An improved Maximum Power Point Tracking For PV System

by

Ramdan B Koad

Supervisor: Dr. Ahmed F Zobaa

Doctor of Philosophy

Department of Electronic and Computer Engineering

College of Engineering, Design and Physical Sciences

Brunel University London

January 2017

Abstract

Working very far from maximum power point diminishes the created power from photovoltaic (PV) system. It is therefore vital, in order to ensure ideal operating conditions, to constantly track the Maximum Power Point (MPP) of the PV panel array. However, this is not easy to identify, due to considerable changes in external influences and the nonlinear relationship of the electrical attributes of PV panels. Therefore, Maximum Power Point Tracking (MPPT) methods can be used to uphold the PV panel operating at its MPP. To date, a number of MPPT methods have been developed, ranging from the simple to the more complex, depending on the weather conditions and the control strategies employed.

This current study offers a novel approach to augment the MPPT method for the PV system, based on the Lagrange Interpolation (LI) formula and the Particle Swarm Optimisation (PSO) method. The LI method is used initially to determine the optimum value of the duty cycle in the case of the MPP, according to the operating point. Starting from that point, the PSO method can then be used to search for the true Global Peak (GP). The proposed MPPT controller essentially initialises the particles surrounding the MPP, thereby providing the initial swarm with information concerning the most effective position. This has the ability to improve PSO efficiency and lead to a more rapid convergence, with zero steady-state oscillations. Additionally, there is no need to restrict particle velocity, as the initial values are closer to MPP. Thus, the proposed technique aims to increase efficiency without adding additional complexity, thereby substantially enhancing potential tracking speeds, while also reducing the steady-state oscillation (i.e. to practically zero) once the MPP is located. This offers a number of significant improvements over the conventional PSO method, in which new operating points are at too great a distance from MPP, and thus require additional iterations.

The algorithm put forward in this work is verified with an OPAL-RT real time simulator and Matlab Simulink tool. A number of simulations are undertaken and compared to: (1) the Perturb and Observe (P&O) method; (2) the Incremental Conductance (IncCond) method; and (3) the PSO based algorithm. The simulation results indicate that the proposed algorithm can effectively enhance stability and fast tracking capability under fast-changing non-uniform insolation conditions.

Table of Contents

Acknowledgements

I owe my most sincere gratitude and thanks to my advisor, Dr Ahmed Zobaa, for his valuable guidance, constructive suggestions, support and strong motivation.

I would also like to express my deepest appreciation to Dr Mohamed Darwish, for his valuable suggestions and guidance. I would also like to thank all those who made this thesis possible.

Finally, I would like to thank my family members, friends, and colleagues, for their warmth, support and patience throughout the research and writing of this thesis.

Declaration

I certify that the effort in this thesis has not previously been submitted for a degree, nor has it been submitted as part of requirements for a degree. I also certify that the work in this thesis has been written by me. Any help that I have received in my research work and the preparation of the thesis itself has been duly acknowledged and referenced.

Signature of Student

Ramdan B A Koad

January. 2017, London

List of Abbreviations

A	Ideality factor of the junction
AC	Alternating current
CV	Constant Voltage
D	Duty-cycle
DC	Direct current
DCM	Discontinuous conduction mode
DSP	Digital signal processor
G	Insolation (W/m2);
I_0	Cell saturation current.
Id	Diode current
I_{load}	Load current
I_{mpp}	PV module Current at maximum power point
IncCond	Incremental conductance
I_{ph}	Photo-generated current
I_{PV}	Current produced by the PV array
I_S	Saturation current (A);
I_{SC}	PV module Short circuit current
I-V	Current vs. voltage
K	Boltzmann's constant (J/K);
LHS	Left-hand side
LI	Lagrange Interpolation
MPP	Maximum Power Point
MPPT	Maximum Power Point Tracking
Np	Number of solar cells connected in parallel
Ns	Number of solar cells connected in series
OCV	Open Circuit Voltage
P&O	Perturb-and-Observe
P_{load}	Active Load Power (W)
P_{mpp}	PV module output Power at maximum power point
P_{pv}	PV power (W)
PSC	Partial Shading Condition
PSO	Particle Swarm Optimisation

P-V	Power vs. voltage
PV	Photovoltaic
PWM	Pulse-width modulation
Q	Charge on an electron
RHS	Right-hand side
R_{ipv}	PV module impedance.
R_{load}	Load Resistance (ohm)
R_P	Shunt resistance;
Rs	Series resistance of the solar cell
s	Second
SCC	Short Circuit Current
t	Time
T	Absolute temperature (K);
T_0	Solar cell reference operating temperature
Tc	Junction temperature, Kelvin (K).
V	Voltage (V)
V_d	Diode voltage.
V_{load}	Load voltage.
V_{mpp}	Voltage at maximum power point for a PV module
Voc	Solar cell open circuit voltage
V_{PV}	Voltage generated across the PV array
A	Temperature coefficient of the current;
B	Temperature coefficient of the voltage.
θ_{ripv}	Load resistance leaning angle.

List of Tables

List of Figures

Chapter One

Introduction

1. The Importance of Maximum Power Point Tracking

Solar energy is widely regarded as the most auspicious source of renewable energy, as (unlike other sources of renewable energy) it has no geographical restrictions. In addition, solar energy cannot be depleted, and is environmentally friendly. In general, a PV cell is a semiconductor material capable of producing direct current electricity once its surface is exposed to direct sunlight. A French experimental physicist was the first to discover a PV effect in 1839, and the first the first PV cell was later made in the United States in 1954, to be used in the space programme. Nevertheless, due to low power output, high costs, and low rates of efficiency, the use of the PV cell did not spread outside the space programme, and was only adopted in the 1970s following a number of oil crises [1,3 and 7].

More recently, the use of PV systems has become a prevalent technique of generating power, because of: (1) its environmental friendliness; (2) respected technology; (3) its production of a free source of energy; (4) minimal maintenance; (5) high levels of efficiency; and (6) reduced costs. Furthermore, a PV system does not require mechanical parts to generate power and is a long lasting method of electricity generation [2-7]. However, PV systems have a number of weaknesses: firstly, PV systems have limited capacity and low conversion efficiency; secondly, they involve high set up costs; and thirdly, they are dependent on weather conditions (i.e. sunlight), which are subject to frequent change. Consequently, the duration of electric current generation by PVs may be limited, as a result of its dependence on the temperature of its surroundings, and sunlight in particular. In addition, the voltage-current (I-V) and power-voltage (P-V) features of PV cell are not linear, since they vary with irradiance and temperature [6-12]. The (P–V) feature of a PV module requires the module to have an optimal operating point (i.e. MPP)) to yield its maximum power output. This point is variable and dependent on local weather conditions and load impedance. Therefore, MPPT methods are necessary for a PV system to maintain the operation of PV panels at their MPP [1, 2] [15- 20].

Furthermore, the efficiency of MPPT controllers is reduced under PSC, due to the assumption that most MPPT controllers operate in such a way that the PV module can only produce its maximum power a one point within the P–V characteristic. However, the P–V characteristic becomes more complex and exhibits multiple peaks in PSC, which in turn affects the performance of the controller, resulting in a reduction in the complete output power of the system [23, 24]. Recently, a large number of modified MPPT methods have been proposed in the literature related to the accurate tracking of MPP, and the improvement in the

dynamic system response, as well as minimising system hardware [24-27]. These methods differ in complexity, accuracy and speed. Yet, even when the tracking was undertaken perfectly with these methods, it resulted in a slow dynamic response speed of the system [21, 26 and 24].

1.1. Problem Statement

The appearance of the output features of PV panels can lead to an assumption that their output is a function of irradiance and the temperature that indicates non-linear characteristics of PV panel power output (P_{pv}) versus the current output. As such, it is important to acquire the highest possible power at all times. Notably, the control of the power electronics by the converter on the PV current ensures the effective function of PV panels at MPP. The variation between MPP and atmospheric conditions is attributed to the changes in the reference value of the PV current. In this case, the PV current is changed according to the atmospheric conditions. The MPPT algorithm frequently exerts an influence on PV current changes, and thus the aim of this current study is to make an introduction to the MPPT system. The MPPT system is intended to foresee and track the MPP of the PV system under environmental changes that could be high within the shortest time possible, with no mistakes being realised and low oscillation. There are a number of setbacks associated with conventional MPPT algorithms, including: oscillation around the MPP; slow speed response; and wrong direction tracking, in particular in the presence of high atmospheric conditions changes.

1.2. Scope of the Research

Two weaknesses exist within PV systems. Firstly, conversion effectiveness is very low (9%-20%) when subjected to low sun energy. Secondly, the current of the PV, and the production of energy, are dependent on weather patterns, leading to constant changes in temperature and solar energy. Moreover, the features of the PV battery are non-linear, i.e. they vary in temperature and irradiance. The PV output feature generally contains a point at which the PV module yields its highest output power and energy, i.e. MPP. At the same time, the actual point is unidentified, and may be arrived at through module computation or through search algorithms, including the MPPT technique [8-20].

According to [23], PV panels present a number of local maximum output power points on the I-V or P-V curves of the PV panels, if allowed to function under non-uniform solar irradiation as a result of covering some of the modules. Conversely, a number of researchers advocate

MPPT algorithms, due to the existence of only a single unique maximum point across the P-V curve. In addition, no suboptimal local maximum exists along the output curves features of the PV panels. More significantly, research into MPPT algorithms for PV arrays indicates more than a single maximum output point on the P-V panel curves or P-I, and is within the scope of this current research. Therefore, the aim of this thesis is to concentrate on methods of improving PSO algorithms, as well as correcting the setbacks of traditional MPPT algorithms.

Recent literature has also proposed a number of modified MPPT methods [28, 43], which differ by characteristics, including: simplicity; cost; conversion efficiency; number of sensors; and application hardware [43]. At the same time, it is not possible to correctly track MPP during a rapid change of weather conditions, and it is not possible to operate the system at MPP under PSC, due to a lack of differentiation between the local MPP and Global Peak (GP) ; this is because of the assumption that most MPPT controllers operate such that there is only one point that the PV module can produce its maximum power within the P–V characteristic. However, when partial shading conditions (PSC) occur the P–V characteristic becomes more complex and exhibits multiple peaks, which in turn affects the performance of the controller and causes a reduction in the whole output power of the system as a result [24, 43-48]. In view of these drawbacks, the following factors have been taken into consideration when developing the proposed MPPT algorithm:

- The dynamic response speed of the system: since a fast dynamic respond can increase the system output power.
- Steady-State Power oscillation: as reducing the power oscillation around the MPP can considerably reduce power loses.
- Tracking direction: in case of rapidly changing weather conditions most of the MPPT algorithm can be confused and track in a wrong direction.
- PSC: the efficiency of MPPT controllers is reduced under these conditions. The assumption made by the majority of MPPT controllers is that on the P-V characteristic there is only one point at which the PV module can produce its maximum power. However, when PSC occurs, the module will have several MPPs, which will impact on the performance of the controller, causing a reduction in the complete output power of the system.

1.3. Aim and Objectives

The aim of this current research is to design and simulate an efficiency controller for a PV system capable of identifying and tracking the MPP of PV in a short time with minimum error and low oscillation under all conditions. To date, the efficiency of the PV system has been approximately 9-20%, an efficiency that can reduce in response to both weather and load conditions [6]. The objectives of this current work are:

1) To study the behaviour of PV modules under different environmental conditions, and their modelling techniques in MATLAB using equivalent circuits, suitable for analysis and simulation.

2) To investigate features influencing the performance of MPPT algorithms, i.e. PV capacitance and PSC.

3) To examine four essential non-isolated DC-DC converters, including contrasting their benefits and weaknesses in various climatic settings, in order to establish the most effective PV system DC-DC converter.

4) To investigate the performance of five widely used MPPT algorithms in the PV system, comparing their performance and efficiency.

5) To propose a new MPPT method for a PV system based on the LI Formula and PSO method capable of dealing with issues arising when searching for MPP.

6) To investigate the performance of the PV system using the proposed algorithm, comparing it to the existing MPPT algorithm using the MATLAB Tools Simulink and RT-lab simulator.

1.4. Organisation of the thesis

The thesis contains eight chapters, as follows

Chapter One gives a brief overview of MPP tracking, and the scope of the work, followed by the organisation of the thesis.

Chapter Two presents a literature review of selected works focussing on different MPPT controllers employed in this field.

Chapter Three presents the background of PV status and types, along with a description and analysis of PV module characteristics, and elements capable of influencing the performance

of a PV cell. This chapter also introduces MPPT, and discusses the main factors capable of limiting its efficiency.

Chapter Four forms a discussion of a number of different types of non-isolated converters (buck, boost, buck-boost, and Cúk).

Chapter Five forms an investigation of five widely used MPPT approaches, as reported in the literature, these being: (1) P&O methods; (2) IncCond methods; (3) open circuit voltage; (4) short circuit current; and (5) constant voltage (CV). This is followed by a discussion of their advantages and disadvantages, and issues relating to their tracking efficiency.

Chapter Six forms an overview of the PSO algorithm, followed by a description of the issue of partial shading. It also forms an introduction to the proposed PSO based MPPT algorithm. This is followed by a comparison of the proposed PSO based MPPT algorithm and existing methods. In addition, there is a proposal for a new MPPT controller based on the Lagrange Interpolation Formula (LIM) and PSO method.

Chapter Seven includes a description of the MPPT system simulation models, and the verification of the proposed algorithm with an OPAL-RT real time simulator and MATLAB/Simulink tool, and which includes undertaking several simulations to be compared to the P&O method, the IncCond method, and the PSO-based MPPT algorithm.

Chapter Eight includes the conclusion suggestions concerning future research and work.

1.5. Author's Publications

The following publications are published from this work.

[1] R. B. A. Koad, A. F. Zobaa, "A Study of non-isolated DC–DC converters for photovoltaic systems," International Journal on Energy Conversion, vol.1, no.4, July 2013, pp.219-227.

[2] R. B. A. Koad, A. F. Zobaa, "Comparison study of five maximum power point tracking techniques for photovoltaic energy systems," International Journal on Energy Conversion, vol.2, no.1, January 2014, pp.17-25.

[3] R. B. A. Koad, and A. F. Zobaa, "Comparison between the conventional methods and PSO based MPPT algorithm for photovoltaic systems," International Journal of Electrical, Computer, Energetic, Electronic and Communication Engineering, vol.8, no.4, April 2014, pp.690-695.

[4] R. B. A. Koad, A. F. Zobaa, and A. El-Shahat, “A novel MPPT algorithm based on particle swarm optimization for photovoltaic systems,” IEEE Transactions on Sustainable Energy.

Chapter Two

Literature Review

2. Literature Review

In recent years, solar energy has become a significant factor in a number of applications. However, the distribution of electrical energy remains a challenge in remote areas, where applications are relatively small, as can be observed from the small size of generators or utility grid. Electricity acquired from an array of solar systems is more expensive in comparison to that acquired from the utility grid, and it is therefore necessary to undertake in-depth research concerning the efficiency of all aspects, in order to establish an effective PV system capable of satisfying a large number of demands at a lower cost [49-51].

The efficiency of PV panel functioning is generally influenced by both external and internal factors, of which there are a considerable number, the most significant being ambient temperature, solar irradiance and wind. Such external factors significantly influence the supply of maximum power and the voltage of MPP of a PV panel. In addition, external influences also cause changes in the position of MPP on the voltage of the current (I-V) curve. On the other hand, load is considered as a primary internal factor capable of causing PV to function at a strict point on the I-V curve in directly matched systems. The intersection between the variance in the load line and the I-V curves under different weather conditions demonstrates the functioning point on I-V curves, and is therefore highly important to MPP of the solar array. Conversely, the tracking control of MPP is a highly complex issue, for which a number of tracking methods have been established to curb, including: IncCond; P&O; neural networks; and CV. The setbacks associated with such methods generally include their high cost, complexity, non-stability and difficulty. The use of the MPPT converter is to ensure the maintenance of the function point of the PV array at the MPPT, while the MPPT controller establishes this takes place by itself directing the PV array's voltage of the load [42-55].

It is significant that the relatively high cost of electricity from PV results from the high cost of PV panels and systems. This could explain the reason that inefficient methods of operation of PV panels leads to designers increasing their number, enabling adjustment in accordance with the energy demand for the load. Thus, the high cost of PV panels results in uneconomic system design. Research concerning the influence and maximum effect on power operation contributes to the construction of the maximum size of PV system. This leads to a large amount of energy being spared by the maximum design PV system, masking that this ensures the cost of the PV system falls. The PV system can generally be widely employed in a number of applications, particularly in remote areas [49, 56].

2.1. CLASSIFICATION OF MPPT TECHNIQUES

As weather conditions do not remain constant, and change over time, PV panel MPP also vary over time. The MPPT controller is required to track the MPP and extract the maximum possible power from the module. The tracking of PV panel MPP becomes more complex during rapidly changing weather conditions, and PSC common in PV systems, due to a number of factors, i.e. passing clouds and dust. The solar cells in practical systems are connected in series, or parallel configuration, to form the modules /arrays, in order to generate the desired value of the voltage. However, the PV module output voltage will be determined by the output current generated, which primarily depends on solar radiation conditions directly proportional to the irradiance. Therefore, an application such as multiple PV modules (which work at different irradiance conditions) will lead to an opportunity to ensure a number of different, rather than just one, MPP, which can result in a substantial reduction of the output power of the complete system, due to its controller being unable to find the true operating point at MPP. This condition can take place due to PSC.

In the case of shading conditions, the shadow PV panel becomes reverse biased, while the un-shaded PV cells become forward biased. Thus, if the reverse voltage is increased beyond the breakdown voltage, this results in the cell/module temperature being raised. These are known as hot spots, and lead to irreversible damage to the cell. The use of a bypass diode has recently become the most popular technique to protect the PV cell/module from the hot spot when connecting the PV cell/module in series. However, the use of a bypass diode results in multiple peaks on the P-V characteristics, which add additional complexity in tracking MPP.

An in-depth study by Esram et al. [59], concerning a number of different MPPT methods employed in PV systems, has established the presence of at least nineteen MPPT techniques recommended for tracking MPP. These methods have been compared by means of the characteristics noted above. These techniques can be classified into three different categories [65], as outlined below:

2.1.1. Online Technique

The first group is known as direct methods, and includes P&O [76], and IncCond [74]. In these techniques, the PV module operating point is perturbed in order to search for MPP. However, its major weakness consists of its tracking ineffectiveness, which ensure it is not the most appropriate preference to function as MPPT, due to the principle of searching for MPP. A further disadvantage of this group is that it is unable to operate the PV panel at its MPP under rapidly changing solar radiations [65, 66].

A number of investigators have asserted that PVs possess a number of MPPT algorithms. One highly utilised algorithm consists of the P&O technique. It is used extensively, due to being easy to execute, needing only a straightforward feedback regulator, and therefore requiring no previous knowledge of the component features. At the same time, it requires fewer factors, since only two sensors are applied, thus implying a reduction in the expense associated with hardware tools [65,66, and 74].

The P&O technique has been defined by [7], and is based on the affiliation linking the output energy and the output current of a PV unit, whereas the MPP is acquired by changing the converter's switching disposition (duty proportion) up to when the dp/dvs becomes zero. The drawback of P&O techniques is the production of a fluctuation around the MPP within the stable condition. Xiao et al. [7] are of the idea that the consequence of a constant oscillation within the P&O method in the stable condition creates a noteworthy decrease during the output energy of the PV module. Furthermore, it cannot run the module at its highest output energy in weather circumstances prone to fast alteration.

The technique of hill-climbing is offered in [6] and [7], and is founded on the belief of perturbation and surveillance of the PV output power. In spite of the execution of this technique being both easy and simple, it has some disadvantages, comprising slow tracking pace, causing fluctuations within the stable state, and a low effectiveness under swiftly changing circumstances.

There are three major setbacks associated with the P&O method. Firstly, it needs to take into consideration the measurement of the PV voltage at every stage, resulting in the loss of a considerable amount of energy in the control unit, which causes inefficient functioning of the PV panel. Secondly, the P&O method requires a high number of iterations, to enable the MPP to be monitored, because of the need for oscillation around the MPP. Finally, a variation in MPP also emerges from the difficulties relating to the zero derivative workings of d_P/dv or d_P/d_I. However, there are a number of methods widely believed to correct the issues associated with the P&O method. Hsiao [57] claims to have established a three-point comparison method that distances itself from the oscillation issues of the observation algorithm and perturbation method. Similarly, the observation algorithm and perturbation method is cited in [60], identifying the capacitor for MPP monitoring in a PV power system. As such, the capacitance is worked upon and applied to correct the differences of the duty ratio, and so obtain the highest mark of MPPT alongside the degradation of PV panels.

The IncCond method has been outlined in [74]. This was developed to overcome issues relating to P&O, due to possessing a higher capacity than the P&O algorithm to track efficiency within rapidly changing environmental conditions. This study analysed the advantages of the P&O method, with the result revealing that the IncCond algorithm has a high efficiency, which successfully tracks MPP of the PV module, even under rapidly changing conditions. However, the result was undertaken through the use of simulation and graphs, and the effect of PSC was not included in the study.

A number of researchers have proposed the IncCond method to overcome the drawbacks of the P&O method, and improve system tracking efficiency under rapidly changing weather conditions. However, the conventional IncCond method retains a number of disadvantages, and its tracking efficiency is low, as it generally employs a fixed step size that depends on tracking speed and efficiency. Therefore, the conventional IncCond method must be modified in order to resolve the trade-off between its dynamic response and reduce the oscillation around the MPP in a steady state.

The IncCond in [10, 74] is considered crucial, since it can be employed to improve the observation algorithm and perturbation method under rapidly changing weather conditions. Thus, the major setbacks associated with the observation algorithm and perturbation method, as well as conductance, consist of a high consumption of energy, resulting from instability due to changes in weather conditions and oscillation around Vmax. Such issues can be avoided in such methods to bring about complexity, particularly in a conventional control unit. The control methods are considered the most popular techniques for reducing setbacks associated with the observation algorithm and perturbation method [14, 31, and 74].

Liu et al. [62] have proposed a variable step size IncCond method capable of adjusting the IncCond step size automatically, according to the characteristics of the PV module, and results have revealed that the proposed technique results in high stability in the steady state. However, even if the proposed method results in accurate tracking, its dynamic response will be low, as a result of the threshold of the duty cycle conversion. Although it has a higher level of tracking efficiency than direct methods, it requires additional sensor devices for the relevant computing, leading to its response time for conversion being slower, and thus resulting in greater power losses. The implementation of these method is more complex, leading to it not being the first preference to function as MPPT in many applications [76-81].

Dezso et al. [76] note the basic operation principles of different MPPT techniques in PV systems, e.g. Hill Climbing (HC), IncCond; P&O; and Fuzzy Logic Controller (FLC). They present a comprehensive comparison between the techniques studied and their tracking efficiencies under varying weather conditions.

In conventional MPPT methods, a fixed step size is applied within the algorithm to track MPP. However, applying a fixed step size results in oscillation around MPP, and a reduction in overall output power. If a large a step size is used, the system will be unable to produce a stable output power, while if small step size is used, the dynamic response of the system will be slow.

Xiao et al. [124] have undertaken a detailed analysis of the P&O and IncCond MPPT algorithms, in order to clarify a number of common misconceptions relating to these two widely used MPPTs presented in the literature. In this study, the two MPPT methods were analysed mathematically, and their practical implementation was thoroughly introduced. The result was confirmed by the use of experimental tests, which revealed that both P&O and IncCond MPP trackers are equivalent. Ishaque et al. [69] evaluated the performance of the P&O and IncCond MPPT technique according to the European Efficiency Test EN 50530, which is specifically devised for the dynamic performance of PV system. The authors implemented both techniques, using a direct control with buck–boost converter, verified through the use of experimental results. This led to the conclusion that both methods are equivalent, and the dynamic response and MPPT efficiency are practically identical. However, the performance of the IncCond method is found to be slightly higher, and its performance at low insolation levels is indicated to be highly sensitive to its perturbation size.

A number of MPPT methods have been reported in the literature, in order to improve the dynamic behaviour of the conventional methods, i.e. the variable step size and perturbation frequency [68-72]. Kobayashi et al. [78] have proposed a variable step-size method to overcome the drawback of the conventional P&O MPPT technique as it oscillates around the MPP at a steady state, resulting in raising the waste of the available output power, and achieving a rapid dynamic response with good tracking performance. However, the variable step-size method also has a number of disadvantages, as a constant value is often used in the algorithm, and the choice of its value is highly significant, since its value cannot be adjusted in response to a change in weather conditions. In addition, its time response is lower in comparison to the conventional method, with less efficiency under PSC and a considerable loss of power during a large variation of solar radiation [65-78].

Chen et al. [77] have presented a novel auto-scaling variable step-size MPPT scheme. The main objectives of the controller are to optimise the PV module output power, and to eliminate issues found in the conventional variable step-size method, as it automatically employs a simple judgment to adjust the step size of the proposed method. This leads to the proposed algorithm having no requirement to attain a reference value, as in conventional methods, enabling it to achieve a fast dynamic response with steady state oscillation, even in an extreme range of weather changes. However, its disadvantages include the low response time of the algorithm, low efficiency during cloudy days, and that it can be confused under PSC.

Rodriguez et al. [80] have proposed a new approach, in which a two-stage method is used to track the MPP. In this method, the equivalent load line is estimated during the first step, from which point the IncCond method is employed to track true MPP. However, under PSC, the control may confuse and track the local MPP instead of GMPP, since the load line is estimated under uniform insolation conditions.

Koutroulis et al. [72] have presented a method for detecting the MPP based on the scanning process, in order to search for the region containing the true MP. A P&O algorithm is then employed in the second stage to track the true MP. Although the accuracy of this method is high, and is capable of correctly tracking the MPP, the tracking speed time is slow, due to all local MPPs requiring to be identified during the first stage, in order to establish GP.

2.1.2. Offline Technique

The second group of indirect methods includes the Fractional Short Circuit Current (SCC) and Fractional Open Circuit Voltage (OCV). The main advantages of these techniques are that they are easy to implement without a complex algorithm and have a relatively rapid response. However, they require additional components [47, 63]. The online measurement of the results of OCV and SCC in reducing the output power of the module and its MPP cannot always be matched. Moreover, the measurements of OCV (VOC) and SCC (ISC) are often necessary in this method, implying a shorting of the module at each instance. Nevertheless, this issue can be mitigated with several loads, although additional components will be required, potentially increasing the cost of the system [47]. A further downside of this technique is the estimation of the factors of voltage and current, as these are likely to change during PSC. Additional valves are also necessary in the converter for the OCV and SCC methods, leading to decreased efficiency and greater power losses. Furthermore, the results lack accuracy, and the MPP is not always attained, and therefore this method only yields optimal power at a single

temperature [47, 48]. The load is required to be detached from the panel for a set amount of a time for the measurement of the OCV, which wastes a considerable amount of energy [63-66], and frequently requires the measurement of SCC (ISC), which leads to shorting the module on each occasion. However, this issue may not arise if several loads are employed, but this requires additional components, and thus increases the cost of the system [47, 68].

Tafticht et al. [64] have established a tracker for MPP founded on the computation of the SCC from the measured OCV, since the SCC method possesses greater accuracy than the OCV method, and OCV measurement is easier in comparison to SCC. In this method, it is necessary to measure OCV, resulting in the importance of inserting a switch between the converter and the PV module. Furthermore, additional valves are required for the OCV technique to compute OCV, alongside the insertion of a capacitor between the converter and the module, in order for the load to access power when the circuit opens from the switch. Both the maximum voltage and OCV ratio are variable, and subject to the temperature of their surroundings, and therefore this technique only attains optimum power at a single temperature.

Masoum et al. [68] have proposed a rapid and accurate MPPT algorithm based on the OCV and SCC of the PV module. This method employs mathematical equations used to describe the PV module I-V characteristics in the algorithm. The proposed method has been verified by using MATLAB, and been tested under different atmospheric conditions. The simulation results reveal that the PV module operating points were close to the theoretical value of the PV module, and the developed algorithm was more rapid and accurate than the P&O method.

2.1.3. Intelligent Technique

The third group contains artificial intelligent techniques, including neural networks and planning, and fuzzy logics [71,72 and 81]. These methods have become popular, with studies recommending fuzzy logic MPPT and neural network methods to deal with the downside of conventional methods. Nevertheless, these methods are limited in terms of flexibility, since the features of the PV module need to be defined to formulate rules to control MPPT. Fuzzy logic controls have commonly been used in MPPT, due to their many benefits, e.g. the capacity to work with inaccurate inputs; addressing nonlinearity; and lacking the requirement of a correct mathematical model. In addition, changes in weather conditions do not influence the FLCs. However, the user is required to choose an appropriate method to calculate the error and formulate the table of base rules to ensure they are effective, and FLCs necessitate a large memory to handle the two extremes.

Chin et al. [83] have proposed an initial voltage tracking function (IVTF) for tracking the MPP of the PV array operating under shedding conditions, in which a fuzzy logic MPPT controller was implemented in the conventional P&O MPPT algorithm, in order to vary the step size of the perturb voltage in case of partial shedding conditions. The results indicate that the fuzzy logic MPPT is able to control the operating point of the PV array at its MPP, after IVTF is initialised with a more dynamic response.

Syafaruddin et al. [67] have proposed a method for tracking MPP based on a radial basis function and a three-layered feedforward neural network. The accuracy of this method primarily depends on the training data, and it lacks versatility, as there is a need to create control rules to meet the PV array characteristics. Furthermore, additional time is needed to acquire the correct MP when updating the data of the PV array, and it is also dependant on expert knowledge. Therefore, in order to track GMP correctly, a computational effort will be required under PSC.

More recently, a number of modified MPPT methods have been proposed in the literature related to accurately tracking MPP and improving the dynamic system response, as well as minimising the system hardware [70, 84 and 86]. However, the conventional P&O and IncCond methods contain a number of drawbacks, including: oscillation around the MPP in the steady state; a failure to track MPP under rapidly changing atmospheric conditions; and a tendency to track the local maxima instead of global MPP in case of PSC. Therefore, a number of researchers have proposed modified P&O and In-Cond methods. However, the associated issues are unable to be completely resolved, particularly under PSC [91]. To improve tracking efficiency, and reduce steady state oscillations, Nguyen et al. [85] have proposed a new method of adaptive reconfiguration of solar PV module operation under PSC. However, this method increases the cost of the system, even if tracking is undertaken perfectly, as it requires additional sensors and switches.

These algorithms have the advantage of working independently, due to knowledge of PV generator characteristics not being a critical factor. Although the majority of these methods are simple to implement [62], they are unable to track MPP correctly during a rapid change of solar radiation. Furthermore, they are unable to operate the system at MPP under PSC, due to their lack of differentiation between the local MPP and the GP [91-96].

Khaehintung et al. [71] have presented a new MPPT controller, known as an adjustable Self-Organizing Fuzzy Logic Controller, implemented on a low cost microcontroller.

Alajmi et al. [98] have proposed a fuzzy based P&O MPPT, with the proposed technique being verified using MATLAB/SIMULINK. Simulation results indicate that fuzzy based P&O MPPT has a high rate of efficiency and increases PV output power.

Khaehintung et al. [53] have introduced a new MPPT algorithm using an artificial neural network, with the proposed method developed by a three-layer neural system, using simple functions. The proposed technique was implemented on a PV charging system on a low cost microcontroller without an outer sensor unit prerequisite. The study was verified using experimental results, demonstrating that, in comparison to conventional methods, the proposed algorithm has high efficiency in terms of tracking speed and stability in the steady state condition, and its efficiency is higher than 90% under all test conditions.

According to [81] a neural network is presented to demonstrate the MPP of PV modules, as well as the design of a PI-type controller for real time optimum power tracking. MPP can be discovered through the suggested neural network, through the application of open circuit voltage from the controlling cells. The suggested neural network has established a real calculation of MPP from the PV modules. In general, the neural networks views functions with more clarity than simple mathematic computing methods. However, a neural network performs random data without human awareness and, as such, it depends largely on the amount of data available to study the network, eventually leading to tedious, and complex, process. Therefore, neural network research method is applied as an end solution selected to resolve issues associated with a low level of knowledge.

Sheraz et al. [81] have presented a more effective MPPT controller, centred on the Artificial Neural Network (ANN) and Differential Evolution (DE). Outcomes have demonstrated that the use of a combination of these methods yields improved tracking, a more rapid response, and minimal fluctuations in the steady state in comparison with the conventional techniques of MPP. However, due PV panels having various features subject to change, the accuracy of the neural network is dependent on the set rules employed by the concealed layer, and the manner in which the neural network has been instructed. Therefore, the neural network requires periodic instructions in order to warrant an accurate tracking.

Wang et al. [91] have described a PV system under PSC, illustrating that the use of a conventional MPPT algorithm under partial shadowing conditions has the potential to result in significant loss of power. According to [92], under PSC, the efficiency of MPPT controllers is reduced, due to the majority operating in such a manner that only one point

remains at which the PV module is able to produce maximum power within the range of its P–V characteristic. However, when PSC occurs, the P–V characteristic becomes increases in complexity, exhibiting multiple peaks. These, in turn, influence the performance of the controller, resulting in a reduction of the entire output power of the system [90-92]. A number of modified MPPT methods have recently been proposed in the literature, in order to ensure the accurate tracking of MPP, to improve dynamic system response and minimise system hardware [80], [94]. These methods differ in their complexity, accuracy, and speed, and even if they resulted in tracking being completed perfectly, the dynamic response speed of the system would remain low [2], [92-94].

An alternative optimisation technique applied to the MPPT controller of a PV system, operating under PSC, is the PSO algorithm [91-93]. The PSO technique exhibits considerable potential, due to its easy implementation, fast computation capability, and ability to determine the MPP, irrespective of environmental conditions. It can also perform a more random search than those performed as part of other evolutionary techniques, i.e. the Genetic Algorithm (GA). The difference between the PSO algorithm and conventional techniques is that the updating of the duty cycle based on the particle velocity is not fixed in the PSO method, while the duty cycle is perturbed by a fixed value when employing other techniques. This results in oscillations occurring around MPP in a steady state, as reported in [91] and [92] - [94]. In standard PSO, particles are generally initialised in a random manner following uniform distribution over the search space. This requires long time delays to enable the particles to converge towards the MPP, thereby resulting in long computation times [26], [93]. However, a correct initialisation of the particles can improve PSO efficiency, resulting in the detection of superior solutions with faster convergence.

Chen et al. [95] have presented a biological swarm chasing algorithm for tracking the PV module. MPP has been introduced with the proposed method known as Bio-MPPT, where every PV module is viewed as a particle used to track MPP automatically. Although this method gives a good performance under uniform conditions in comparison to the conventional P&O MPPT method, the case of PSCs was not addressed.

A new MPP tracker based on PSO for PV module arrays has been presented by Chen et al. [96], with the result demonstrating that the proposed algorithm is capable of tracking global MPPs under PSC. However, the dynamic response of the system was low when tracking global MPPs, as fixed values for weighing were employed within the algorithm. Although traditional PSO algorithms are fast and accurate when tracking global MPPs with a single

peak characteristic, the tracking performance is found to be lacking when a number of PV modules are shaded, due to fixed values of weight in the conventional PSO that need to be readjusted when tracking global MPPs of multi-peaks characteristics.

Phimmasone et al. [100] have projected a novel MPPT, founded on the PSO algorithm, by adding extra coefficients to model PSO equations in order to enhance the algorithm computational load. Nevertheless, it is not apparent whether the algorithm is capable of tracking the correct MPP continually, as when particles reach the MPP within the PSO algorithm, their speed falls to extremely low, or nil. One of the frequently encountered difficulties with the PSO algorithm is that, under conditions of slow difference in solar emissions, the alteration of the duty cycle needs to be small to track MPP accurately. Nevertheless, this leads to the need to employ a definite amount of power utilised during the investigative process, and determines that the conversion towards MPP will be gradual. In contrast, if the adjustment to the duty cycle is large, it is then not possible to accurately trace the novel MPP [97, 98].

Ishaque et al. [92] have introduced a new MPPT method based on a PSO algorithm, proposed to increase the tracking performance of the conventional PSO, as one of the common problem in the slandered PSO algorithm is the length of time required for convergence. Therefore, the author has suggested removing the random numbers of the standard PSO acceleration factors in order to reduce the search time. The advantage of the proposed method include: (1) the use of a small number of number of particles; (2) an easy structure; and (3) the need for only one inertia weight to be tuned. The results have demonstrated excellent performance in comparison to the conventional PSO. However, there needs to be a restriction of the change in particle velocity. Furthermore, there is no guide as to how its values have been selected, as a low value of velocity leads to additional iteration to reach GP, while a large value may lead to an escape from GP.

Lian et al. [88] have proposed a two-stage algorithm through the implementation of the P&O method in first stage to set the nearest local MP. From this point, the PSO method is employed to search for the true GP. The advantage of this hybrid method is the reduction in the PSO searching area. The proposed method was verified using an experimental setup, with the result demonstrating that the hybrid method reduced the search space for the PSO, while its convergence time was greatly improved. However, P&O can be confused during the time intervals characterised by changing weather conditions, which can move the system operating point away from the LMPP, and it takes a considerable amount of time to reach the local

MPP. Moreover, when PSC occurs, the proposed scheme may track LMP in the second stage instead of GP, due to the lack of a guide to the way PSO parameters were tuned, while in the conventional PSO algorithms the three basic parameters (i.e. the inertia factor and acceleration coefficients) need to be toned to accelerate convergence. This leads to a need to modify the learning factors and inertia weight in the conventional PSO when PSC occurs. However, there are difficulties in choosing its values, and tuning generally takes place by means of experimentation.

A re-initialised PSO-IncCond process has been suggested in [138]. The IncCond process was employed to discover the locality of MPP, following which, the averages of the function cycle and the output power within the IncCond technique were employed to re-initialise the standards for identifying the finest duty cycles and the highest power rate in the PSO process, in that order. Despite the benefits of precise tracking (which is possible when using PSO-founded techniques) a key drawback consists of tracking taking considerably longer than when using traditional processes, particularly under PSC.

Chapter Three

PV Systems

3. Introduction

This section will firstly, examine the background of the PV system, an overview of the MPP, and the parameters influencing the performance of MPPT in the system. Secondly, it will focus on a description of modelling PV cells in Matlab, using an accurate equivalent circuit, and including the parameters impacting on its performance.

3.1. Renewable Energy and Photovoltaic system

There has recently been a considerable rise in global energy usage, attributed to the increase in industrialisation as well as elevated living standards. The majority of energy is currently sourced from non-renewable traditional energy supplies (i.e. fossil energy, including coal) and has resulted in two main challenges to the sustainability of human evolution: (1) global warming and (2) an energy crisis [110]. This has led to an appreciation of the potential harm to the natural world resulting from rising amounts of CO2 discharged from traditional energy supplies, leading to global warming, as well as to adverse effects on nature and a number of ecological challenges. This has resulted in an increased focus on identifying effective alternative resources to satisfy global energy requirements through the use of environmentally friendly energy supplies, which have no need to burn the fossil fuels currently causing a discharge of CO2. Consequently, renewable energy supplies are regarded as the solution to increasing energy needs and have sequentially caused the growth of this area as a significant prerequisite for the future of humankind [104-111].

The use of renewable sources of energy has increased in popularity as a result of their sustainability. Furthermore, they cause no damage to the environment, and are free from carbon emissions. As a result, the use of renewable sources of energy has been embraced as a remedy for issues resulting from the use of non-renewable fossil fuels. The generation of power through renewable sources of energy remains limited by the weather conditions of each locality, i.e. the use of wind, rain, and sun in the generation of wind power, hydro power, and solar energy, respectively. Moreover, renewable sources of energy are more costly than traditional sources, particularly when power is required in large volumes.

In essence, the research for renewable energy focuses on minimising cost in order to increase the efficiency of output. Most recently, PV energy and wind power have been the focus areas of research and development [102-111]. The field, however, requires additional effort in order to improve the efficiency and reliability of renewable energy. The popularity of the PV system in power generation has increased since advancements in the field of

semiconductors, which have improved production to realise the load power requirements. Therefore, PV systems are viewed as the most effective alternative energy of the future, due to: (1) their energy source never being depleted; (2) they are environmentally friendly; and (3) they have no need of mechanical parts (i.e. which would increase maintenance costs) [105].

3.2. The Fundamentals of Photovoltaic

The term 'photovoltaic' originates from Greek words *phos* (implying light) and *voltaic* (implying electrical). Therefore, voltaic was named after an Italian physicist referred to as 'Volta', which could also mean measurement or volts. The term photovoltaic has been widely used among English speakers since 1849. Bequerel was the first to identify PV effects in 1839, however, the commercial applications of PV forms of electricity were not discovered until the late 1950s. PV power production costs have, in the past, proved relatively higher than equivalent forms of conventional power sources [103,105]. However, there is currently less focus on cost, due to a considerable fall in prices, i.e. 12 to 19 % nationwide in 2013 and another drop 3 to 12 % in 2014, depending on the market and the system location [109].

The process involving the conversion of light energy into electricity in a direct manner is known as PV. One of the most significant factors is that PV power generation is only possible under certain conditions that warrant suitable absorption of the solar energy, accumulation of charges, creation of flexible electron/hole pairs, and linking of contacts that are oppositely charged. A solar cell is frequently a source of electrical current operated by the rate of flow of radiation. In the PV panel, semiconductors contribute an approximate 60% of general usage. The efficiency of PV systems for commercial purposes is approximately 10-20%, yielding energy in a normal daylight at a rate of 1-2kWh per square metres daily. Thus, the average energy generation of a full solar radiation of kW per square metre yields a potential difference of an estimated 0.5 V and a current density of 200 A per square metre of a cell. This implies that a typical industrial cell of 100 square centimetres yields a current of approximately 2 A., while a typical cell has a lifespan of at least twenty years.

In addition, the stationery nature of the system enables it to remain isolated in its location without any need for maintenance. There are a number of strengths associated with the use of PV systems over other widely known sources of power throughout the globe: firstly, the systems are characterised by long life periods, ranging from twenty years and above; secondly, solar PV systems are able to function in any given climatic conditions, and have an immediate response to solar radiation; and finally, solar PV systems are more reliable, sturdy,

and modular, resulting in little need for maintenance, as PV systems functions silently. However, PV systems also have a number of limitations. Firstly, they have a relatively high initial cost and demand high levels of investment. Secondly, as PV systems largely depend on climatic conditions to function efficiently, they require energy storage in the form of batteries, with their costs therefore being increased by the installation of batteries. Thirdly, power production is unstable, as it relies largely on climatic conditions. Fourthly, the general efficiency of the PV system is relatively lower than power generator technology. Fifthly, PV systems can easily become less efficient over time. Finally, numerous losses emanating from the PV module's active group reflection prevent photons from travelling through the semiconductor. Therefore, during production, the ground of the PV module is dressed with a specialised anti-reflecting material to have a pyramidal texture, with the treated layer disappearing over time.

3.2.1. Classifications of Photovoltaic Power Systems

As demonstrated in Figure.3.1, PV systems can be divided into two types: (1) a stand-alone system and (2) a grid connected system. Stand-alone systems generally operate independently, and can be used in a number of applications, including: satellites; space stations; remote areas; and water pumping systems. There has recently been an increase in the use of grid-connected systems capable of supplying utilities with solar energy through the grid, with 93% of PV grid connected systems being installed in 2004 [5,10, and 21].

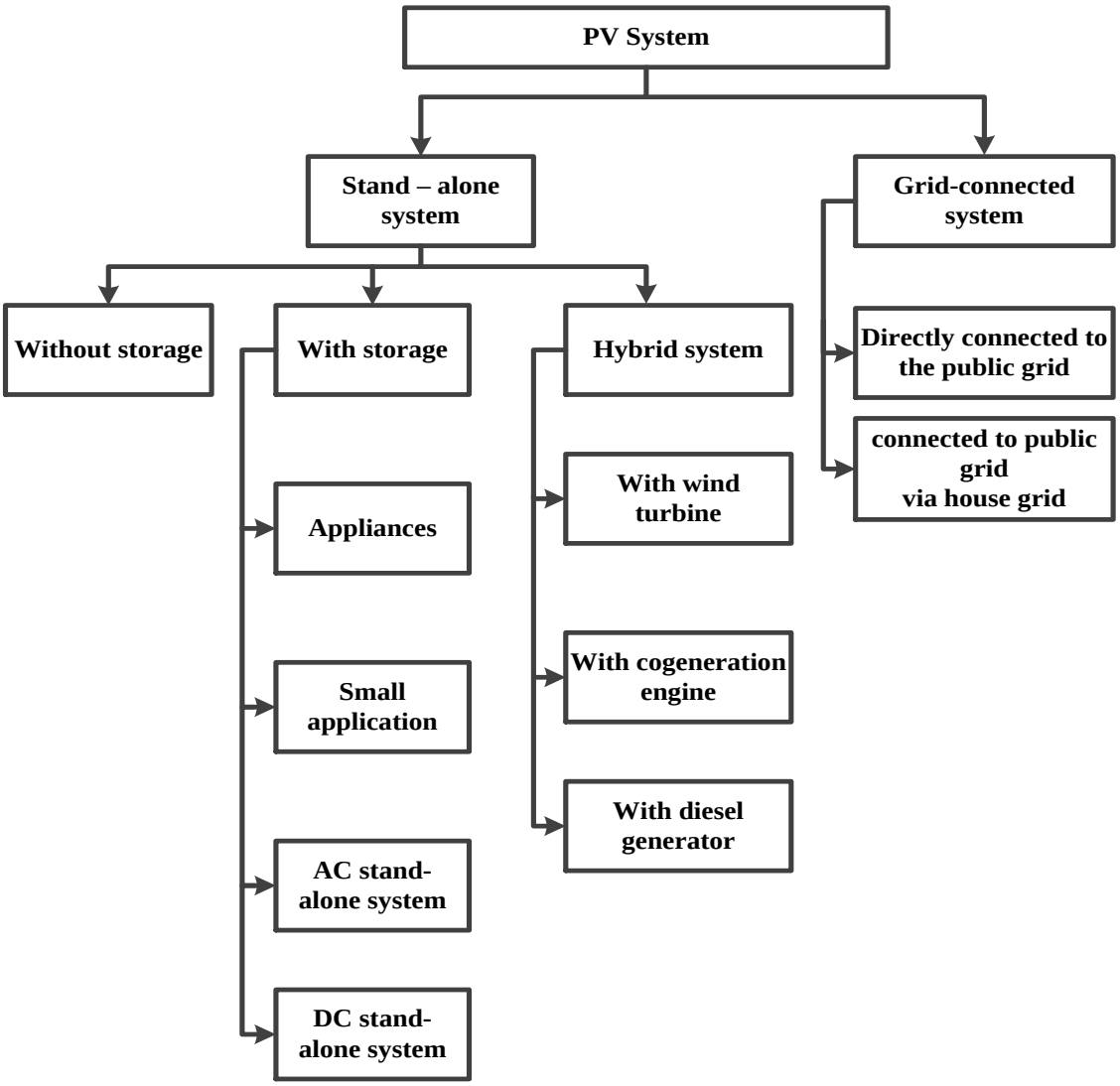

Figure 3.1: Classifications of PV systems [5].

3.2.2. Stand-alone PV systems

In a stand-alone form of PV system, the load is supplied by the energy directly from the system, particularly in remote areas that have no access to an electricity grid [4], i.e. charging of batteries, water heating systems, solar lighting and water pumping systems. Figure 3.2 (below) demonstrates the simplest block of a stand-alone PV system. The PV system in this type of configuration provides the energy to the load during the day, i.e. water pumps [4, 24].

Figure 3.2: stand-alone PV system [11].

3.2.3. Grid connected PV systems.

This form of PV system is appropriate for those regions with plentiful space, combined with lengthy and unobscured periods of sunlight. It consists of a grid connected system, with its output power directly supplied to the grid. However, the output voltage of the PV module is DC, and thus need to be converted to an AC current by means of power electronic devices. The PV output power needs to be initially increased, followed by feeding its output power into a DC link to be inverted into alternative current (AC) through an inverter fulfilling the demand quality of AC voltage [21, 23]. Figure 3.3 demonstrates the grid connected type when the PV system is connected to other sources in parallel [1].

Figure 3.3: grid-connected type [11].

3.2.4. Techniques of Photovoltaic Power Systems

The Figure 3.4 (below) demonstrates a typical block of a PV system. While the output power of PV systems has been improved, its installation remains expensive in comparison to conventional sources, as it requires additional components to meet the required output power, e.g. a controller; power storage; a DC/DC converter; and a DC/AC inverter, to be used as a power interface between the panel and the load [101]. These components are used to control and regulate the output power produced by the PV module.

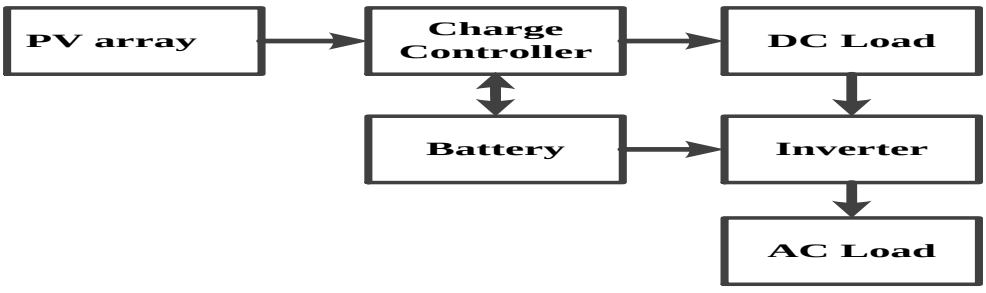

Figure 3.4: typical PV system [11]

3.2.5. Photovoltaic cell

A solar cell or photoelectric (PV) cell is primarily a semiconductor device capable of converting sunlight into a direct current DC. An electron will be produced where the energy of the photon is greater than the band gap energy, while a direct current can be produced by the flowing of electrons.

PV cells are typically formed as a PN junction and two terminal sides (i.e. front contact and rear contact). Fig, 3-5 demonstrates the working of silicon based solar cells. When the sunlight hits the PV surface, a number of photons will be reflected, or passed through the cell, while the remainder will be absorbed, thus generating the hole-electron pairs. The p-n junction subsequently produces the current separating the holes and electrons, resulting in a direct current flow (i.e. electricity) if the load is connected to the solar cell [3, 113, and 117].

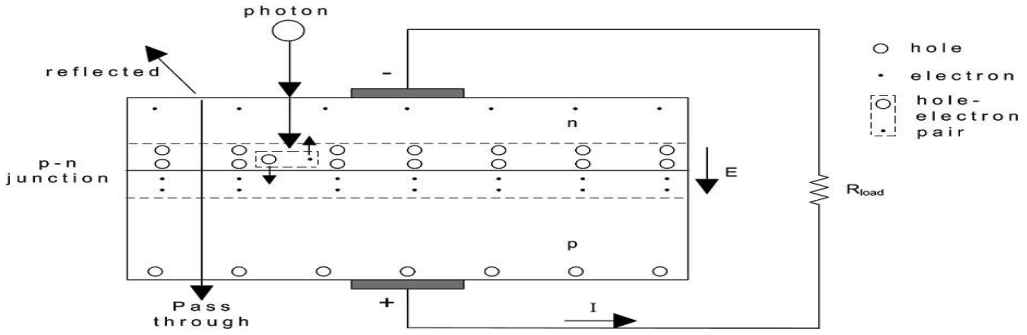

Figure 3.5: Structure and working of a typical PV cell [11].

For the majority of loads, the output voltage of a single PV cell is generally small, i.e. approximately 0.6v, for crystalline silicon (Si) cells. The required output voltage can therefore be achieved by connecting a number of PV cells in series which known as the PV module (see Figure 3.6) [11, 19, and 120].

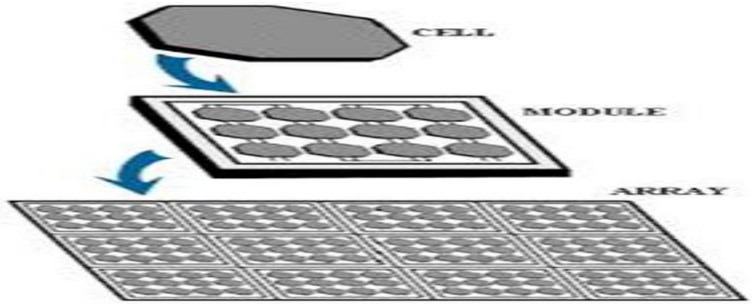

Figure 3.6: PV Cells, Modules, and Arrays [119].

3.3. Maximum Power Point Approaches for PV panels

It is significant that aging plays a vital role in the solar array system, and it is thus important to accurately establish the functionality of the complete PV system, in order to create an effective system capable of fulfilling demand with lower cost. However, wind speed, solar irradiance and ambient temperature are major external factors dictating the highest power capable of being generated from a PV panel. It appears that the position of the MPP on the I-V curve is changed through the influence of external factors. In directly coupled machines, the load forms the major internal factor capable of driving PV panels to function at a strict point on the I-V curve, as illustrated in Figure 2.5. In fact, MPP changes its position and operates furthest from the highest power point, decreasing the output power of the PV system as a result of external influences. As such, it is important to track the MPP of a PV solar array. There are a number of difficulties in measuring these parameters, as (due to a considerable fluctuation in external influences) the electrical appliances of PV panels are modified on a regular basis. This leads to difficulties in identifying the highest power point mathematically as a function of internal and external factors.

MPP of a PV system has been proposed as a control technique for tracking with traditional and artificial techniques. However, research has, over a number of years, focused on many highest power point control algorithms to produce the maximum power of PV panels. These methods primarily employ different research methods with different control strategies, and thus the main directions of these MPPT techniques can be grouped into four main methods: (1) computational artificial intelligence; (2) P&O; (3) IncCond; and (4) computational. Their required features (i.e. simplicity, efficiency, and stability) have been evaluated under a number of different climatic conditions. They are of low cost, and can be used with different types of loads, while also having the potential to adapt to different types of converter and low tracking iterations under different environmental conditions [117-122].

3.3.1. Maximum Power Point Tracking

MPPT is employed to ensure that the highest power is obtained from the PV modules under all environmental conditions (in particular, solar insulations and temperature). This is achieved by matching the functioning voltage and current of coordination power converters. Figure 3.7 shows the outline MPPT block figure in combination with a DC-DC converter. To link a standalone DC-DC structure (as designated within the figure) the use to a grid linked PV system is expanded through inclusion of extra electronic devices, together with inverter and grid units. MPPT purposes concentrate on detecting the present electrical energy of the

PV range, with this data facilitating the array energy to be added and differentiated with the current MPP value.

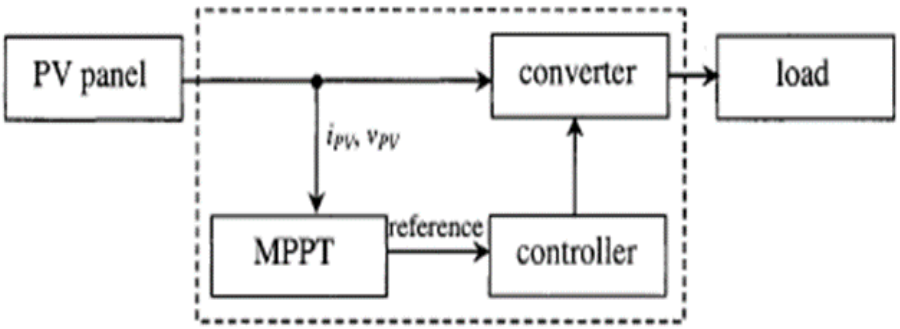

Figure 3.7: simple block of MPPT system

Similarly, the duty cycle of the converter is set using a PI or hysteresis controller to suit MPP, which in turn forces the converter to extract the highest available power from the array. However, an alternative control structure is distinguished by an automatic update of the power converter duty cycle (i.e. direct duty cycle MPPT control). It is notable that this scheme includes an elimination of PI block and duty cycle facilitated by the MPPT algorithm.

Despite PV systems containing a number of major advantages, they also have a number of specific disadvantages, i.e. high cost; limited capacity in comparison to other low and zero carbon energy sources; low conversion efficiency; and (as they generally rely on atmospheric conditions) a dependence on weather conditions [1, 10 and 21]. Consequently, MPPT is capable of only generating electric current for a short period each day, conditional on both energy from the sun and the prevailing temperature. In addition, differences in climatic setting cause PV systems to have non-linear features, while a PV unit has a position within each climatic condition at which it is capable of generating its highest output current, as well as power, i.e. MPP. It is thus necessary to regulate the PV unit to manage it at MPP [13, 21]. As established by the references, MPPT is capable of raising the generation of electric current to 25% [7, 122]. This illustrates the I-V plus P-V output features of a standard PV module at STC (1kw/m^2, 25ºC) (see Figure 3.8). The techniques of MPPT will be discussed in further detail in Chapter Five.

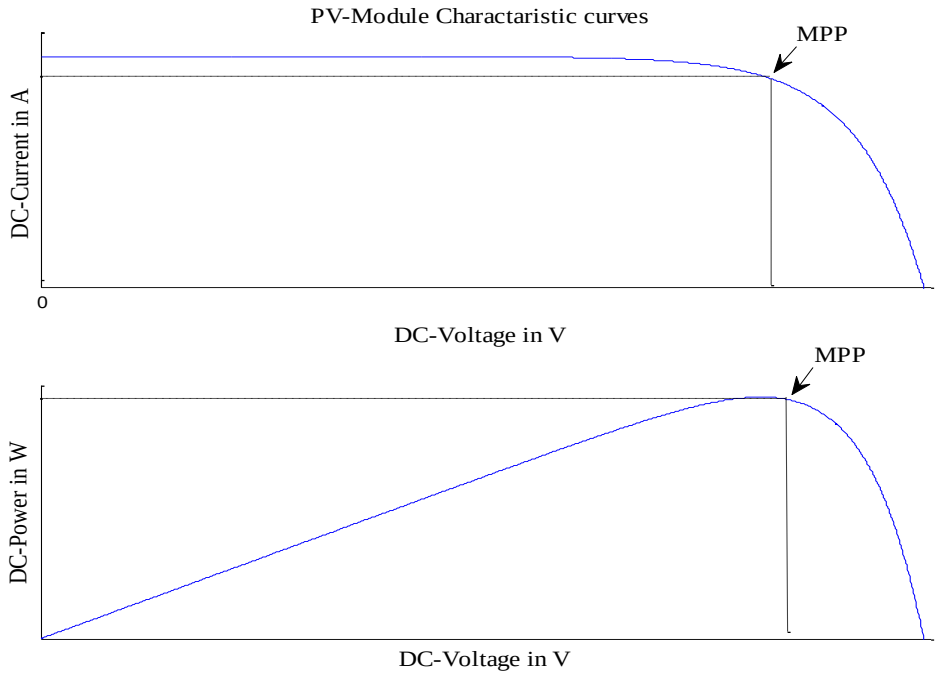

Figure 3.8: Typical (I-V) and (P-V) characteristics of PV cell

3.3.2. Problems of Maximum Power Point controller

Notably, the absolute power point tracking techniques are applicable in the extraction of maximum available power from PV systems in various environmental conditions, with various types of load. DC-DC converters are employed to suit the highest power point of PV systems with various loads. However, issues that need to be addressed in MPPT systems include: different shapes of load line; the nonlinearity between the duty cycle and the voltage ratio of most types of converters; and the wide degree of fluctuation in weather conditions.

3.3.3. The restrictions of Maximum Power Point Tracking

This section will define a number of important factors capable of affecting the performance of MPPT in the system.

3.3.3.1. Variation of photovoltaic cell materials

The majority of PV cells can be made from the following materials: single-crystalline silicon; amorphous silicon; and thin films. These can be classified in terms of their cost, performance and output characteristics [122].

3.3.3.2. Non-optimal conditions

A PV cell is unable to deliver its designated output power under a number of specific conditions. The two major situations influencing MPPT efficiency consist of: (1) partial shading and (2) low irradiance [3, 7, 122].

3.3.3.3. Partial shading

Figure 3.9 demonstrates typical generation features and I-V curve for two parallel-connected cells under different generating conditions, in particular in relation to irradiance, with PV_1 and PV_2 representing a shaded and non-shaded cell, respectively. In parallel connections, the point of intersection of the vertical functioning channels Oa-c provides the functioning point of each single cell, i.e. uniform cell voltage, as well as the I-V curves of each single cell. In the PV system, the increase in production rises from zero to the optimum current. The functional point of each single cell changes as illustrated in Figure 3.9(b), Oa1 → Ob1→ Oc1 for PV_1 and Oa2 → Ob2→ Oc2 for PV_2 in PV. The functional features demonstrated in the figure reveal that both shaded and non-shaded cells can function effectively in a region in which each single cell is able to produce power.

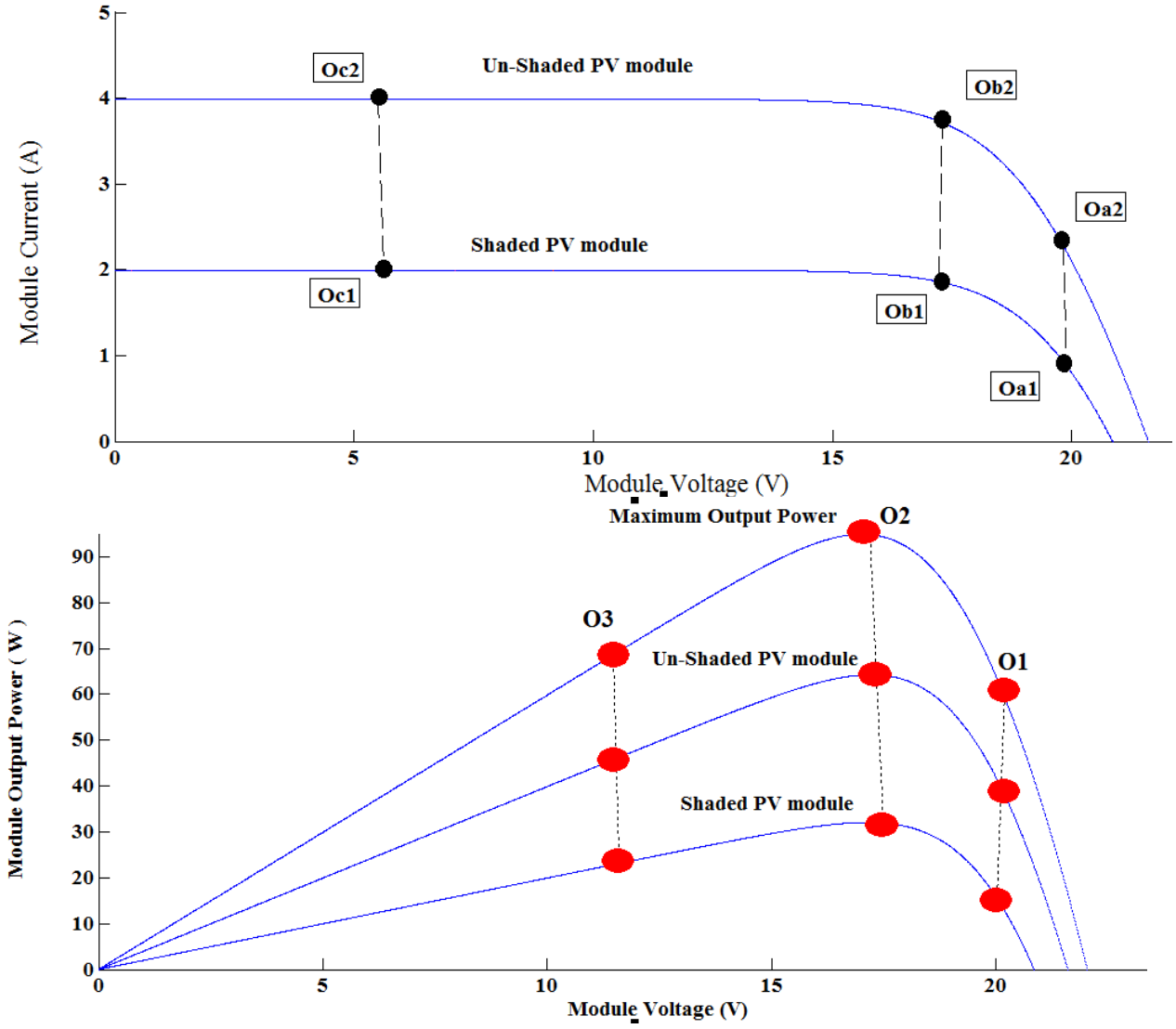

Figure 3.9: Typical generation I-V and P-V characteristics of two parallel-connected cells

Figure 3.9 demonstrates the way in which the total production of the P-V features of these cells is achieved, as illustrated in b. At this point, the total power produced is illustrated by equation 3.1, where there is power production on PV_1 is P_{1out}, and the production power on PV_2 is P_{2out}.

$$P_{total} = P_{1out}t + P_{2out}t \quad (3.1)$$

The functioning of each single cell in the series connection is granted by the point of intersection of the horizontal function line, such as the I-V characteristic of the cell, and uniform cell current. The increase in the production of the current system from zero to optimum causes the functional point of each single cell to move, as illustrated in Figure 3.10 (a), $O_{a1} \rightarrow O_{b1} \rightarrow O_{c1}$ for PV_1 and $O_{a2} \rightarrow O_{b2} \rightarrow O_{c2}$ for PV_2. Thus, a maximum production of

power is achieved on the operation line Sb (i.e. the shaded cell). However, none of the shaded cells (in this case PV_2) produce their maximum power at that time. Hence, the move of the function line to O_c makes the function point of every single cell PV_1 and PV_2 to move to O_{c1} and O_{c2}, in that order, as the production of power on PV_2 increases.

The non-shaded cell (PV_2) forces the shaded cell (PV_1) to release an additional current to the new short circuit current. The shaded cell functions well in a reverse bias position, resulting in a net voltage reduction to the system. Notably, it is considered as a point of breakthrough in the pn-junction, where there is the application of the electric field that overcomes the intrinsic electric field. This is commonly referred to as the avalanche effect. The end results of the negative voltage and the current (i.e. avalanche voltage) provide the power dissipated by the shaded cell. To be precise, the shaded cell dissipates power heat causing hot spots [9]. At this point, the non-shaded cell (PV_2) produces power, i.e. P_{2out}. On the other hand, the shaded cell (PV_1) results in power reduction, i.e. P_{1loss}. Therefore, the output power which is P_{out} on the system is decreased to the following equation:

$$P_{total} = P_{2out} - P_{1loss} \tag{3.2}$$

The total power production features of this system demonstrate the reason why the P-V curve is arrived at in a similar manner. A clear illustration of this is found in Figure 3.9 (b). The two highest points of power in the figure are relatively small in comparison to those in the parallel-connected condition illustrated in Figure 3.10 (b). Only two-cell connections are explained here. However, the mechanism for power reduction occurs for a number of series-connected cells similar to that of the two-cell connection.

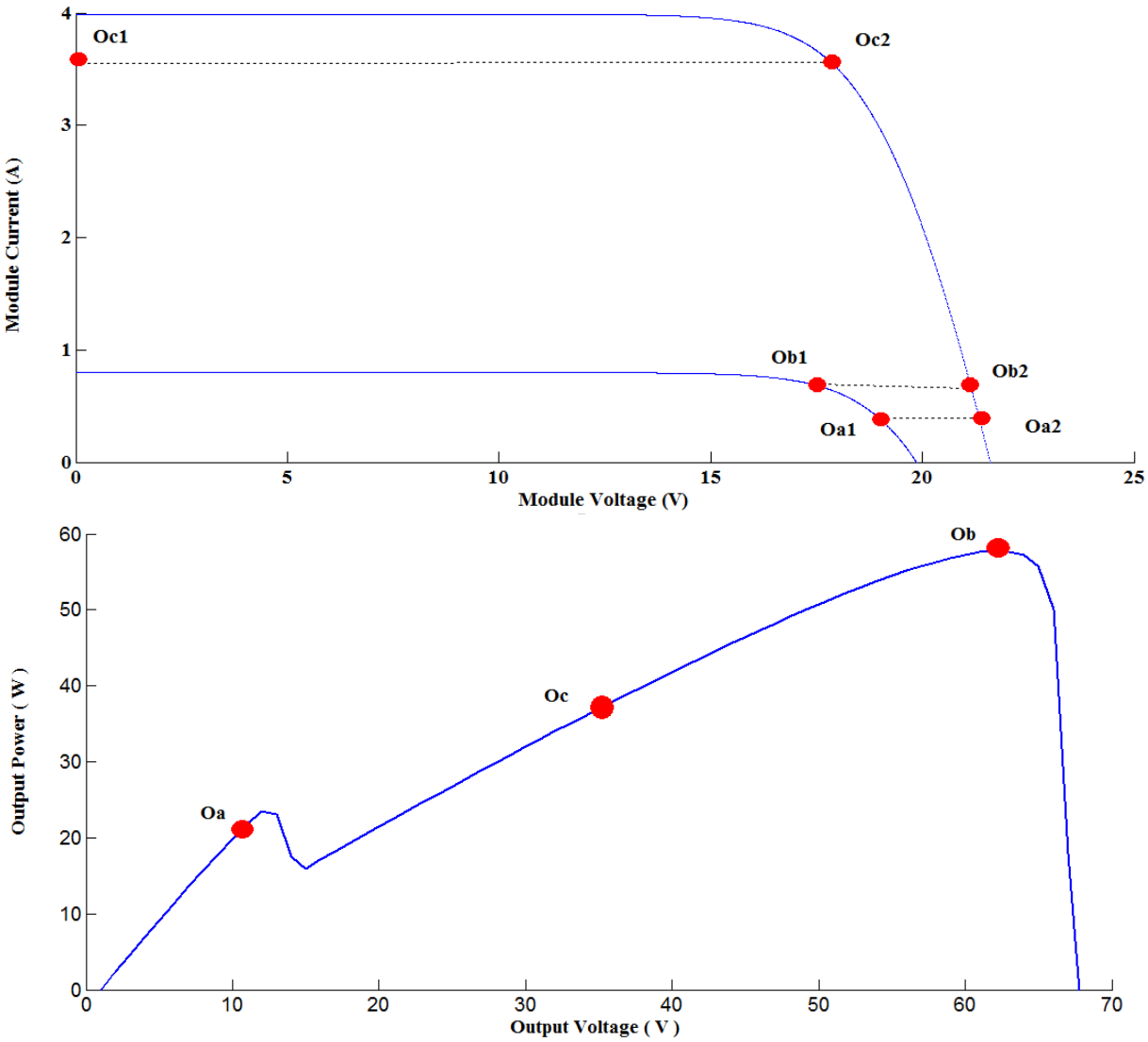

Figure 3.10: Typical generation I-V and P-V characteristics of two series-connected cells

The solar cells are primarily connected together to create strings capable of producing a desirable voltage. As such, the voltage is the total voltage of the device, and the current of the string is limited to the current of the least productive device of the string.

When configuring the PV cell or module in a series connection, and during the recurring issue of partial shading, the cell or module will operate as a load. The system generates more photon current than the shaded cell/module (reversed biased), resulting in raising the cell/module temperature (known as hot spots), which are capable of damaging the module and effecting the whole system. Hot spots can also occur in a parallel configuration if the PV module is shaded, leading to it to consume (rather than produce) power, thus raising its temperature and potentially resulting in damage to the module, should its temperature become too high. The use of a bypass diode has recently become the most popular technique used to protect the PV cell/module from the hot spot when connecting the PV cell/module in series.

This can be placed in the PV string or across the modules, while blocking diodes are usually preferred to be in a series configuration with the module, in order to avoid the issue of hot spots when connecting the PV modules in parallel, as shown in Figure 3.11, below.

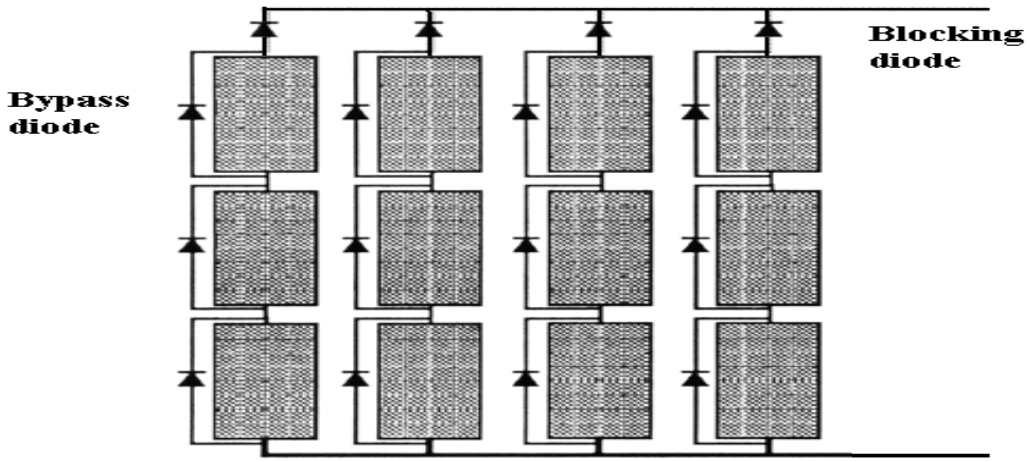

Figure 3.11: The PV cell/modules with by-pass and blocking diodes [91]

Ref [91] reports an experiment to establish the effect of partial shading on the PV system, in which four identical PV modules MSX60 in series configuration were used. When one of the PV modules was shaded, its irradiance was 750 W/m^2, while the others were 1000 W/m^2

. In this case, the shaded PV module reduced the maximum output power of the system from 244 W to 204 W, i.e. approximately 83.6% of the maximum output power of the system under normal conditions [122-127]. According to Ref [92], under PSCs, the efficiency of MPPT controllers is reduced. The assumption made by the majority of MPPT controllers is that there is only one point on the P-V characteristic at which the PV module can produce its maximum power. However, when the PSC occurs, the module will have several MPPs, affecting the performance of the controller, resulting in a reduction in the whole output power of the system. Therefore, removing the shaded PV module from the system could prove the preferable method of preventing the system from low conversion efficiency [92-94]. This condition and its effect on the controller will be addressed in detail in Chapter Six.

3.3.3.4. Low solar radiation

The issue of low radiance can impact on the MPPT controller. It has been highlighted out that a number of MPPT methods (e.g. the perturbation and observation method) have low efficiency at low solar radiation. Hence, it is important to improve a suitable MPPT algorithm, whose performance cannot be affected by conditions of low solar radiation [46, 127].

3.3.3.5. The effect of load on PV panels curves' operating point

The load is considered to have no effect on I-V features, however, it can affect the functioning point on the I-V curves. The direct load coupling to the PV panel results in a mismatch between the solar generator's optimum, and the actual functioning, voltage, which reduces the generated power from the PV panels. The functioning voltage, along with the functioning current on I-V curves points, relies on the load. The intersection taking place on the different load line and I-V curves under different climatic conditions identify the functioning point on I-V curves, as illustrated in Figure 3.12 for resistive and battery loads. Any change in climate conditions modifies the I-V curve, causing changes in the function voltage and current supply in the PV system. More frequently (as illustrated in Figure 3.12), the point of intersection is not the P_{max}, and therefore the load type influences the range identifying the functioning point in IV curves.

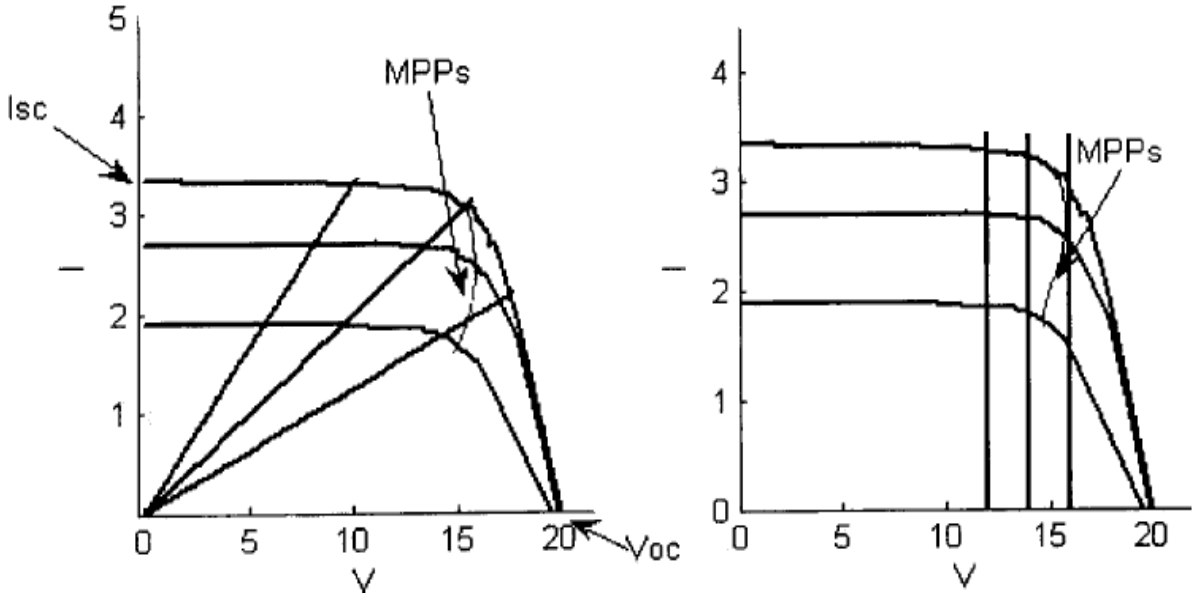

Figure 3.12: Different load line and I-V curves under different climatic conditions

The PV system supplies two major types of load, (1) resistive loads consist of the DC pumps and battery loads, and form examples of the CV load, and (2) the battery forms the widely known load in the standalone PV system. As demonstrated in Figure 3.12, the type of load has an impact on the range of function points of I-V curves. In general, a battery load has a CV that differs narrowly. However, as illustrated in Figure 3.12, the resistant load pushes the PV panel to function at a very wide interval on I-V curves. The resistive load voltage linearly relies on the current produced by the PV panels. The sudden increase (or reduction) of the irradiance level during conditions of partial cloud causes a wide range of variance in the production of voltage. This leads to the existence of a high number of approximately 15V

in every 36 cell PV panels. It appears that the battery voltage relies on the PV current, due to the low internal resistance from the batteries, while there is also a slight change of 1V to 12V during the charging period. The divergences seen in the functioning voltage, as a result of variance in load types, has an effect on the required changes of the duty cycle DC-DC switch converter.

3.3.3.6. DC-DC converter switching-mode

The most important components in the PV system are the DC/DC converter and DC-AC inverter, while their switching-mode generally has nonlinear characteristics variable over time. Therefore, the switching mood converter needs to be closely controlled through the use of appropriate techniques. Furthermore, MP can be extracted from the PV system if the DC-DC converter is well designed and its switching mood is correctly controlled. In addition, the DC-DC converter needs to draw low ripple current from the system, causing conversion loss and reducing the maximum power tracking efficiency. This can be reduced by using high switching frequency [46,122,126].

As a result of the recent improvements in electronic devices, PV systems are now able to generate a large amount of energy. DC-DC converters tend to be of several kinds, categorised into two groups: (1) the isolated (i.e. generally utilised in a grid-linked system) and (2) the non-isolated (i.e. suitable for detached systems requiring equal (or less) power PV module production energy. They may also be formed into three groups: (1) buck/step-down; (2) boost/step-up; and (3) buck-boost converters [10, 18]. The DC-DC converter method is significant within MPPT, since MPP may be attained if the converter's button mode is correctly regulated. Thus, the major concern within PV is the creation of an effective regulator for the DC-DC converter. Further information, and an inclusive examination of the topologies of the four fundamental non-isolated converters (i.e. buck, boost, buck-boost, and Cúk) will be take place in Chapter 4).

3.4. Photovoltaic source model

It is important when building a PV system to understand its behaviour and ensure system stability, in order to specify its size and its location, as installing the module in a perfect location with widespread sunlight can extract the system's maximum possible power. One of the most common (and unavoidable) issues with a PV system consists of partial shading, which has a considerable influence on the output power of the PV module. In general, PSCs at a low latitude are less acute than at higher latitudes, as, in the latter, the sun is at a

considerable distance on the horizon. Therefore, during installation, the location of a PV system needs to be taken into account, including its direction and installation rise angle. According to [46], a considerable reduction in PV module output power will result in a small shading of the module. Therefore, operating the module in a case of PSC needs to be investigated in order to improve MPPT performance, and extract the maximum power the PV module is capable of generating.

The most important issue when designing a PV system is understanding PV module behaviour, including accurately determining its characteristics. Therefore, modelling a PV module becomes a significant issue when modelling a MPPT module, and requires considerable knowledge of the characteristics of a PV module, along with its performance under different circumstances, e.g. low solar radiation, temperature, and PSCs. This is necessary to ensure improvements in the design, and to simulate the behaviour of the MPPT system. This chapter will therefore: firstly, define the modelling of a PV module, employing a simple equivalent circuit, and secondly, the more accurate module will be used to simulate MPPT algorithms. The simulation result will demonstrate the suitability of the proposed model for the design and analysis of the MPPT system.

3.5. The terminal characteristic of photovoltaic cells

3.5.1. The simple model

Figure 3.13 symbolises the most straightforward corresponding path of a solar battery with two characteristics: (1) a diode and (2) a separate photon power supply. This produces DC energy when rays from the sun shine on the cell, and can be steady in a continuous climatic condition [4]- [12].

The I-V characteristic is generally calculated by computing the following two factors: A) the short-circuit current, which is obtained by shorting the terminals of the PV cell (i.e. setting V=0, hence this gives I_{ph} = *Isc*); and B) the open circuit voltage (Voc). The values of these factors are generally provided by the manufactory datasheet [4, 25].

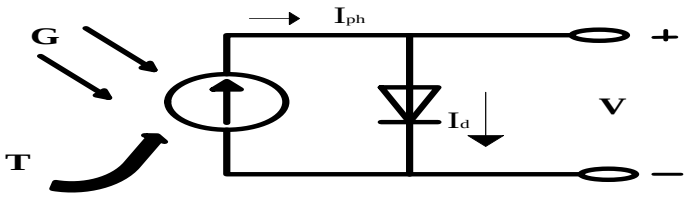

Figure 3.13: Simple circuit of PV cell [10].

The output current of the cell on the circuit presented in Figure 3.13 can be calculated using Kirchhoff's current law (KCL);

$$I = I_{sc} - I_d \quad (3.3)$$

Where:

I_{sc} is the cell short-circuit current, and

I_d is the diode current.

Shockley's diode equation can be used in order to establish the value of I_d;

$$I_d = I_0 \left(e^{(qV_{d/KT_c})} - 1\right) \quad (3.4)$$

Where:

I_0 is the cell saturation current (A),

Q is the electronic charge = 1.6×10−19C,

V_d is the diode voltage (V),

K is the Boltzmann's constant = 1.38×10−23 J / K, and

T is the junction temperature, Kelvin (K).

By substituting I_d of equation (3.3) with equation (3.4) the voltage and current characteristics of PV cells can be described as;

$$I = I_{Sc} - I_0 \left(e^{(qV_{q/KT_c})} - 1\right) \quad (3.5)$$

Where:

V and I are the PV cell terminal output voltage (V) and current (A) respectively.

3.5.2. The more accurate model

Nevertheless, the PV system outlined above does not provide a correct I-V characteristic of PV systems, as it disregards a number of factors that impact on its functioning [11, 23]. The system may be enhanced through the addition of a chain resistance to the current path, which symbolises PV cell wastes. However, despite this enhancement, this system is unable to form the correct model for the PV system, since it disregards the exposed circuit power coefficient

[15]. A number of scholars [10, 14, 25] recommend the addition of additional resistance separately to the single diode model, as illustrated in Figure 3.14 (shunt-resistance, Rp). This addition raises the number of factors to five; then again through applying this archetype, the PV feature precision may be enhanced [10-16].

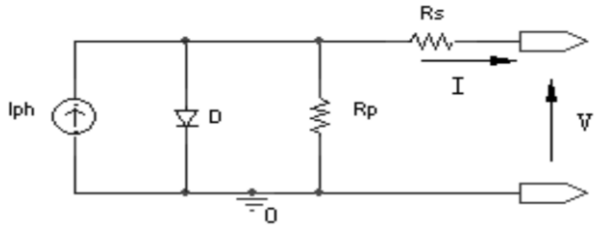

Figure 3.14: Single-diode circuit of PV cell [11, 12].

However, the recombination losses are ignored in a single diode module, which is not the case in a real solar cell, where these represent considerable losses. As a result, an additional enhancement is attained through the addition of a separate diode to form a two-diode model [13]. Nonetheless, this raises the PV units' factors to seven, while the principal objective when creating the PV system is to maintain a rational calculation attempt if calculating the figures of every factor [15]. (Figure 3.15 illustrates the corresponding circuit known as a two-diode model).[11-14].

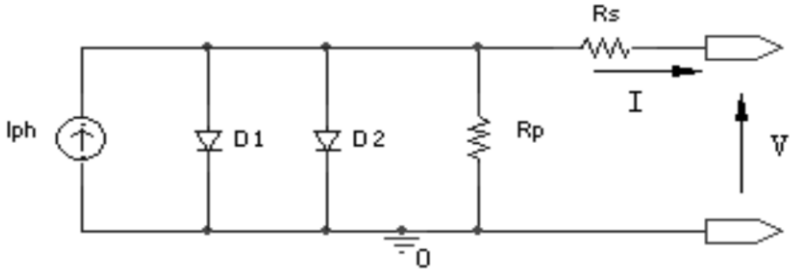

Figure 3.15: The equivalent circuit of two-diode model [11].

The output voltage and current characteristic equation are given as:

$$I = I_{Sc} - I_{01}\left(e^{(qV_{q/KT_C})} - 1\right) - I_{Sc} - I_{02}\left(e^{(V+I.R_S/KT_C)} - 1\right) - \left(V + I.\frac{Rs}{Rp}\right) \qquad (3.6)$$

The techniques recommended by D'Souza et al. [12] are the most accurate methods for computing the values for R_s and R_p, and, despite accuracy declining at low radiation, it has a lower computation effort. In the two-diode model (in which PV module parameters increase to seven), a number of authors estimate the PV parameters by using the Thevenin equivalent

circuit, calculated as a function of its series resistance [25]. Nevertheless, further factors need to be introduced to these calculations. Moreover, it is difficult to approximate the initial value of the PV factors [126]. In addition, the majority of the above methods award an estimated value of $a_1 = 1$ and $a_2 = 2$ to the ideality factor. However, even when this estimation is used, it is not always accurate [17,18].

Although, owing to its precision, the two-diode model is the favoured method, it requires a far higher re-assemblage struggle in contrast to the single diode unit [12, 25 and 126]. This struggle renders the single diode unit a highly appealing system, considering the required enhancements [45,126].

Consequently, by merging the two models (D1, D2) Equation 3.6 can be simplified as follows:

$$I = I_{Sc} - I_{01}\left(e^{(V+I.R_{s/AKT_C})} - 1\right) - \left(V + I.\frac{Rs}{Rp}\right) \qquad (3.7)$$

Where:

A is the p-n junction ideality factor, which commonly takes a value between 1 and 2 [11] and [12].

The selected PV module is MSX-60 module, and is able to generate an output power of 60 watt, with its electrical specifications shown in Table 3-1.

A number of elements are capable of influencing the performance of the PV cell, including: (1) the ambient temperature; (2) solar radiation; (3) the series resistance (R_s) of the cell; (4) shunt resistance (R_p); and (5) the ideality factor (A). A number of authors have analysed the effects of these elements, as outlined below.

Table 3.1: The PV module electrical specification

Maximum power (*Pmax*)	60 W
Voltage @ *Pmax* (*Vmp*)	17.1 V
Current @ *Pmax* (*Imp*)	3.5 A
Open-circuit voltage (*Voc*)	21.1 V
Short-circuit current (*Isc*)	3.8 A
Temperature coefficient of *Short-circuit current (Isc)*	.(0.065±0.015)%/°C
Temperature coefficient of *Open-circuit voltage (Voc)*	–(80±10)mV/°C

Temperature coefficient of power	–(0.5±0.05)%/°C

3.5.3. The effect of the environment on PV characteristics

The major factors influencing the functioning of the PV systems consist of irradiance level, wind speed, and the ambient temperature. I_{sc}, Vmax, V_{oc}, and the max are the commonly known factors assisting in the specification of the I-V curves of the PV panels systems. I-V curve features and the cell junction temperature of PV panels are able to function well in response to climate change conditions. The illustration below demonstrates the ways in which PV output features, and the cell-junction temperature, changes because of climatic conditions. At the same time, this section also discusses the impact of cell junction temperature on electrical features of PV curves panels.

3.5.3.1. The environmental effect on the cell temperature

The calculated temperature of PV cells relies largely on the ambient and irradiance temperature, as illustrated in the following linear relationship.

$$Ts = Ta + C*G \quad (3.8)$$

T_S Cell temperature in °C

T_a Ambient temperature in °C

G Irradiance level (mW/cm2)

In this case, the value of C (which is constant) lies between 0.32°C/ (mW/cm2 and 0.27 for commercial modules. The assumption overlooks the effect caused by wind velocity (the Ts.) This neglect of the wind effect on the PV panel causes the constant increase in the PV temperature with irradiation of the solar cell. Therefore, the wind reduces the surface temperature of the solar cell, which eventually reduces the cell junction temperature [129].

3.5.3.2. The cell junction effect on the Maximum Power Point

The ambient temperature increases the temperature of the PV solar cells at the PV junction. As such, the junction cell temperature is the commonly known factor acting to decrease the optimum power production of the PV panel. Figure 3.16 illustrates the ways in which the power curves and the I-V curves adjust with the temperature of the PV cell from the cell junction temperature. Figure 3.16 illustrates the I-V curves, including the ways in which the

maximum power produced from the PV panel is reduced as a result in the rise in the cell temperature. This increase is facilitated by the irradiance being in constant motion [128, 129].

In addition, Figure 3.16 illustrates the ways in which Vmax reduces in line with the cell junction temperature. In this case (as illustrated in Equation 3), the cell junction rises due to solar irradiance and the ambient temperature. Thus, the rise in the cell junction temperature decreases the Voc, as illustrated in Figure 3.16.

The ambient temperature effect: any change in temperature has a strong effect on the output voltage and slightly affects the short circuit current.

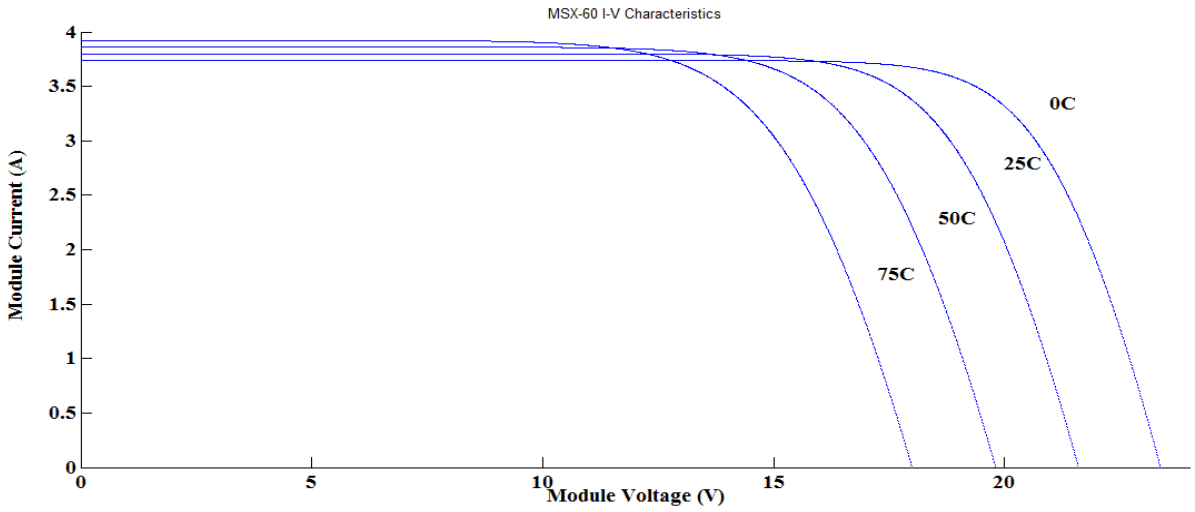

Figure 3.16: The I-V characteristics of MSX-60 module under different temperature values and constant radiation ($1kw/m^2$)

3.5.3.3. The irradiance effect on photovoltaic characteristics

It is believed that in the PV panel system the output power and irradiance level are directly proportional. Figure 3.17 illustrates the ways in which the I-V curves change with the irradiance. The figure also illustrates the way maximum power rises alongside the irradiance level when the cell temperatures are at a constant point [128-131]. The changes in the irradiance level demonstrate the existence of differences in current and voltage, in particular MPP. Therefore, any rise in solar radiation results in an increase in the optimum power voltage. The following three issues are experienced during the establishment of the relationship between cell junction temperature, irradiance and Voc level: firstly, nonlinear links exist between open circuit voltage and irradiance; secondly, the effects are associated with the irradiance level on cell junction temperature and ambient temperature [52]; finally,

difficulties are encountered during the measurement of the impact of wind on cell junction temperature as a Voc result.

Figure 3.17 demonstrates the effect of radiation on the I-V–P characteristic. If solar radiation increases, the short current will increase proportionally, while its effect is slightly less on the output voltage. Therefore, output power will increase as the output current increases, and reduce when it declines. The output power is defined by P=V×I

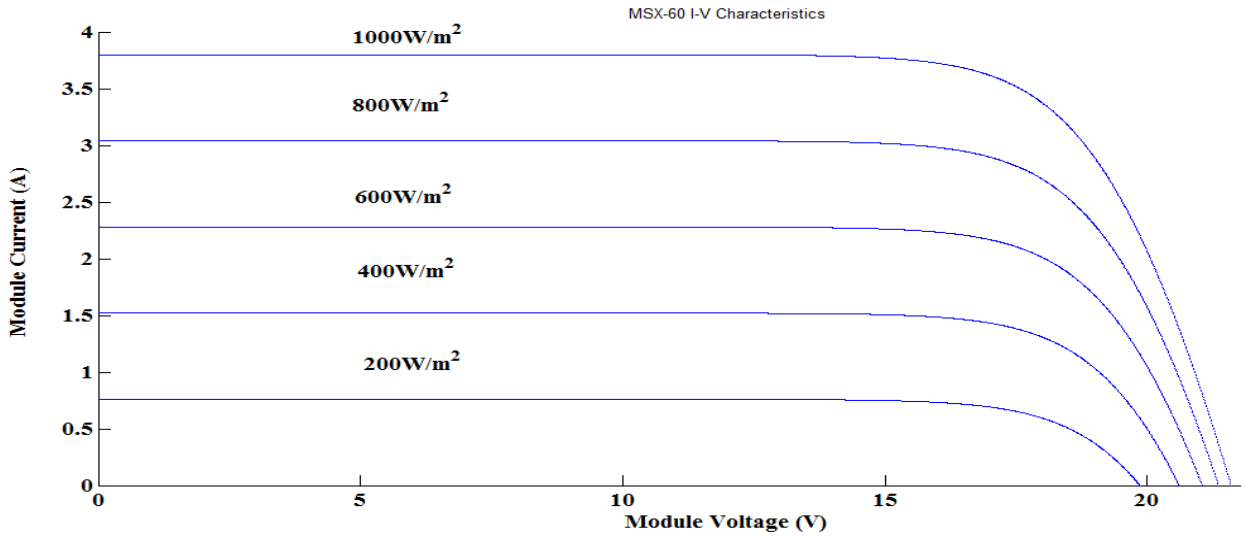

Figure 3.17: The I-V characteristics of MSX-60 module different irradiance values and a constant temperature (25°C).

3.5.3.4. The effect of series resistance

The series resistance (R_s) has (as demonstrated in Figure 3.18) a strong effect on PV module curves. If the value of R_s increases, the output power will decrease, as it reduces the output current.

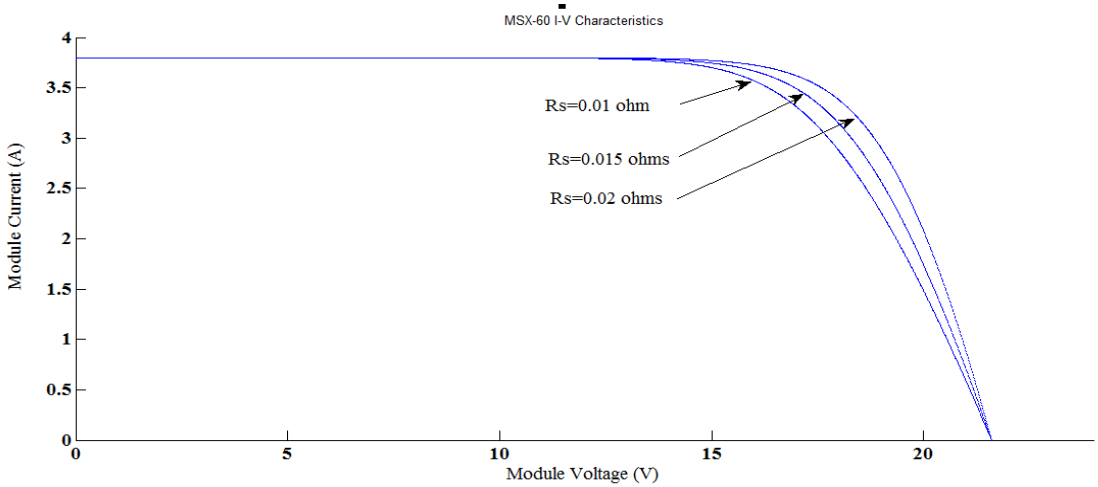

Figure 3.18: Effect of series resistances at 1kw/m2, 25°C

3.5.3.5. The effect of parallel resistance

Figure 3.19 demonstrates the effect of R_p on PV output characteristics. It can be seen that, when the value of R_p is decreased, the open circuit voltage is also reduced, without any impact observed on the I_{SC}.

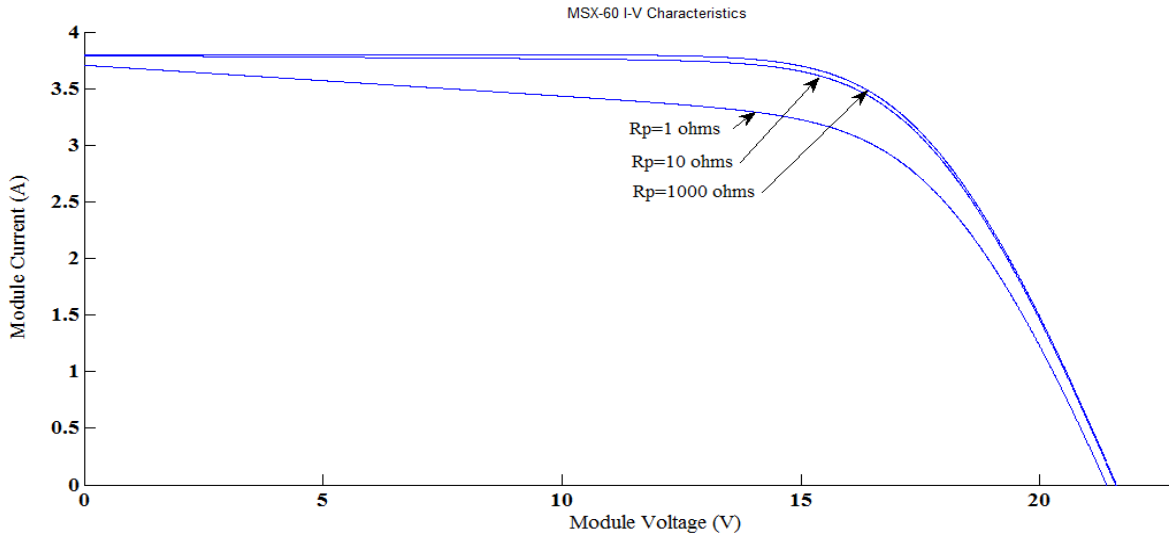

Figure 3.19: Effect of parallel resistances at 1kw/m^2, 25°C

3.5.3.6. The effect of diode ideality factors

As stated previously, the ideality factor has an estimated value ranging between one and two. Figure 3.20 highlights the influence of any change to its value.

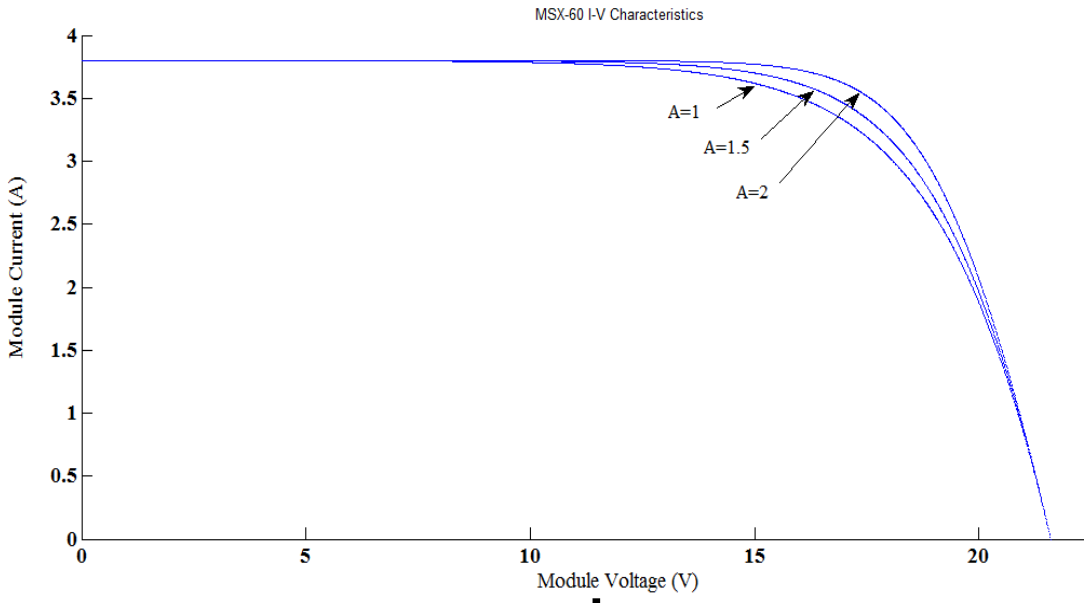

Figure 3.20: Effect of changing the ideality factors at 1kw/m^2, 25°C

3.6. Solar cell modelling

As noted in Section 3.6.2, the R_p model has proved more accurate than the R_s model, and therefore the R_p module will be used throughout this study. Figure 3.21 (below) represents the equivalent circuit of the module containing five components: a current source (*Iph*), a diode (*D*), a series resistance (R_s), and a parallel resistance (R_p).

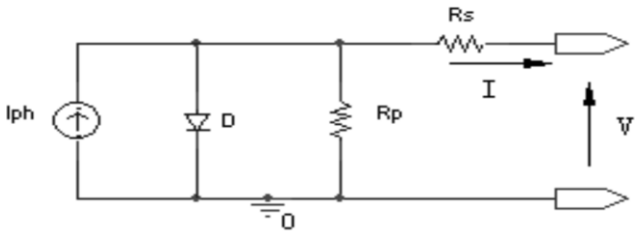

Figure 3.21: Single diode PV cell model with Rs and Rp.[146].

The one-diode model with series and parallel resistances of PV cell is shown in Figure 3.21 (above), and its corresponding current - voltage (I-V) characteristics equation can be expressed as follows:

$$I = \mathrm{Iph} - \mathrm{Io}\left\{\left[\exp\left(\frac{\mathrm{q(V + IRs}}{AKT}\right) - 1\right\} - \frac{\mathrm{V + IRs}}{Rp}\right. \quad (3.9)$$

Firstly, for a more accurate characteristic, the value of the short-circuit current (*Isc*) must be calculated at a given cell temperature (*T*), and solar radiation (G), as follows:

$$I_{Sc}\big|_{Tc} = I_{Sc}\big|_{T_{ref}}\left[1 + a(T_c - T_{cref})\right] \quad (3.10)$$

Where

Isc at *Tref is* provided by the cell manufacture datasheet at STC,

Tref is the PV cell reference temperature in *Kelvin* (*K) and its equal to* 298*K* (25*oC*),

a is the short circuit current *Isc* temperature coefficient provided by the cell manufacture datasheet at STC.

As the solar radiation has an influence on the short circuit current of the PV cell, its value at a given solar radiation (G) can be represented as:

$$I_{Sc}\big|_G = I_{Sc}\big|_{G_o}\left[\frac{G}{G_o}\right] \quad (3.11)$$

Where

($Isc\big|_{Go}$) is provided by the cell manufacture datasheet at STC,

(G_o) is the value of solar radiation at STC, which is generally 1000W/m^2.

In general, the characteristic of a PV cell has three main operating points, these being: (1) the short circuit current I_{sc}; the open circuit voltage V_{oc} (where V = V_{oc} and the PV cell current equal to zero (I=0)); and MPP. The saturation current (I_o) value can be calculated at the open circuit voltage, where V_{oc} =V and the PV cell current is equal to zero as:

$$0 = \text{Isc} - \text{Io}\left\{\left[\exp\left(\frac{\text{q(Voc}}{AKT}\right) - 1\right\} - \frac{\text{Voc}}{Rp} \quad (3.12)$$

Equation 2.4 can be rewritten as:

$$Io = \text{Isc} - \left(\frac{\text{Voc}}{Rp}\right)\exp\left(-\frac{\text{Voc}}{AVt}\right) \quad (3.13)$$

The reverse saturation current (I_o) is primarily dependent on the PV cell temperature. Therefore, its value can be obtained as follows:

$$I_o\big|_{Tc} = I_o\Big|_{Tc_{ref}}\left(\frac{T_c}{T_{cref}}\right)^{\frac{3}{A}}.e^{\left[\frac{-qE_g}{AK}\left(\frac{1}{T_c}-\frac{1}{T_{cref}}\right)\right]} \quad (3.14)$$

When the open circuit voltage is equal to zero at the short circuit current, where I= I_{sc} equation (3.4) can be rewritten as:

$$Isc = \text{Iph} - \text{Io}\left\{\exp\left[\frac{\text{qIscRs}}{AKT}\right] - 1\right\} - \frac{\text{IscRs}}{Rp} \quad (3.15)$$

At MPP at which the PV module output voltage V= V_{mp} and its current I=Imp equation (3.15) can be rewritten as:

$$Imp = \mathrm{Iph} - \mathrm{Io}\left\{\left[\exp\left(\frac{\mathrm{q(Vmp + ImpRs}}{AKT}\right) - 1\right\} - \frac{\mathrm{Vmp + IRs}}{Rp}\right. \quad (3.16)$$

And the PV output power can be expert as:

$$P = \mathrm{I} \times V \quad (3.1)$$

The ideality factor of a diode is unknown and can be calculated by using the following equation, or by estimation as it takes a value between one [7.19]:

$$A = \frac{\mathrm{Vmp + ImpRs - Voc}}{Vt\left\{Ln\left(Isc - \frac{\mathrm{Vmp}}{Rp} - Imp\right) - In\left(Isc\frac{\mathrm{Voc}}{Rs}\right) + \frac{\mathrm{Imp}}{Isc - \left(\frac{Voc}{Rs}\right)}\right\}} \quad (3.2)$$

A number of authors have suggested the value for the ideality factor of a diode to be generally between one and two, calculated by using trial and error until the accurate PV curve is obtained [7, 19, 126].

The value of R_s, the series resistance of the PV cell, has a considerable influence on the slope of the I-V characteristic, as discussed in Section 3.5. Its value can therefore be calculated by evaluating the I-V slope dI/dV at the open circuit voltage, and its value can be identified by differentiating equation 3.12 and rearranging it in terms of R_s, as follows:

$$dI = 0 - I_o q\left(\frac{dV + dIR_s}{AKT}\right).e^{q\left(\frac{V+IR_s}{AKT}\right)} \quad (3.3)$$

And at the open circuit voltage:

$$R_s = -\frac{dV}{dI}\Big|_{Voc} - \frac{AKT/q}{I_o.e^{q\left(\frac{V_{oc}}{AKT}\right)}} \quad (3.20)$$

Where

$\frac{dV}{dI}\Big|_{Voc}$ The I-V characteristic slope at the open circuit voltage (V_{oc}), and its value can be determined from the PV cell manufactory datasheet.

The value of parallel resistance R_p can be determined by evaluating the PV cell I-V curve, with its equation derived by differentiating equation 2.6 and rearranging it in terms of R_p as:

$$Rp = \frac{1}{\left(\left|\frac{dV}{dI}\right|_{Isc} + Rs \right) + \frac{1}{q\frac{Io}{AKT}\exp\left(q\,Isc\frac{Rs}{AKT}\right)}} \tag{3.21}$$

Finally, equation 3.4 can be solved using a numerical solution starting with the initial value employing algorithms used for solving a nonlinear equation. The Newton Raphson method has been chosen for this current study, for rapid convergence for solving equation 3.21. This method can described as:

$$x_{n+1} = x_n - \frac{f(x_n)}{f'(x_n)} \tag{3.22}$$

Therefore, the PV module output current can be computed iteratively as:

$$In + 1 = \mathrm{In} - \frac{\mathrm{Iph} - \mathrm{In} - \mathrm{Io}\left\{\exp\left[\frac{\mathrm{q(V + IRs)}}{\mathrm{KAT}}\right] - 1\right\} - \mathrm{V} + \mathrm{IRs/Rp}}{-1 \_ Io(\frac{qRs}{AKT})\{\exp\left[\frac{q(V + IRs)}{AKT}\right] - \frac{Rs}{Rp}} \tag{3.23}$$

The MATLAB function written in this thesis has been iteratively performed three times to obtain the accurate converge result.

Figure 3.22 demonstrates the PV cell Simulink module created to signify the output features of the PV unit. It possesses two changeable inputs, i.e. the solar radiation G and the temperature Tac. Furthermore, it utilises the production power as a reaction input that is utilised to push the PV component production current for obtaining a precise I-V curvature resulting from the current sun energy, as well as temperature. The parameters' figures for the chosen PV model are represented in Table 3.1:

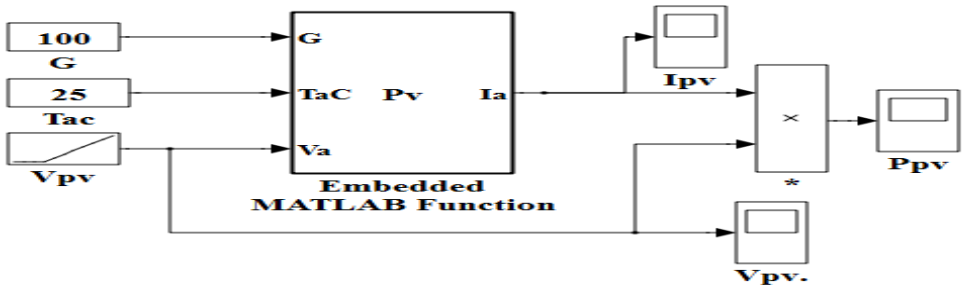

Figure 3.22: the PV cell model

Considering STC, the I-V and P-V characteristics of a selected PV module are shown in figures 3.23 and 3.24 (below), simulated with the Matlab model. The simulated results reveal

effective matching between the simulated P-V and I-V curves, with the data provided by the PV module manufacture.

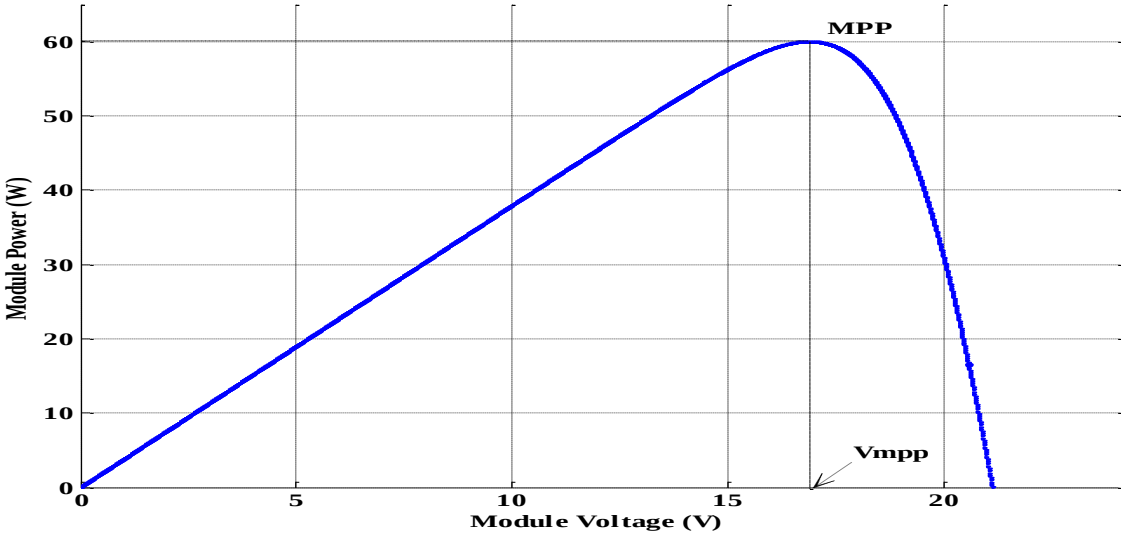

Figure 3.23: simulated P-V curves of a selected PV panel

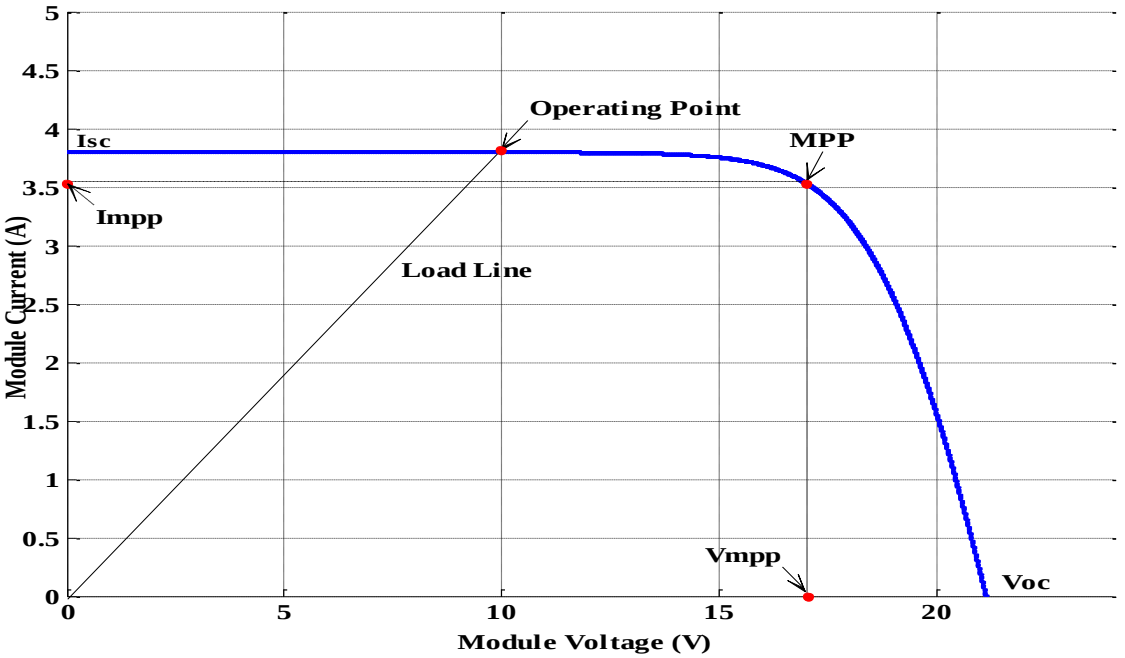

Figure 3.24: The I-V curves of a selected PV panel

As it can see from fig (3. 24), the operating point of the module is mainly depending on its characteristic and the load impedance. At the open circuit voltage when there is no load, the operating point of the PV module will be on the right side of MPP when V=Voc and the PV module output current is equal to zero (I=0), and this is an initial operating point, if the load increases, the operating point of the module will increase as well resulting in reducing the

open circuit voltage while its output power increases till it reaches the MPP, where can extract maximum power from the module. Any increase of the load beyond this point will move to the right side of MPP resulting in a reduction in the output power as the PV output voltage decreases, till it reaches the point where(I= Isc) and module output voltage at this point is equal to zero (V=0).

3.6.1. Validation of the PV module characteristics

As outlined in section 3.6, the PV cell/module parameters vary according to weather conditions, with temperature and solar radiation being the most important factors in its output current and voltage.

Figure 3.25 demonstrates the (current I- voltage V) characteristics of the selected PV module for a number of different environment conditions, temperature and irradiance, employing the equations established above (in conjunction with the electrical specifications of the selected PV module given in in Table (3.1), as simulated in Matlab using an m-file function (see Appendix (A.1)).

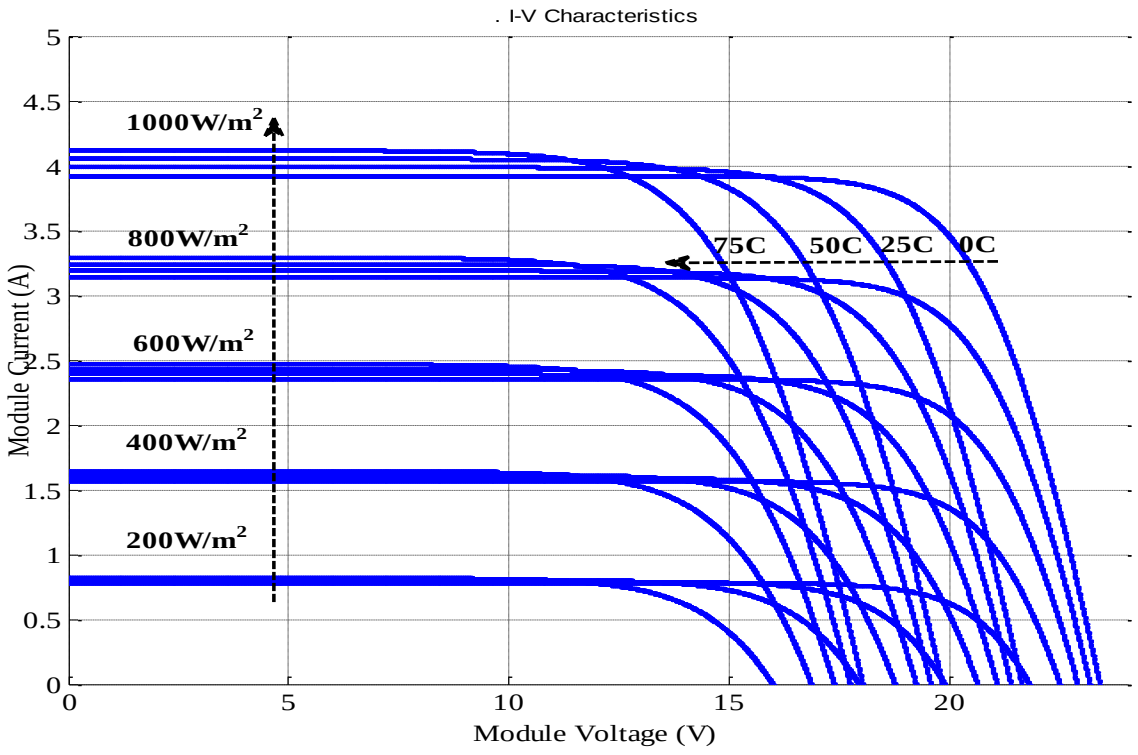

Figure 3.25. The simulated I-V curves under different irradiance and temperatures.

3.6.2. The photovoltaic module source under non-uniform weather conditions

PV cells are generally connected in parallel, or in a series configuration, to meet the load demand energy. When PV cells are connected in a parallel connection, its output voltage is identical to that of the single solar cell, while the generated current is the total of each cell current. On the other hand, when solar cells connect in a series connection, its output current will be the same as that of a single solar cell, while the output voltage will be the sum of the voltage in each cell. This is demonstrated in This is demonstrated in Figure 3.26 (below).

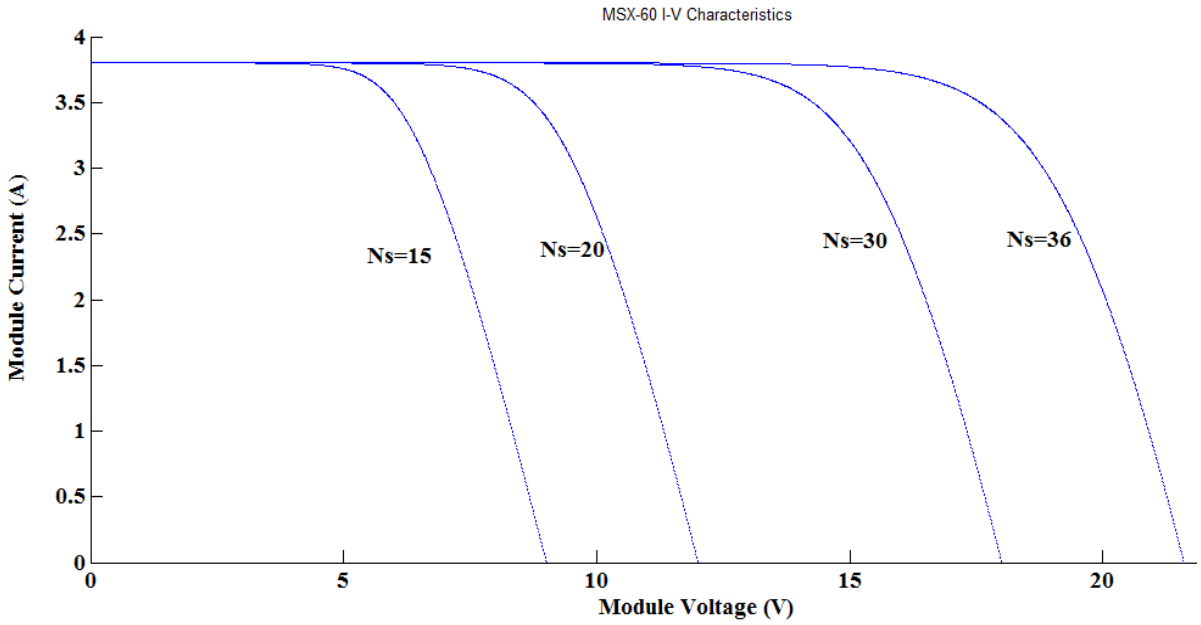

Figure 3.26: The PV cells series configuration to make up a PV module

The solar cells in a practical system are connected in series, or in a parallel configuration, to form the modules/arrays to generate the desired value of the voltage. However, the PV module output voltage is determined by the generate output current, which (due to it being directly proportional to the irradiance) primarily depends on solar radiation conditions. Therefore, in an application such as multiple PV modules working at different irradiance conditions, an opportunity will arise to have a number of different maximum output power points, instead of one MPP. This can result in a substantial reduction of the output power of the entire system, as its controller is unable to establish the true operating point at MPP. This condition can occur as a result of PSCs [92-95].

3.7. Summary

This chapter has provided a brief description of the modelling of PV cells in Matlab, using an accurate equivalent circuit, including a number of important factors with the potential to

influence the performance of MPPT in the system. It can be inferred that this remains an inaccurate model for a PV component, notwithstanding the enhancement undertaken on the single diode model through addition of a chain resistance to the current path, which denotes the PV cell wastes. This is due to disregarding the exposed circuit energy coefficient. This has led to the Rp component being applied in this research.

Chapter Four

DC-DC Converter for PV systems

4. Introduction

Based on the theory of maximum power transfer, the transfer of MP is made from source to load at the point at which the source impedance and the load impedance are equal (i.e. load matching). It is possible to accomplish load matching by making an adjustment to the DC/DC converter's duty cycle. The ratio of the switches switching on time to the switching period is known as the duty cycle. The operation of the converter must be undertaken with its corresponding duty cycle, if the MPP is to be tracked. Extracting maximum power from the PV module at different atmospheric conditions requires the adjustment of the DC/DC converter's duty cycle. A high proportion of DC/DC conversion circuit architectures are capable of being utilised for this purpose. This section proposes a realistic examination of the four essential non-isolated DC-DC converters, within a number of varied weather settings, as a means of putting in place the most effective DC-DC converter that should be utilised in the PV technique.

4.1. DC-DC converters

PV generating systems frequently integrate DC-DC converters serving as an interface device between PV panels and loads to match load voltages and MPP voltages of PV panels. These converters are primarily designed to mediate the efficient transformation of input power $P_m=V_{in}*I_{in}$ into output power $P_o=V_o*I_o$ through increasing, or decreasing, the input voltage. Equation 4.1 demonstrates the manner in which DC-DC converter efficiency (i') is determined:

$$\tau = \frac{P_o}{P_{in}} = \frac{V_o \times I_o}{V_{in} \times I_{in}} \quad (4.1)$$

Equation 4.2 indicates the expression taken by the correlation between input and output parameters:

$$V_o \times I_o = \tau \times V_{in} \times I_{in} \quad (4.2)$$

Efficiency is maintained at approximately the same level at particular converter voltage and current values. Thus, a V_0 or I_o increase in Equation 4.2 is the direct result of a V_{in} or I_{in} increase. The increase or decrease of the DC-DC converter input voltage is generally achieved through one of three types of converters, i.e. a buck converter (step down converter); a boost converter (step up converter); and a buck-boost converter (step up/step down converter).

A common feature of all three types of converters is an inductor capacitance (LC) electrical circuit, which is regulated in an electronic manner. A pulse width modulator (PWM) controls the duty cycle (D) of the electronics switch, which takes the following form:

$$D = \frac{t_{on}}{T} \tag{4.3}$$

In the above equation, T represents the switch oscillation period (otherwise known as time period of square pulse), which governs the electronics switch, while t_{on} denotes the on time regulation of square pulse.

Continuous current conduction and discontinuous current conduction exhibit considerable feature discrepancies, and form the two operation modes associated with DC-DC converters. In the former, there is a more straightforward relationship between the duty cycle of the electronics switch duty cycle and voltage ratio. The converter operation will occur in a continuous mode, provided that the current through the inductor does not decrease below zero. In order to ensure the inductor current stays above zero, the load resistance needs to be lower than the combined value of PWM pulse signal frequency and the inductor inductance (L). This lead to a need for a selected mode operation to be imposed on the converter parameters and control frequency. In such a design, the highest and lowest required current and voltage of appliances must be taken into account. Operation in continuous current conduction is standard for converters in the majority of applications. This operation mode requires careful selection of converter parameters, in order to ensure that the current through the inductor does not decrease below zero [118,132, 135,144].

4.2. Maximum Power Point Tracking from the DC-DC converter point of view

After the PV component is linked straight to the load, the unit will function at the T-junction position of its I–V distinctive and the load arc. Figure 4.1 shows that the PV component has a non-linear distinctive that varies in accordance with solar emission, heat, and load state. As a result, MPPT is needed to equal the PV unit impedance with the load impedance, proportionate to oscillations during weather circumstances. So as to resolve this matter, a DC–DC converter is normally put in between the PV component and the load applied like the power stage translation to uphold the function of the PV component at its MPP [20]. This can be attained through regulating the task cycle of the converter to imitate a changeable weight from the PV terminals standpoint, even after a permanent load is linked.

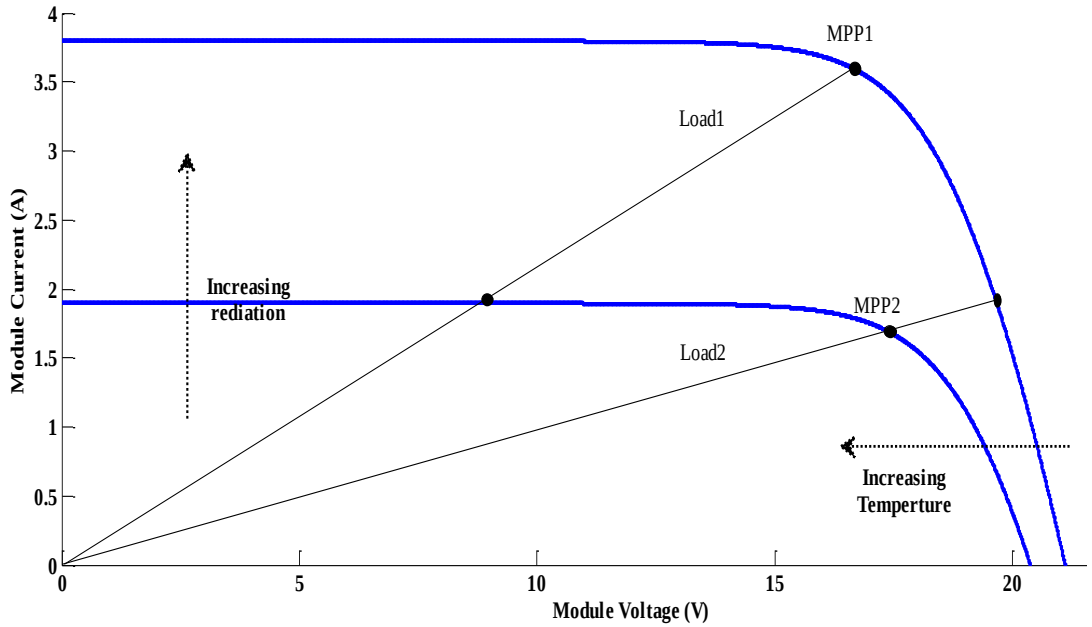

Figure 4.1. The PV module operating point

4.3. Topologies of DC-DC converters

The major component of the MPPT regulator consists of the DC-DC tracker converter. This is due to its ability to influence the functioning of PV, in addition to removing the highest energy from the PV through equalising the PV component impedance with its load. This compels the unit to function close to its MPP within diverse degrees of sunrays, as well as in various weather settings. Many scholars have studied the DC-DC buck or boost converters in the absence of any handbook outlining the manner in which such converters should be employed, or which converter is the most suitable for a PV system.

The diversity of DC-DC converters fall into two categories: (1) the isolated form (generally employed in a network linked system); and (2) the non-isolated form (highly suitable for stand-alone methods requiring a level of power that is identical to, or lower than, the PV component output energy). The non-isolated forms can be further classified into three groups: (1) buck (step-down); (2) boost (step-up); and (3) buck-boost and Cùk converters (step-down/step-up) [133,134].

4.3.1. Buck Converter

DC-DC buck converters have the ability to stand down the production power if the production is classically lesser than the input energy. Hence, these forms of converters are commonly utilised if the supply power is higher in comparison to the load power [6, 7].

Figure 4.2 illustrates the DC-DC buck converter possessing two power keeping units: (1) the inductor (L); (2) the output capacitor (C). In addition, it is in possession of a Mosfet (S), which is utilised for turning the converter on or off, by means of the Pulse Width Modulation (PWM) [122, 134 and 135].

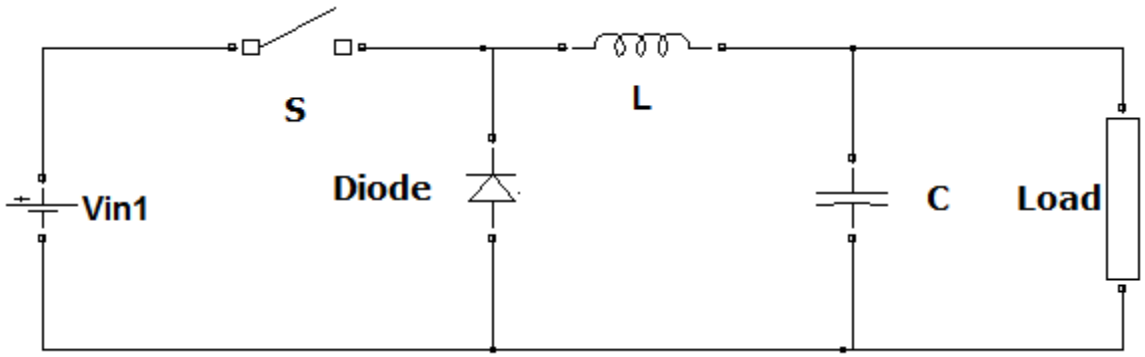

Figure 4.2. Buck converter electrical circuit.

The connection linking the produced voltage to the converter's current (i.e. the PV component production power and energy and the duty cycle) is as follows:

$$\frac{V_{load}}{V_{pv}} = \frac{T_{on}}{T_s} = D \tag{4-1}$$

$$\frac{I_{pv}}{I_{load}} = D \tag{4-2}$$

The correlation involving the load voltage and load current may be expressed as:

$$V_{load} = I_{load} * R_{load} \tag{4-3}$$

In which: D is the duty cycle; V_{load} is the load voltage; V_{pv} is the PV module output voltage; I_{load} is the load current; and Ipv is the PV output current.

When the expressions (4.4) and (4.5) are placed in expression (4.6), the correlation involving the PV unit's impedance, along with the load impedance, may be expressed as:

$$\frac{V_{pv}}{I_{pv}} = \frac{R_{load}}{D^2} \tag{4-4}$$

Furthermore, equation (4.7) can be rewritten as:

$$R_{ipv} = \frac{R_{load}}{D^2} \quad (4\text{-}5)$$

In which R_{ipv} represent the PV module impedance. At the time of linking the load to the PV, the PV's component functioning spot is at the meeting point connecting the load with its I-V curvature, and derived from expression (4.8), the line that denotes that the load is straight. Thus, the leaning angle may be calculated as expression [132- 135].

$$\theta_{Ripv} = \text{atan}\left(\frac{D^2}{R_{load}}\right) \quad (4\text{-}6)$$

A hypothetical constraint exists in relation to the converter's duty cycle, which assumes a figure between 0-1. As a result, the leaning angle (θ_{Rpv} maybe expressed in the following way:

Its minimum limit:

$$\theta_{Ripv} = \text{atan}\left(\frac{0}{R_{load}}\right) = 0 \quad (4\text{-}7)$$

Its upper limit:

$$\theta_{Rpv} = \text{atan}\left(\frac{1}{R_{load}}\right) \quad (4\text{-}8)$$

Expressions (4.10) and (4.11) provide the functioning and non-functioning area of the DC-DC buck converters. Thus, in accordance with expression (4.9), the load's figure establishes the inclination angle maximum level; to enable the PV to function in the non-functioning area if the load is shifting. Consequently, the input of the DC-DC buck converters' impedance is not lesser compared to the load impedance. Furthermore, it may not control the PV component closer to the short-circuit I_{sc}. As a result, these converters may only be run when $R_{load>=} R_{MPP}$ [126,133, 135].

Table 4.1 illustrates the correlation of diverse non-isolated DC-DC converters with regard to their input resistance, duty cycle, and load resistance inclination angle (θ_{Rpv}. In addition, it demonstrates the conversion ratio of the converters, obtained through the application of the expression above.

Table 4.1: The input resistance of PV Module, load and D of different DC-DC converter

Type	R_{ipv}	D	$\boldsymbol{\theta_{Ripv}}$
Buck	$R_{ipv} = \frac{R_{load}}{D^2}$	$\frac{V_{load}}{V_{pv}} = D$	$\theta_{Ripv} = \text{atan}\left(\frac{D^2}{R_{load}}\right)$
Boost	$R_{ipv} = (1-D)^2 * R_{load}$	$\frac{V_{load}}{V_{pv}} = \frac{1}{1-\text{D}}$	$\theta_{Ripv} = \text{atan}\left(\frac{1}{(1-D)^2 * R_{load}}\right)$
Buck-Boost and Cùk	$R_{ipv} = (\frac{1-D}{D^2})^2 * R_{load}$	$\frac{V_{load}}{V_{pv}} = \frac{D}{1-\text{D}}$	$\theta_{Ripv} = \text{atan}\left(\frac{D^2}{(1-D)^2 * R_{load}}\right)$

Through the application of the expression within Chart I, the inclination angle (θ_{Ripv}) may be placed as its minimum and maximum limits ($90 > \theta_{Ripv} > \frac{1}{R_{load}}$[126, 135, and 136].

4.3.2. Boost Converter

Under these converters, the size of the output energy is consistently higher in comparison to that of the input energy. Thus, these forms of converters may be applied if the PV unit output power is lesser compared to the load power. Fig. 4.3 [126,134-136] illustrates the fundamental electrical path of boost converters:

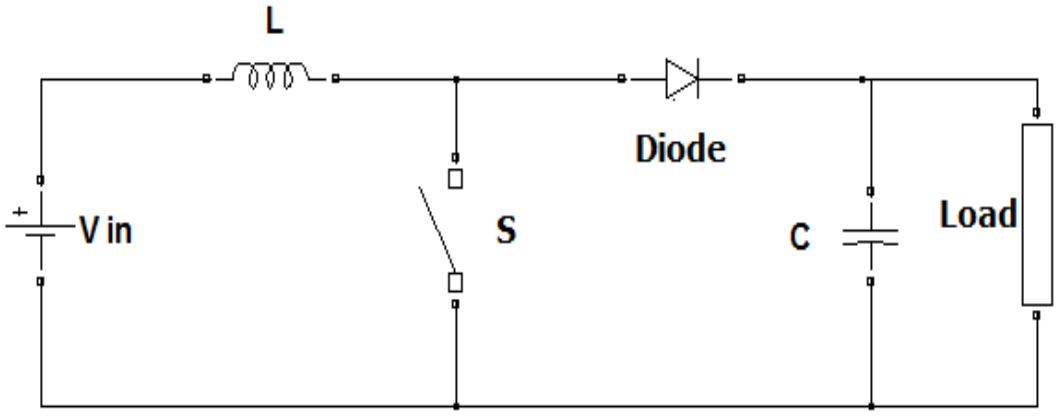

Figure 4.3. Boost converter electrical circuit.

4.3.3. Buck-Boost Converter

Under these converters, the output power size may be greater or lesser in comparison to the size of the input power. The atypical characteristic of the buck-boost converters consist of their output power polarisation being reverse to their input power, thus, transformers known

as inverter controllers are frequently utilised within buck-boost converters. The benefits of utilising the buck-boost converters consist of their increased effectiveness, as well as simple execution of a short circuit current safeguard. Nonetheless, their major weakness consists of their irregular input current, increased peak current via the control switch, as well as increased intricacy in contrast to other converters. Figure 4.4 demonstrates the essential electrical path of buck-boost converters. It bears an inductor (L), diode (D), capacitor (C) and a switch which may be Mosfets or transistors [133, 135].

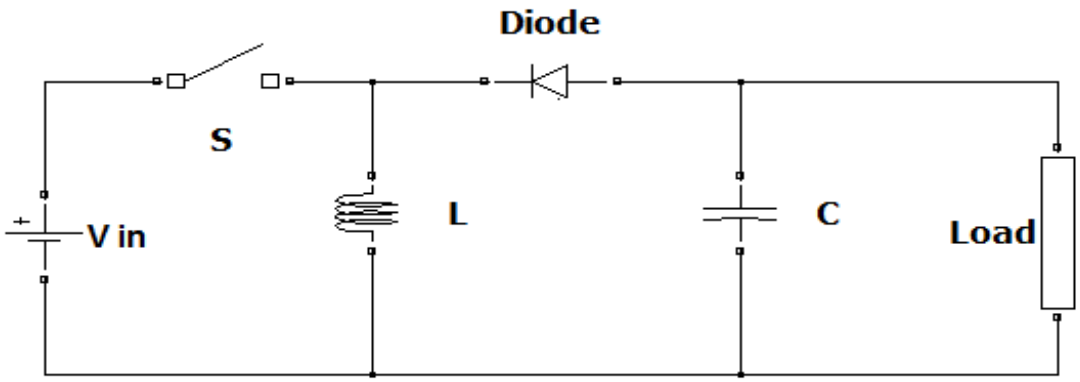

Figure 4.4. Buck-Boost converter electrical circuit.

The leaning angles (θ_{Ripv}) of these converters are expressed in this manner:

$(90 > \theta_{Ripv} > 0)$.

Consequently, derived from the expressions under Table II, these converters may function from an open circuit power position to the short-circuit current, i.e. these converters have no area of non-operation. The lack of such a non-operating area is due to whichever rise within the duty cycle decreases the input impedance. Consequently, the inclination angle or PV unit functioning spot drifts to the left of the I-V feature, whereas decreasing the duty ratio raises the input impedance, causing the drifting of the functioning spot to the right of the I-V curvature.

4.3.4. Cùk Converter

The functioning of these converters is identical to that of buck-boost converters. The main electricity path of Cùk converters is illustrated within figure 4.5. The major distinction between these and buck-boost converters consists of their additional input inductor, which may be utilised as the DC input sieve, as well as the capacitor C1 that is utilised as a transfer-energy tool.

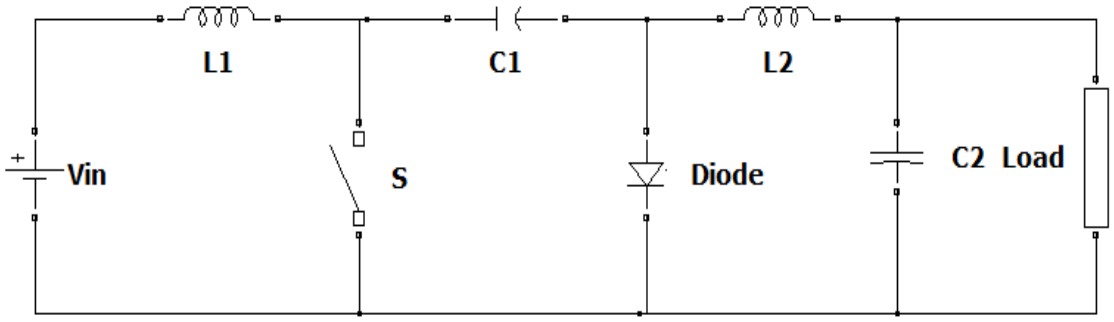

Figure 4.5. Cùk converter electrical circuit.

The leaning angles of these converters are similar to those of buck-boost converters. As a result, these forms of converters also lack the non-operating area [134, 135].

4.4. The conduct of non-isolated DC-DC converters within various sun radiation as well as temperatures

Based on the expression under Table II, it is apparent that buck converters are in possession of operating, as well as non-operating, areas described as; $(0 > \theta_{Ripv} > \frac{1}{R_{load}})$. Whereas, the corresponding description for the boost converters is: $(90 > \theta_{Ripv} > \frac{1}{R_{load}})$, although the leaning angles of the Cùk converters are similar to those of the buck-boost converters, with their operating area being between 0°- 90°.

So as to certify the concept, buck, boost, buck-boost, and Cùk converters are all created in addition to being executed within the Matlab.

Table 4.2: The electrical specification

Type	V_{in}	V_{out}	D	R_{load}
Buck	17.5	6	0.71	2.4
Boost	17.5	40	0.57	26.66
Buck-Boost and	17.5	12	0.41	24
Cùk	17.5	40	0.7	26.66

Through the application of the figures in Table 4.2, the leaning angle (θ_{Ripv}) of every converter was computed with the obtained outcomes plotted to the I-V curvature at diverse

sun radiations, so as to establish whether the MPP is within the functioning or non-functioning area of the converters (see Figures 4.6, 4.7 and 4.8).

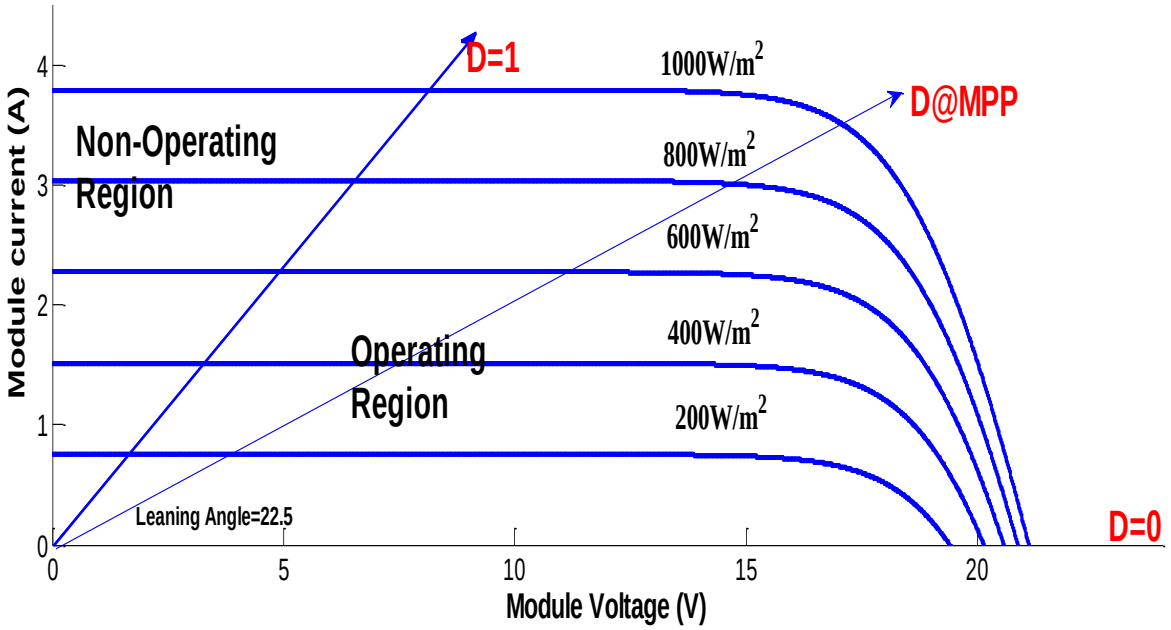

Figure 4.6. The buck converter operating and non-operating zone in different conditions [144].

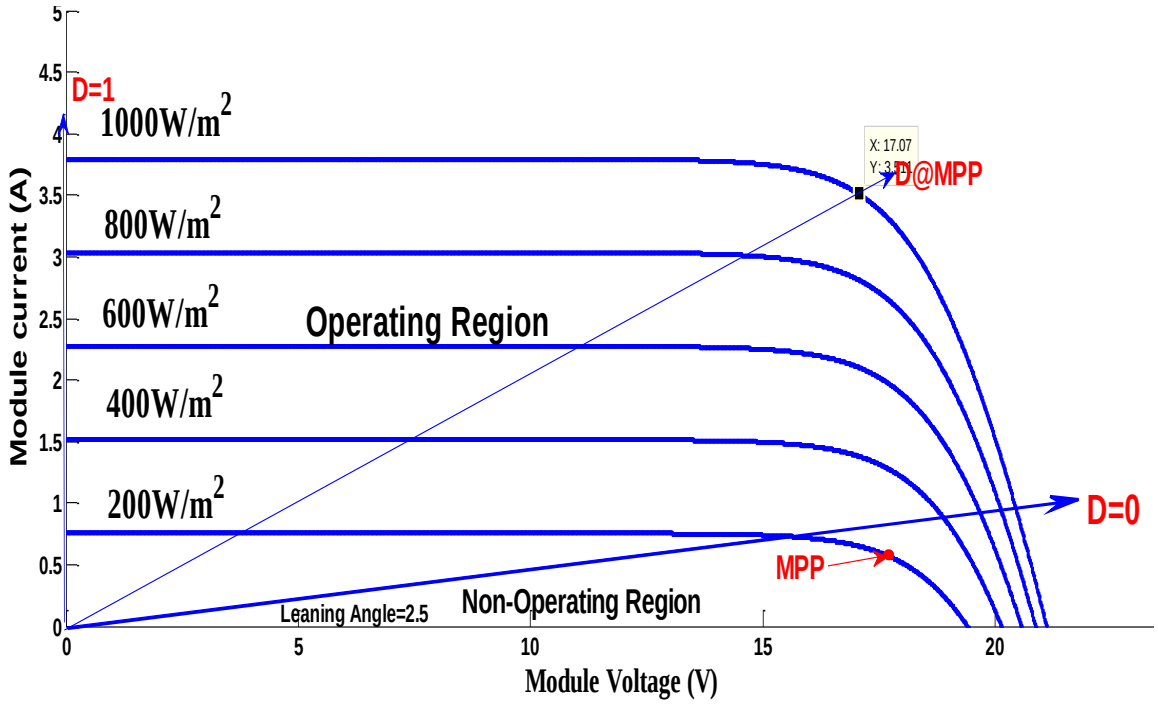

Figure 4.7. The boost converter operating and non-operating zone in different conditions [144].

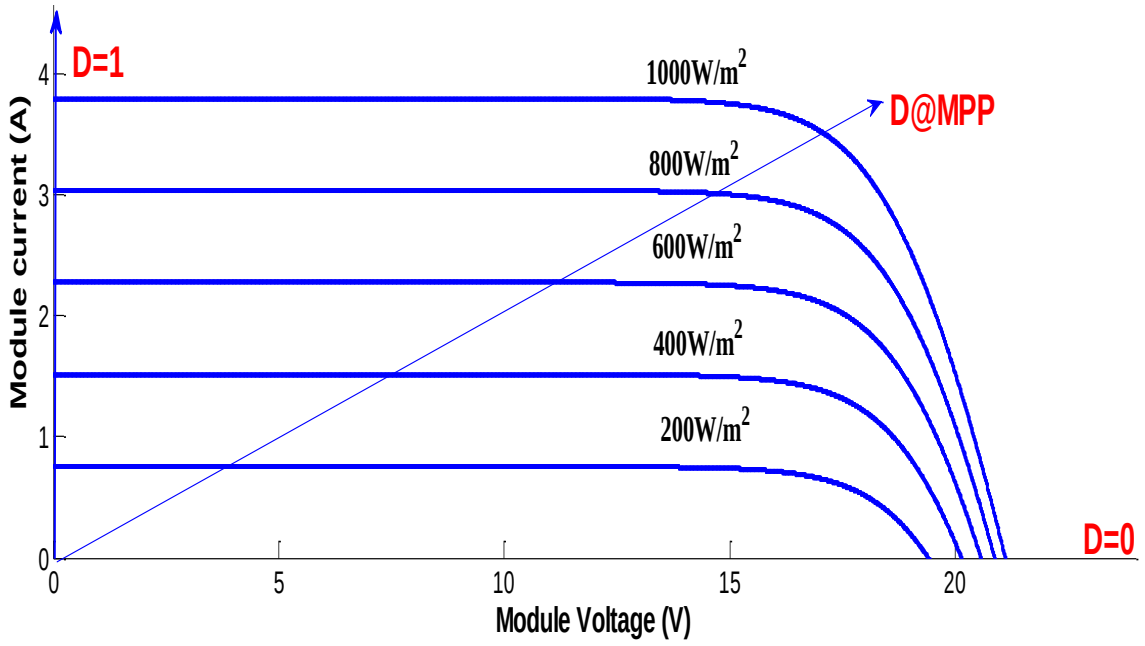

Figure 4.8. The buck-boost and Cùk converters operating and non-operating zone in different conditions [144].

The outcomes above were reproduced at diverse sun radiations ($0W/m^2<G<1000W/m^2$), from which it is apparent that DC-DC buck converters may often control the PV unit within its MPP, since it is positioned within its functioning area (refer to Figure 4.6). Nevertheless, in cases in which the load shifts, the operating spot has the potential to drift out of the functioning area. On the contrary, the boost converters (see Figure 4.7) are incapable of operating the PV unit within its MPP in conditions of low sun radiation, since it falls out of the functioning area. The functioning area of both DC-DC buck-boost and Cùk converters (refer to Figure 4.8) is 0°-90°. They are therefore capable of controlling the PV unit under its MPP in every climatic condition, due to being situated within the functioning areas. Coelho et al. investigated the impact of both sun radiation and temperatures on various forms of non-isolated DC–DC converters, and deduced that, when the converter's duty cycle shifts in line with climatic conditions, the parameters of the converter also shifts [122,126, 135].

The DC-DC analysis reveals that, despite being commonly used in tracking applications, buck and boost converters are unsuitable for this operation mode, due to being capable of MPP tracking in a single portion of the I-V plan. By contrast, Cùk converters, as well as buck-boost converters, provide a more appropriate alternative for tracking applications, due to their ability to track the MPP throughout the I-V plan.

It therefore is necessary to establish an effective operation of both DC-DC converters and tracking algorithms, in order to achieve an enhanced tracking system. The use of a Cùk converter together with the MPPT technique enables the fulfilment of this specification.

4.5. Simulation result and discussion

Figure 4.9 demonstrates the recommended electricity circuit created to signify PV component output features. Firstly, the model possesses dual changeable inputs, i.e. the sun radiation (G) as well as the temperatures (T_{ac}). Secondly, it applies the output power as a reaction input utilised for compelling the PV unit's output current to attain a correct I-V curvature originating from sun radiation as well as temperature. Thirdly, the non-isolated DC-DC buck, boost, buck-boost, as well as the Cùk converters, are created and linked to the PV component. Finally, the P&O algorithm was applied in the role of MPPT regulator, in order to assess the enquiry.

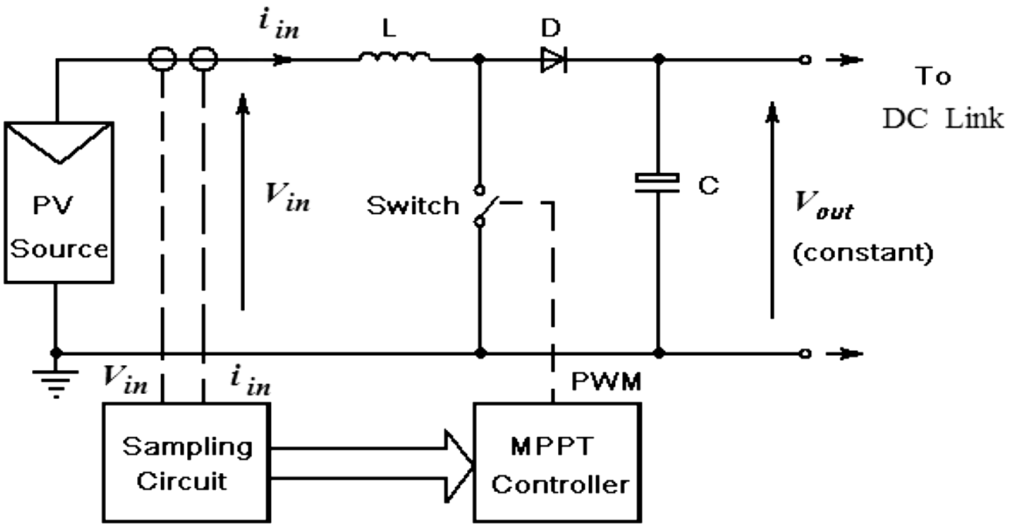

Figure 4.9**:** Circuit of the PV system [144].

Figure 4.10, illustrates the PV unit output power, at the time when the PV was replicated at low sun radiation (G=200 W/m^2). The effectiveness of the buck-boost, as well as the Cùk, converters was established as being superior in comparison to that of the boost converters within the identical setting. However, the boost converters may not control the PV component close to the MPP, due to its location outside its functioning area. Nevertheless, the buck converters may accurately trail the MPP. The buck-boost (as well as the Cùk) converters are capable of trailing MPP in all climatic settings, despite boost converters being incapable of tracking MPP at minimal sun energy. It possesses a number of advantages in relation to buck and buck-boost converters, due to being cost-effective, and having a more effective dynamic reaction. Furthermore, boost converters have an additional benefit to buck converters, due to possessing a diode or Mosfet within its system to obstruct any opposite

current, if the PV's output power is lower in comparison to the load power. Thus, boost converters are extensively utilised at the time of charging a battery requiring constant input energy.

Conversely, the boost functions require an increased switching rate. This (1) raises switching deficits; (2) is strident; and (3) increases pressure on the boost units, which leads to a decrease in energy. Buck converters, on the other hand, require an added diode, implying increased expense, leading to a fall in power, but raising the current loss. In addition, in order to ensure the PV unit's wave current is even, the buck converters require an input capacitor that is both sizeable and costly.

Figure 4.10 demonstrates that voltage losses escalate at the time of operating the buck, as well as the buck-boost, converters, as a consequence of escalating the PV component output power and energy waves, due to their irregular input energy. An input capacitance needs to be employed to resolve this challenge in the buck converters, resulting in additional losses. However, the buck-boost converters require input, as well as output sieving that implies a rise in the losses alongside the expense. Figure 4.10 emphasises Cùk converters as having an easy output power, as well as current, due to their output point inductor. Furthermore, they possess additional functioning and efficacy in comparison to buck-boost converters, despite these being cost-effective. In addition, buck-boost converters have less effectiveness in comparison to Cùk converters, due to: (1) their irregular input current and (2) pulsated output power resulting in additional switching wastes, together with additional pressure on the power unit.

Figure 4.11 illustrates the PV system output power, and replication outcome for the sun radiation at the figure 1000W/m^2. One remarkable consequence is that buck–boost, as well as Cùk converters, are able to operate the PV unit within its MPP, regardless of the load or climatic surroundings. The boost converter displays improved functioning with elevated effectiveness demonstrated by each of the converters.

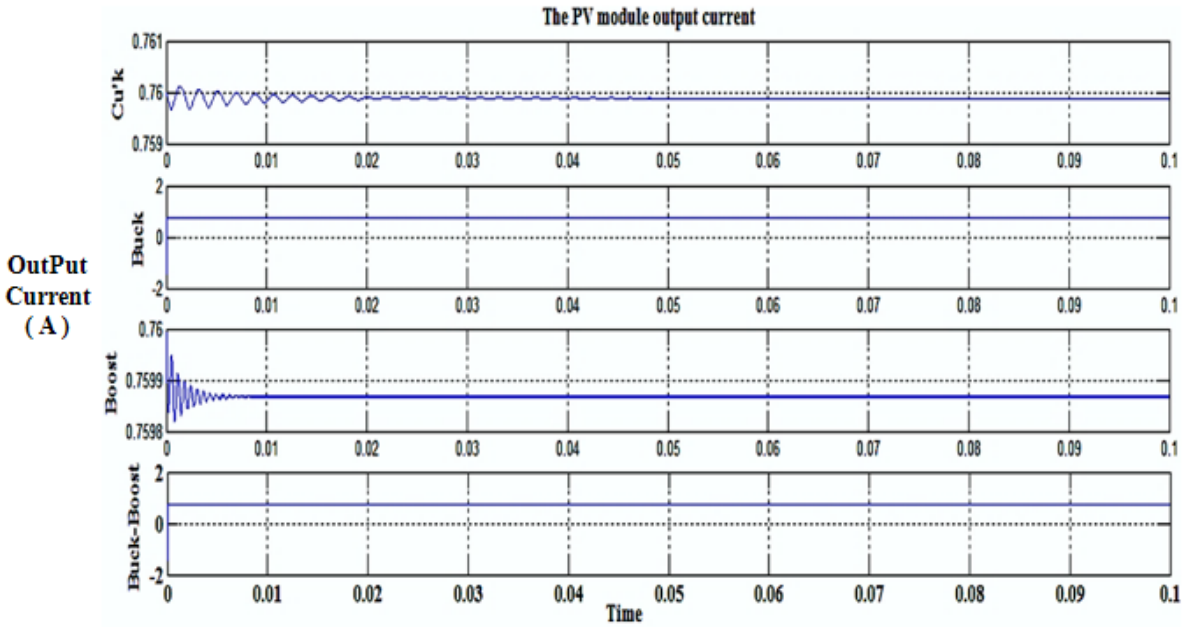

Figure 4.10. The simulated PV module output voltage (V) at (200W/m^2, 25°C) [144].

In general, the buck, along with the boost, converters are incapable of accurately tracking MPP, and their effectiveness tends to be minimal when contrasted to the Cùk and buck–boost converters. However, their ease (as well as cost-effectiveness) renders these converters highly attractive in comparison to other converters. The buck–boost converters are capable of tracking the PV system's MPP of the climatic surrounding, as well as the load notwithstanding. However, it undergoes irregular input power, since the converter's control switch has been connected in series to the component causing additional noise. An additional weakness of this form of converter consists of the elevated wave input power, which intensifies pressure on the switch.

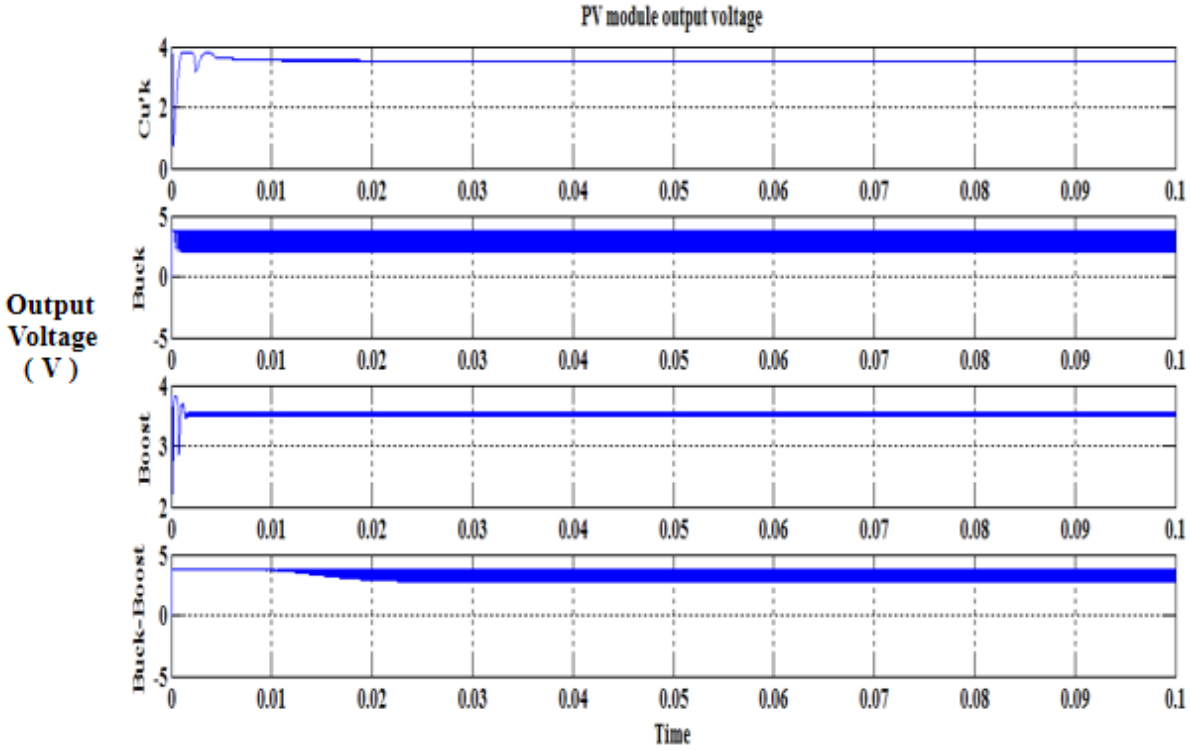

Figure 4.11. The simulated PV module output voltage (V) at STC [144].

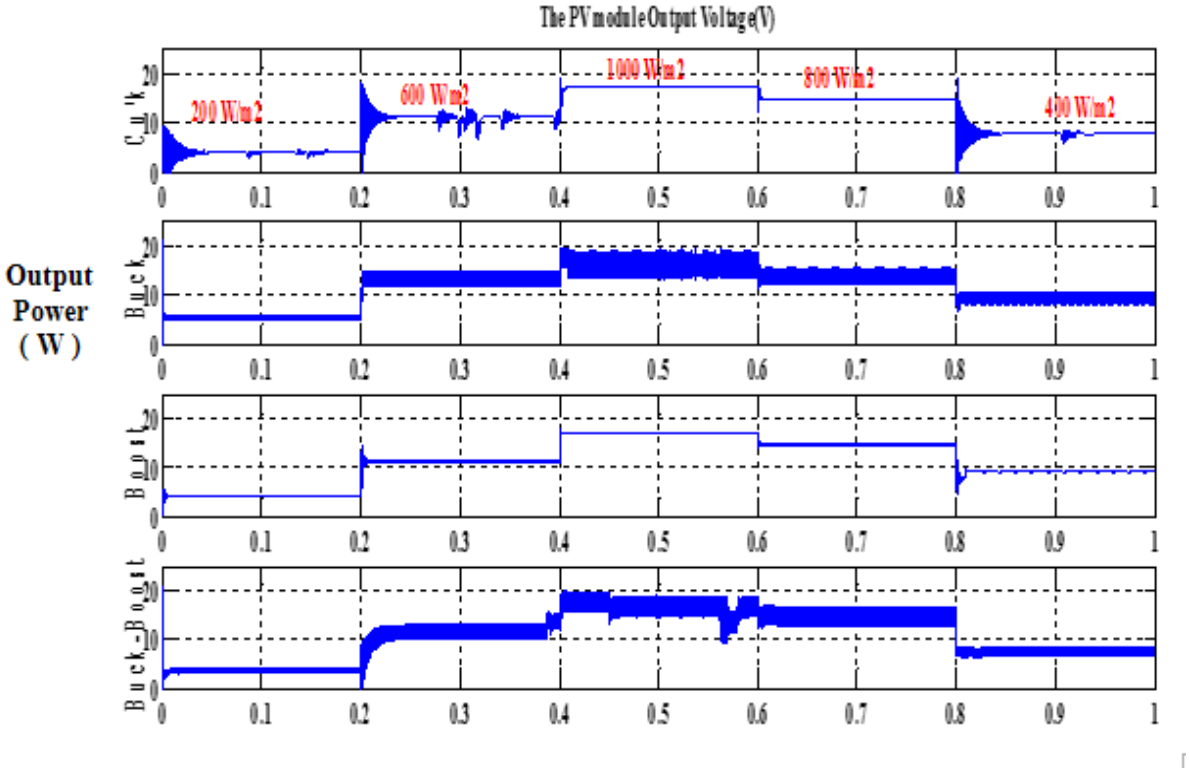

Figure 4.12. The simulated PV module output voltage (V) under (G=200W/m^2 to 1000W/m^2 and constant T= 25°C) [144].

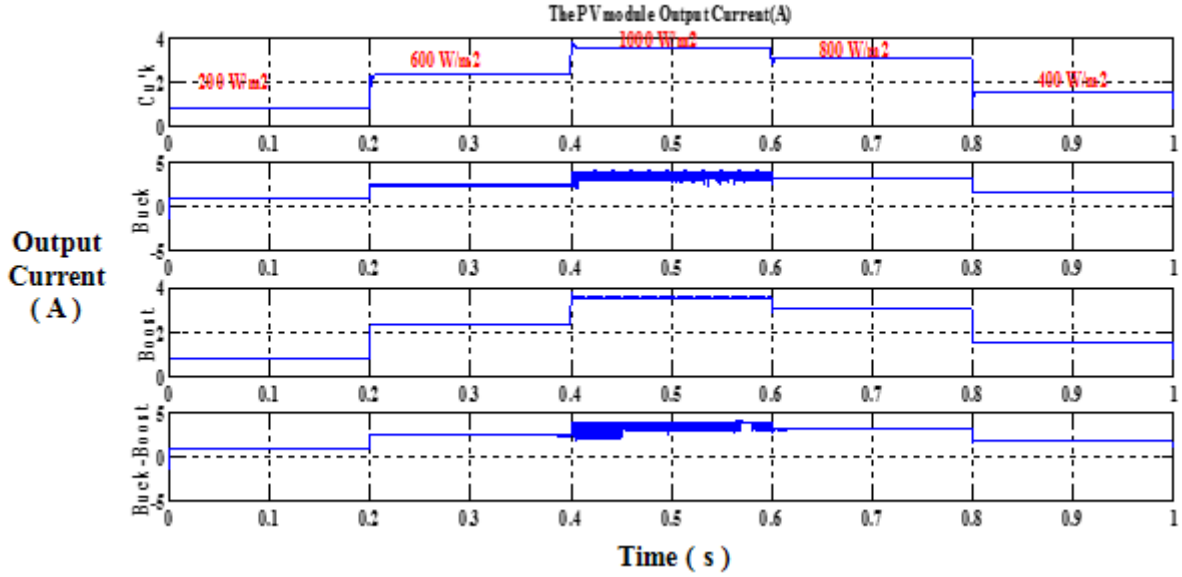

Figure 4.13. The simulated PV module output Current (A) under (G=200W/m^2 to 1000W/m^2 and constant T= 25°C) [144].

Figures 4.12 and 4.13 both illustrate the PV component output energy, in addition to the output current model outcomes of swift shifting surroundings, and sun radiation altering between 200W/m^2 - 1000W/m^2. The buck–boost with the Cùk converters have been established as having the capacity to function the PV unit close to MPP. The boost converter displayed improved functioning; however, it also demonstrated lower effectiveness at minimal sun energy, in comparison to other converters. In addition, its functions lead to the unit using lower levels of power, as well as current. Both the buck and buck-boost converters function in the unit, using a high degree of power and energy wave, resulting in increased loss of energy.

4.6. Summary

This chapter has offered a succinct appraisal of the various non-isolated DC-DC converters, as well as the simplest technique of selecting an efficient converter for application within the MPPT. This aids creators to ensure effective selections. The investigation has revealed that both the buck and boost converters are extensively applied due to their ease of use and cost-effectiveness. However, these converters are not the first choice to function as MPPT, due to having lower levels of effectiveness in comparison to other non-isolated DC-DC converter kinds within shifting climatic surroundings. The buck and boost converters are the most effective forms of converters in relation to price. Nonetheless, their major shortcoming consists of minimal tracking effectiveness. In addition, the replication outcomes have revealed that the boost converter demonstrates lower efficacy in minimal irradiance, in

contrast to other kinds of converters. It has been established that both the buck–boost and Cùk converters are capable of tracking the MPP accurately in a number of climatic surroundings, notwithstanding the load. This capability renders these converters perfect preference for MPPT uses. In addition, the Cùk converter was seen to produce the maximum efficacy. Further analysis of the Cùk converter and its voltage transfer function will take place in Chapter Five, Section 5.1.

Chapter Five

Existing MPPT Algorithms

5. Introduction

MPPT is a technique permitting power controllers to maximise their output in solar powered systems. This extraction of maximum power is achieved through regulation of the current taken from the solar panels or the voltage to achieve the MPP, and is independent of operating conditions, e.g. temperature, aging or solar irradiation. There are a number of reported techniques for achieving this MPP, which have been classified as being either on-line or off-line. Those that are off-line provide a reference signal based on previously obtained information on parameters concerning the PV array, i.e. solar irradiation levels; the temperature of the modules; the short-circuit current; or open circuit voltage of any sample PV panels. On-line methodologies involve taking reference signals and developing algorithms to calculate the true power, creating comparisons with previously calculated values and adjusting the MPP accordingly.

Figure 5.1 demonstrates a previously created Simulink module in Chapter 3, connected to a resistive load, as shown in Figure 5.1 without an MPPT controller. This was tested within a MATLAB environment, employing various radiation conditions under a constant temperature, with the results being recorded to enable a comparison with the operating point of the PV module when directly coupled to the load, with the actual recorded operating point as stipulated in the data sheets.

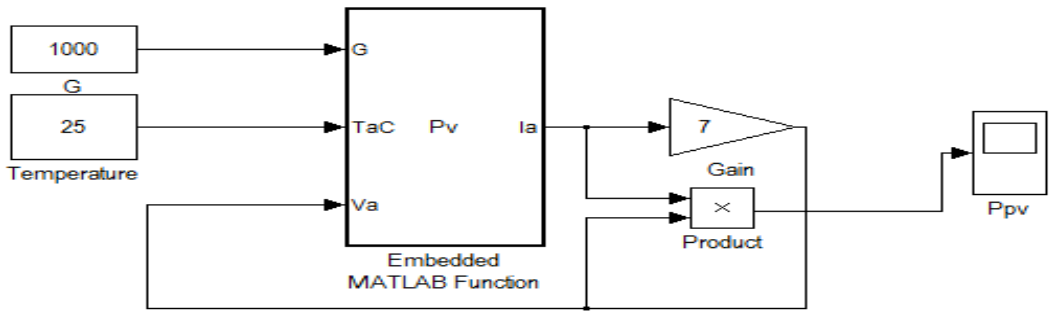

Figure 5.1: SIMULINK model of the PV module with a resistive load.

Table 5.1: the theoretical operating point of selected PV with variable irradiance and Constance temperatures (25°C).

G(w/m2)	The theoretical values			The operating points			(%)the efficiency of the PV module
	I_{MPP} (A)	V_{MPP} (V)	P_{MPP} (W)	V_L (V)	I_L (A)	P_L (W)	
100	16.02	0.358	5.74	2.66	0.387	1.01	17.95
200	16.4	0.721	11.84	5.36	0.76	4.043	34.14
300	16.7	1.077	18	7.98	1.14	9.097	50.53
400	16.9	1.431	24.2	10.64	1.52	16.16	66.77
500	17	1.785	30.36	13.26	1.895	25.14	82.80
600	17.02	1.145	36.52	15.62	2.231	34.84	95.39
700	17	2.507	42.63	17.13	2.447	41.92	98.33
800	17	2.863	48.68	17.96	2.565	46.07	94.63
900	16.95	3.225	54.67	18.47	2.639	48.74	89.15
1000	16.8	3.607	60.6	18.83	2.691	50.68	83.63

As outlined in section 4.1, when the PV module is connected directly to the load, it will operate at the intersection point of its I–V characteristic and the load curve. Figure 5.2 (below) demonstrates the PV module I-V characteristic with resistive load.

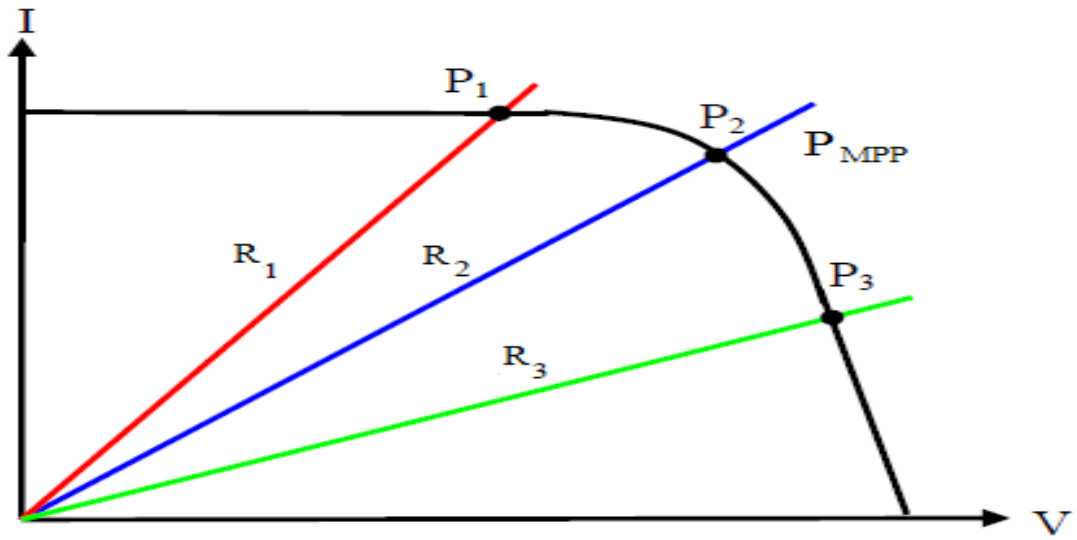

Figure 5.2: I-V characteristic with resistive load

As previously noted, research has confirmed that the electrical energy conversion capacity of a solar panel is approximately 30-40% of incident energy. An MPPT algorithm needs to be applied to improve the effectiveness of the panel. This can be achieved through a range of methods, including: P&O (i.e. the hill climbing method); IncCond; Fractional Short Circuit Current; Fractional Open Circuit Voltage; Fuzzy Control; and Neural Network Control. Of these, the most frequently employed are the P&O and IncCond techniques. These are advantageous due to: (1) being easy to implement; (9) being capable of rapidly tracking MPP; and (3) are cost-effective [106]. Factors such as MPPT duration, cost and degree of application difficulty all dictate the type of algorithm selected.

This study will now focus on a discussion of five MPPT algorithms popularly used in the available PV system, followed by utilisation of MATLAB tools to compare their tracking efficiency. Their application techniques are widely utilised in the MPPT controllers as a result of their simplicity and ease of implementation. A number of different proposals concerning a number of MPPT techniques have been advanced, but no wide-ranging comparison has yet been undertaken between the numerous techniques and their efficiencies in terms of tracking under different weather conditions. The objective of the current study is to establish a bridging of this gap. This chapter will therefore direct its focus on a comparison study of simulation between these extensively applied MPPT techniques, taking solar radiation variation into consideration, to establish the technique capable of performing most effectively under rapidly changing weather conditions. This section will be organised as follows: firstly, Section 5.2 will outline the description of the PV system modelling and the illustrations of the respective P&O, INC, CV, OCV, and SCC principles of operation techniques; secondly, Section 5.3 will illustrate the results, analysis, and discussion; and finally, Section 5.4 will form the conclusion.

As distinguished in parts 3.2.3 and 3.2.4, sources of PV demonstrate an MPP within their steady-condition attribute, one that differs in accordance with changing circumstances, e.g. levels of irradiance and heat. To warrant the most efficient application of the sources of PV, it is necessary to function at the MPP. There are some factors to think about when assessing an MPPT algorithm, such as tracking pace; steadiness; ease; cost of execution; and tracking effectiveness. Some MPPT techniques have been built on for application within PV systems, so as to attain the MPP, varying from easy to more intricate techniques based on weather circumstances and the use [7-9]. The main objective of MPPT is to take out utmost output energy from the PV component underneath diverse sunlight emission and temperatures.

5.1. Cùk Converter

As discussed in Chapter 4, both buck-boost and Cùk converters can offer either lower or advanced output power. The buck-boost adapter has a lesser effectiveness compared to the Cùk converter since it has some drawbacks, that is, (1) the high voltage pressure on the power module stops input voltage; and (2) it spends a longer time than the Cùk to achieve the transitory reaction. In spite of being more costly than the buck-boost adapter, the Cùk converter has definite benefits, such as its constant input power; low converting loss; and the supply of a ripple-free output power because of the output phase inductor. Thus, among the different DC-DC converters, the Cùk adapter is the mainly suitable for use in an MPPT method. Figure 5.1 shows the Cùk converter circuit using a capacitor like its major power storage, and thus having a constant input power, therefore facilitating it to take out free power wave from the PV , causing lesser switching losses and advanced levels of effectiveness [104,135].

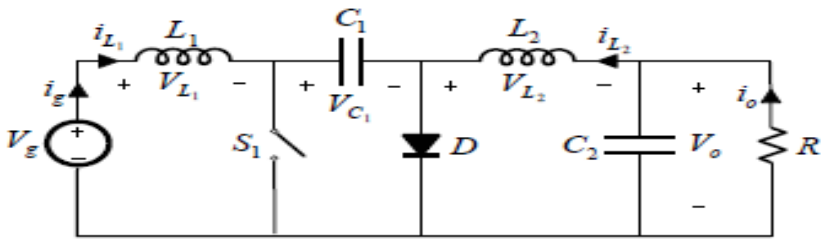

Figure 5.3: The Cùk Converter Electrical Circuit [104].

Therefore, the voltage transfer function can be written as following:

$$V_{OUT}/V_S=D/(1-D) \quad (5\ 1)$$

The electric specification the Cùk converter are shown in Table 5.1, below:

Table 5.2: ELECTRIC SPECIFICATIONS OF CÙK CONVERTER

Specification	
Input Voltage (V_s)	12-18V
Input Current (I_s)	0-5A(<5% ripple)
Output Voltage (V_o)	40V(<5% ripple)
Output Current (I_o)	0-5A(<5% ripple)
Maximum Output Power (P_{max})	60W
Switching Frequency (f)	10KHz

Duty Cycle (D)	0.6≤D≤1

The Cùk converter components employed for simulation have been calculated as follows:

5.1.1. Input Inductor (LI)

The assumption made when calculating the inductor size is that the change in the current across the inductor is not more than 5%, with the change in the inductor current calculated as follows:

$$\Delta I_L=(V_S.D)/ (L.f) \quad (5.2)$$

Where: V_s the input voltage, D the duty cycle, and f the switching frequency.

Therefore, the inductor L can be determined as:

$$L=(V_S.D)/ (\Delta I_L. f) \quad (5.3)$$

And the current ripple is 5% of the average current, therefore ΔI_{L1} is given as:

$$\Delta I_{L1}=5\%.I_{L1} \quad (5.4)$$

Therefore, the inductor (*L1*):

$$L1=(V_S.D)/ (\Delta I_{L1}.f) \quad (5.5)$$

Using the same assumption, the output inductor (*L2*) size can be calculated as:

$$L2=(V_S.D)/ (\Delta I_{L2}.f) \quad (5.6)$$

5.1.2. Capacitor selection

In choosing the capacitor size, the voltage ripple across it should be no more than 5%.

The voltage across the input capacitor can be calculated as:

$$Vc1=Vs+Vo \quad (5.7)$$

The load resistance can be calculated as:

$$R = \frac{V_O^2}{P_O} \quad (5.8)$$

To calculate the value of *C1*, the following equation is used :

$$C1=(V_O.D)/ (R.\Delta Vc1.f) \quad (5.9)$$

The output capacitor (*C2*) can be calculated by using the output voltage ripple equation as:

$$\frac{\Delta V_O}{V_O} = \frac{1-D}{8.L_2.C_2.f^2} \quad (5.10)$$

Then, the value of C2 can be calculated as:

$$C_2 = \frac{1-D}{8.L_2.\left(\Delta V_O / V_O\right).f^2} \quad (5.11)$$

5.1.3. Matching the load

When the PV module is directly connected to the load, the PV module operating point will be at the intersection point between its (I-V) characteristic and the load line.

The load impedance is calculated as follows:

$$R_{Load} = \frac{V_O}{I_o} \quad (5.12)$$

The optimal load of the PV module can be given as:

$$R_{Optimal} = \frac{V_{MPP}}{I_{MPP}} \quad (5.13)$$

Where: *VMPP* is the PV module output voltage at MPP, and IMPP is the PV module output current at the MPP. When matching the value of R_{load} with the value of R_{opimal}, the maximum power can extract from the PV module. However, this matching is rarely likely to occur in practice. Therefore, MPPT is required to match the impedance of the PV module with the load impedance.

An example has been undertaken in this study, during which the PV module was directly connected to the load without the MPPT controller, in order to study the load matching using a high efficiency Cùk converter.

Equation (5.14) gives the relations between output and input voltages, and duty cycle:

$$V_S = \frac{1-D}{D} \times V_{OUT} \quad (5.14)$$

And equation (5.10)

$$\frac{I_S}{I_O} = \frac{I_{L1}}{I_{L2}} = \frac{V_O}{V_S} \quad (5.15)$$

Therefore

$\frac{I_S}{I_O} = \frac{D}{1-D} \gg I_S = \frac{D}{1-D} \times I_O$ (5.16)$\frac{I_S}{I_O} = \frac{D}{1\text{-}D} \gg$

$I_S = \frac{D}{1\text{-}D} \times I_O$(5-1)

From the above equations (5.15) and (5.16), the converter input impedance is given as:

$$R_{IN} = \frac{V_S}{I_S} = \frac{(1-D)^2}{D^2} \cdot \frac{V_O}{I_O} = \frac{(1-D)^2}{D^2} \cdot R_{Load} \quad (5.17)$$

As it can see from the above equation, the impedance that appears from the PV module is the converter input impedance R_{in}. Therefore, the value of R_{in} can be adjusted by changing the duty cycle (D), till the value of R_{in} matches that of PV R_{op}, where the PV module operating point is at MPP.

5.2. Techniques of Maximum Power Point Tracking

The main characteristic of the electronic system of MPPT is a specific form of operation enabling PV modules to yield maximum power. Rather than being a mechanical tracking system, capable of making the PV modules point straight to the sun by physically moving them, MPPT is a completely electronic system that stimulates the modules to generate as much power as possible by varying their electrical operating point. This results in additional power derived from the modules being available, which takes the form of elevated battery charge current. MPPT and a mechanical tracking system can be operated together, despite having no similarities in common.

The electrical energy conversion capacity of a standard PV module does not exceed 30-40% of the incident solar radiation; however, its effectiveness can be increased through the application of MPPT. The theorem of Maximum Power Transfer specifies that the Thevenin circuit impedance (i.e. source impedance), along with the load impedance, need to be identical to achieve maximum circuit power output. Thus, the challenge of tracking the MPP is, in reality, a challenge of impedance matching [110,145].

To increase the output voltage, and ensure it is appropriate for use in various applications (e.g. motor load), a DC-DC converter linked to a PV module should be employed within the source side. The source impedance can be matched to the load impedance by modifying the duty cycle of the converter, accordingly.

Given that the energy attained through employing the PV system is principally based on solar emission, heat and load hindrance, it is significant to run the system at its MPP. Where

applications require power greater than that a PV module is capable of producing, a power conversion system can be used to maximise the output power from the system. a power translation method can be applied to capitalize on the output current from the system. Some writers have lately provided various accounts to describe the matters linking to the MPPT regulator. There are a large number of different methods capable of maximising the power from a PV system, ranging from the use of simple methods, to a more complex analysis [108, 110]. This chapter will discuss in detail a comparative study of existing MPPT algorithms, including: P&O Methods [88]; IC Methods [102]; CV; Open Circuit Voltage (OCV) [47]; and Short Circuit Current (SCC) [63].

5.2.1. Perturb and Observe algorithm

This technique is founded on an exploration of the affiliation between PV component output power and its output voltage. The Power-Voltage (P-V) characteristics are demonstrated in Figure 5.4, wherein the PV module operating point is on the left of the P-V arc (dp is positive), indicating that once the output current of the PV component raises, the PV unit current perturbation will persist within the same course in the direction of the MPP. If the functioning point of the component was on the P-V arc right side, subsequently the regulator would shift the PV unit functioning point back, looking for the factual MPP. This can be attained through overturning the perturbation course. This method flowchart is demonstrated within Figure 5.5 [76, 88,145]:

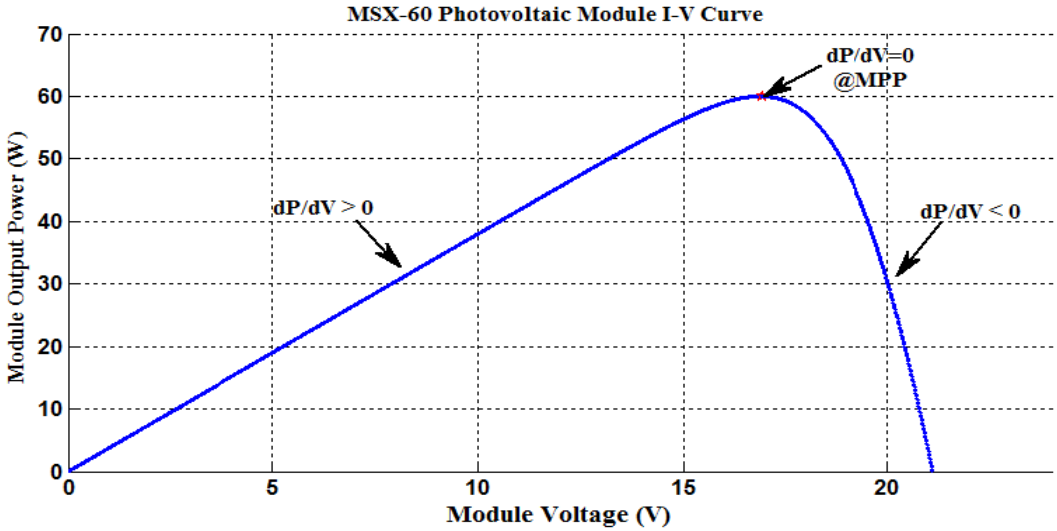

Figure 5.4: The PV muddle P-V characteristic at STC (1kw/m^2, 25°C).

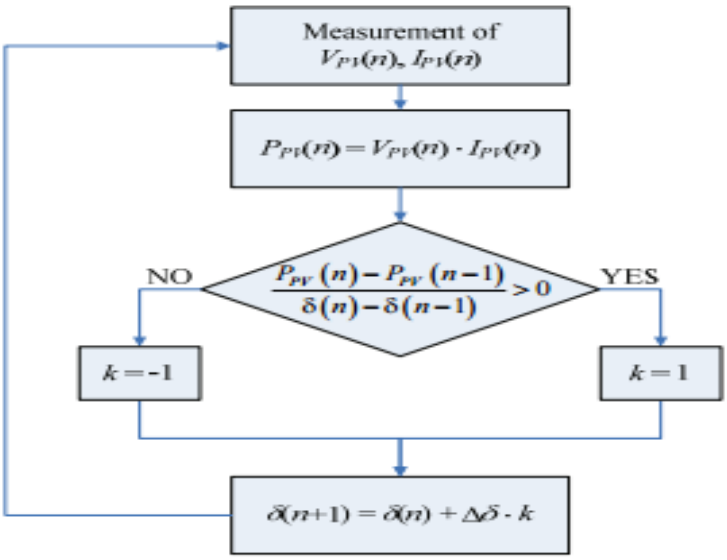

Figure 5.5: Flowchart of P&O[107].

There are two commonly used techniques when using the P&O method: (1) the reference voltage; and (2) the converter duty ratio [76, 88]. In the reference voltage, the PV module output voltage is adjusted by a PI controller operating the PV module at its MPP under standard test conditions. In the converter duty ratio, the duty ratio of the DC-DC converter is perturbed to extract the maximum output power from the PV module. This method is founded on the association between the PV component output energy and the duty proportion of the DC-DC converter; whereas MPP is attained by amending the switching disposition of the adapter (duty proportion) until dp/dd is equivalent to zero. The downsides of P&O techniques are that they generate osculation near the MPP within the stable state. Ref [88] shows that a constant fluctuation in P&O techniques within the stable state leads to a decrease in the PV component output energy. Additionally, it is not capable to run the component at its utmost output energy during swiftly changing weather circumstances [3, 9, and 88].

Digital circuits can implement P&O MPPT algorithms without difficulty. As discussed in Section 2.2, the output power of PV panels is computed based solely on the terminal voltage and current of a PV panel. A comparison is then undertaken between this result, and that preceding, in order to establish the orientation of the subsequent perturbation. This process is facilitated by digital circuits. The primary advantage of the use of P&O algorithms is their capacity for acting to slow fluctuations, not only in solar irradiation and temperature, but also in the properties of the PV panels. On the other hand, P&O algorithms fail to respond with sufficient rapidity when searching for the most effective operating point to generate maximum output power. A further reason for the slowness of these algorithms consist of the clocked

perturbation of the electrical feature performed by the systems, as a result of which they are required to stand by until the perturbation effect is produced. The speed of the process is also limited by the average voltage, power or current in the majority of implementations being used by perturbation methods to supply data relating to derivatives. A number of different studies have demonstrated that the MPP is tracked by standard P&O systems at a couple of tens of milliseconds or more [3-9], [82]. Once the MPP is tracked, the PV panel operating point will still suffer perturbations, due to the ongoing use of perturbations in MPPT. Under stable conditions, PV power is lost, due to the rising P&O system fluctuations around the MPP. P&O algorithms have an additional limitation, as addressed in [108, 102]. Furthermore, atmospheric conditions undergoing rapid changes may trigger a temporary deviation of the operating point from the MPP.

The assumption underpinning P&O algorithms is that perturbation is the cause of fluctuations in output power. Since they cannot rely on measured values to detect unexpected fluctuations in atmospheric conditions, any deviation from the MPP can occur if the direction of the perturbation responsible for increasing output power is maintained, i.e. it is impossible to prevent tracking in the incorrect direction. However, faster tracking cycles can help to diminish duration and power loss [145].

5.2.2. Incremental Conductance

IncCond was built by a Saga University student, and has been applied to prevail over the P&O technique drawback under fast altering ecological circumstances. The technique is attained by computing the symbol of dp/dv employing the PV component incremental and its straight conductance (dI/dV and I/V) [62, 74]. Just two feelers (the current and voltage sensors) are needed within the IncCond system to determine the PV unit output energy and voltage, presuming the existence of simply one point on the P-V distinctive, wherein the PV component can generate its MPP (see Figure 5.2) [145].

The relationship between the output voltage and power are expressed as follows;

$dP/dV = 0$ at MPP (5 18)

$dP/dV > 0$ on the left side of MPP (5 19)

$dP/dV < 0$ on the right side of MPP (5 20)

The slope (dp/dv) of P-V characteristic can be calculated using the PV module output voltage and current, as follows:

$$dP/dV=(dI)/dV=I\times dV/dV=I\times dV/(dV)+V\times dI/(dV)=I+VdV/dI \quad (5\ 21)$$

Hence, the operating point of the module at its MPP can be calculated based on equation (5.21), as follows:

$$dI/dV= I/V \quad \text{at MPP} \quad (5\ 22)$$

$$dI/dV > I/V \quad \text{on the left side of MPP} \quad (5\ 23)$$

$$dI/dV < I/V \quad \text{on the right side of MPP} \quad (5\ 24)$$

These equations reveal that the PV unit functions at its MPP once the IncCond I/dV is equivalent to its straight conductance I/V. Nevertheless, if the PV component IncCond dI/dV is above its conductance I/V, then the regulator will augment the PV unit voltage through regulating the duty proportion of a DC–DC adapter. If this was not the situation, the perturbation could be in the conflicting course, or would amplify the duty proportion of the converter so as to decrease the current and change the functioning position back to the MPP [62, 74 and 102]. The IncCond algorithm flowchart is shown in Figure 5.6.

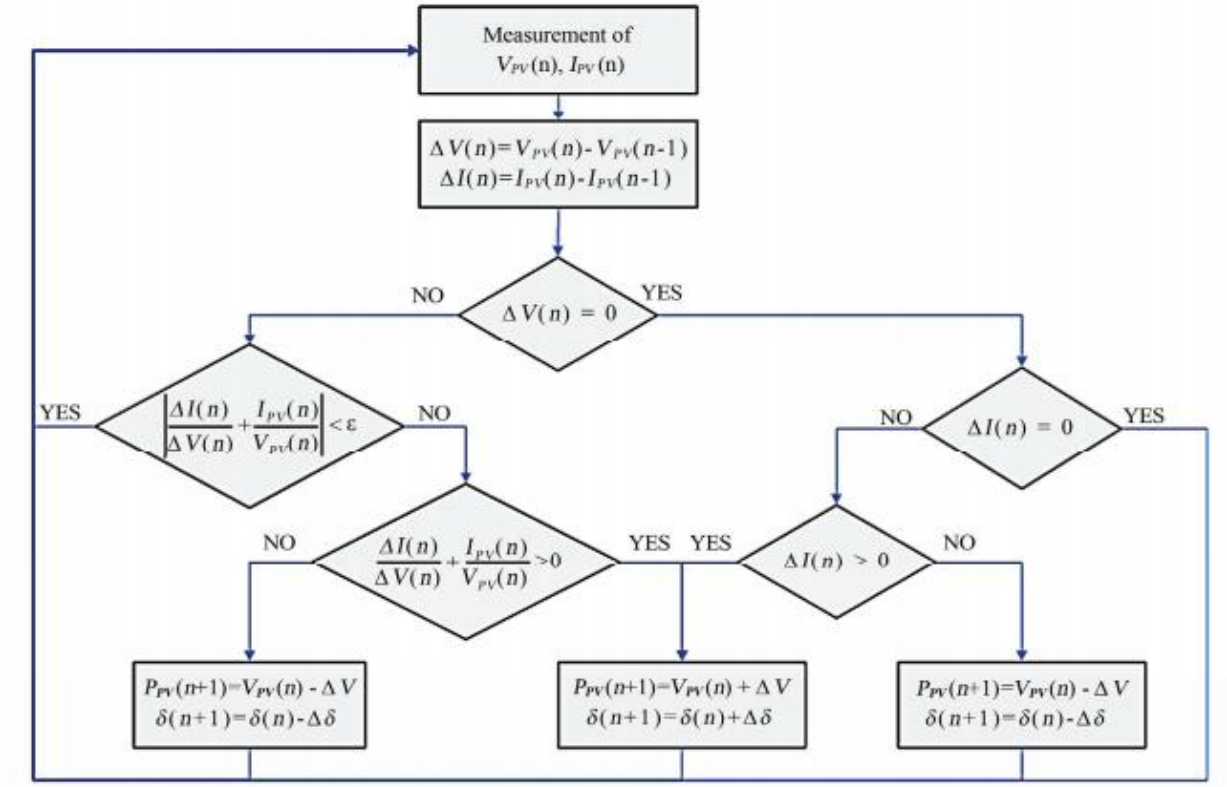

Figure 5.6: Flowchart of IncCond method [107].

In Theory, fluctuation around the MPP can be prevented by IncCond algorithms. As revealed in the flow chart, the operating point needs to remain fixed upon fulfilment of the

condition di/dv = -I/V, which denotes successful tracking of the MPP. On the other hand, if the condition is unfulfilled, the relationship between di/dv and –I/V may be employed to establish the direction in which the MPPT system operating point needs to be modified. The principle of the above-mentioned relationship is that the positioning of the operating point to the right or to the left of the MPP is indicative of negative or positive dp/dv, respectively. Furthermore, frequent fluctuations in atmospheric conditions have no effect on the MPPT ability of IncCond algorithms. To establish whether the position of the operating point is to the left or right of the MPP, the condition di/dv = -I/V (or dp/dv = O) is applied by these algorithms. More specifically, the operating point is located to the left of the MPP if the dp/dv differential is above zero (i.e. di/dv > -I/V), while it is located to the right of the MPP if dp/dv is below zero (i.e. di/dv < -I/V).

Therefore, regardless of the pace of change in atmospheric conditions, the operating point is, in theory, moved by the IncCond algorithms towards the MPP. Nonetheless, these algorithms are not without limitations, including a lack of cost-efficiency due to the complex nature of the control circuit and the necessity of rapid computation for the IncCond di/dv. An estimation of di/dv is typically achieved based on the relationship di/dv = I(k) – I(k-1)/V(k) – V(k-1) [145].

Under circumstances of rapidly changing atmospheric conditions, a slow computation speed will result in an invalid di/dv estimation. Hence, it is not possible to guarantee the advantage displayed by IncCond algorithms regarding the movement of the operating point towards the MPP, regardless of the pace of change of atmospheric conditions. This leads to an issue comparable to the P&O algorithm deviation from MPP under rapidly changing atmospheric conditions.

5.2.3. Constant Voltage

The CV process algorithm is the easiest MPPT regulator, and has a fast reaction. Like it can be observed within Figure 5.7, CV techniques have no necessity of extra tools or input, aside from the dimension of the PV voltage that needs a PI regulator to regulate the function cycle of the converter so as to uphold the PV voltage close to MPP [32, 48]. Within this technique, the regulator controls the PV component voltage, running it near its MPP by harmonizing the PV component output energy to a steady reference voltage (Vref). The worth of Vref is equivalent to the calculated PV unit utmost output voltage in standard test circumstances (STC) or set to a permanent estimated value [48, 59].

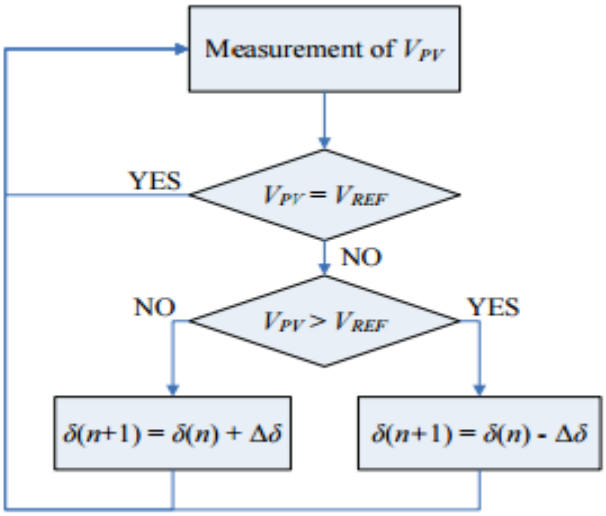

Figure 5.7: Flowchart of CV method [107].

5.2.4. Open Circuit Voltage

The method of the Open Circuit Voltage (OCV) is a more recognized MPPT regulator, founded on the proportion between the PV component utmost output voltage and its open circuit voltage being equivalent to constant K:

$$V_{mpp}/V_{oc} \approx K1 \approx 0.76 \quad (5\ 1)$$

Where: V_{mpp} is the PV module maximum output voltage; V_{oc} the module open circuit voltage and K1 is a constant; and (assuming it is slightly changed with solar radiation) the operating point is set to a fixed value of the open circuit voltage. A number of authors have suggested good values for K within the range 0.7–0.80 [108, 145].

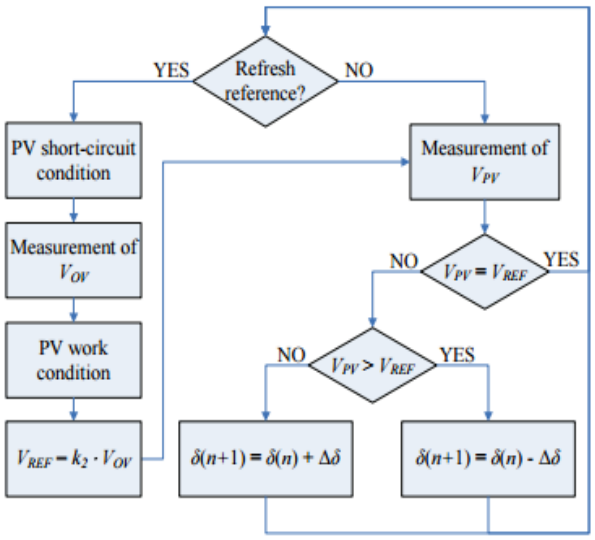

Figure 5.8: Flowchart of OCV [107].

The ratio between the OCV and the PV module MPP voltage (Voc/Vmp) at STC is approximately 76% for crystalline silicone panels [108]. In order to measure the OCV, the load has first to be disconnected from the panel for a set amount of a time. The measurement of the OCV occurs when the short circuit current is set to zero, then the MPPT controller calculates the new operation point using Eq. (2), and sets up the PV module voltage to MPP. This is repeated continuously, in order to operate the module at its maximum output power. Figure 5.8 demonstrates the flow chart of this method. Despite this method being low-cost, its implementation is more straightforward than other methods, and requires only one feedback-loop control. Its efficacy is low, as the K value is not constant, due to it being temperature and solar radiation dependent [59]. Moreover, either over-voltage or current can be caused. In addition, the load has to be disconnected from the panel for a set amount of a time to measure the OCV, which leads to a waste of energy [48, 59].

The OCV technique is advantageous, due to it being simple and inexpensive, and having no need of expensive multipliers or digital controllers. The main feature of this technique is a quasi-MPPT. The controller relies on prior knowledge of the location of the MPP, rather than continuously searching for the real MPP in relation to the voltage curve. However, this technique is associated with a loss of energy during the open-circuit period, and requires a sample PV module or cell whose exposure to solar irradiation and temperature matches that of the primary PV modules [145].

5.2.5. Short Circuit Current

The technique of the short circuit current (SCC) is founded on the dimension of the PV component SCC, while its output voltage is equivalent to zero, and the PV unit highest output current at MPP is linearly comparative to its SCC [65, 108, 110]. So as to match the two currents, the error current is employed to control the duty proportion of the DC-DC adapter as the connection between the PV unit output current and SCC at MPP is:

$$I_{MPP} \approx k2 * ISC \quad (5\ 2)$$

In which K2 is a constant (K2<1) able of being determined from the curve of the PV. Its worth has been approximated by some writers. Ref [32] mentions it to be amid 0.78-0.92, whereas Ref [9] proposes a method of determining the real value of K2 by trailing the PV component MPP under altering weather circumstances, and recommends the worth of the relative K2 to be around 0.92 [32,48]. The flowchart of the SCC is demonstrated within Figure 5.9.

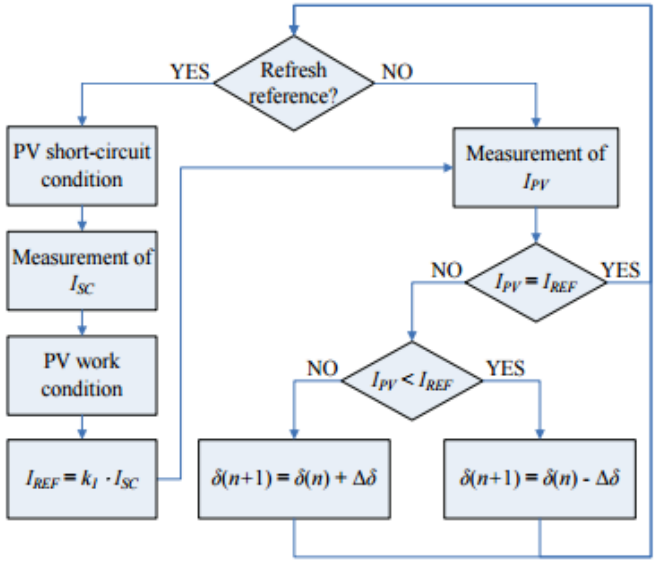

Figure 5.9: Flowchart of SCC [107].

The major benefits of this process comprises: (1) ease of execution with no intricate algorithm; (2) a shortage of any fluctuations about MPP; and (3) it has a comparatively fast reaction. Nevertheless, it needs extra units, together with a current sensor needed to determine the SCC. Furthermore, this technique cannot at all times run the PV unit at its highest output energy because it employs an assessment of the K2 aspect that is incapable to symbolize the exact MPP value within a real state. This is because of the PV component with a non-linear

distinctive that differs with ecological circumstances. Moreover, the online dimension of the SCC leads to decreasing the output energy of the module, and its MPP is not at all times harmonized [65, 110]. Additionally, the dimension of the SCC (ISC) is often needed in this technique, which implies shorting the component on every incident. The application of numerous loads can guarantee this matter does not take place. Nevertheless, this needs extra components, thus raising the price of the method [108,110,145].

This technique offers the advantages of rapidity, ease of implementation and lack of complexity. However, the disadvantage consists of the necessity of monitoring PV modules for the measurement of the short-circuit current. This gives rise to a number of issues, including the incompatibility of system characteristics between the monitor and primary PV modules, and energy loss due to system shorting of the PV modules to derive the short current in the sampling interval. Fluctuation in the proportional parameter (which is generally deemed to be constant) is an issue in both approaches to obtaining the short-circuit current. This parameter can undergo modifications, if the distribution of solar irradiation on the surface of the PV modules lacks uniformity due to the presence of shade and dirt.

5.2.6. Characteristics of different Maximum Power Point Tracking techniques

Table 5.3: Characteristics of different MPPT techniques

MPPT Technique	PV array dependent	Convergence speed	Rank	Periodic tuning	Sensed parameters
Perturb Observe	No	Varies	2	No	Voltage, Current
Incremental conductance	No	Varies	1	No	Voltage, Current
Constant Voltage	Yes	Medium	3	Yes	Voltage
Fractional Voc	Yes	Medium	5	Yes	Voltage
Fractional Isc	Yes	Medium	4	Yes	Current

Under changing atmospheric conditions, the on-time tracking of MPP by off-line MPPT systems is generally only achieved upon reaching the subsequent sampling time and acquiring a new reference value associated with the new MPP. In order to diminish the loss of energy during sampling, the sampling time period is lengthier in comparison to the switching cycle of the MPPT converter. Moreover, due to the characteristic incompatibility between monitor and primary PV modules, the tracking precision of the off-line MPPT systems is not optimal.

On the other hand, these systems afford the advantage of ease of implementation and cost-efficiency. They are particularly appropriate for PV conversion systems with a power capacity that does not exceed a couple of hundred watts and minimum total costs. By contrast, atmospheric conditions, PV module types and ageing do not affect the ability of on-line MPPT systems to track MPP constantly, leading to their tracking accuracy and rapidity exceeding those of off-line systems. However, on-line systems have the disadvantage of making PV generation systems more complex and expensive, and thus their use is restricted to PV systems with medium or large power levels. Nonetheless, the costs added by the on-line MPPT technique to PV generation systems are not as high as the overall cost of medium or large power level PV systems. The IncCond technique has numerous benefits over other methods of algorithm, including: superior effectiveness under swiftly shifting weather circumstances; its capacity to run the component at a precise MPP with no fluctuation around the MPP (i.e. different from the P&O technique). Nevertheless, the execution of this technique is more intricate compared to that of the P&O technique because it needs a speedier regulator having elevated sampling precision, leading to an augment in the system price.

5.3. Modelling and Implementation of Maximum Power Point Tracking algorithms

The circuit (Figure 5.10) illustrates the Simulink module of the MPPT system employed in the current study, in which the PV module output was fed to the DC-DC Cùk converter, and the converter output was coupled to the load. A number of different MPPT algorithms were used to control the switch of the converter, in order to study and compare their efficiency under various conditions.

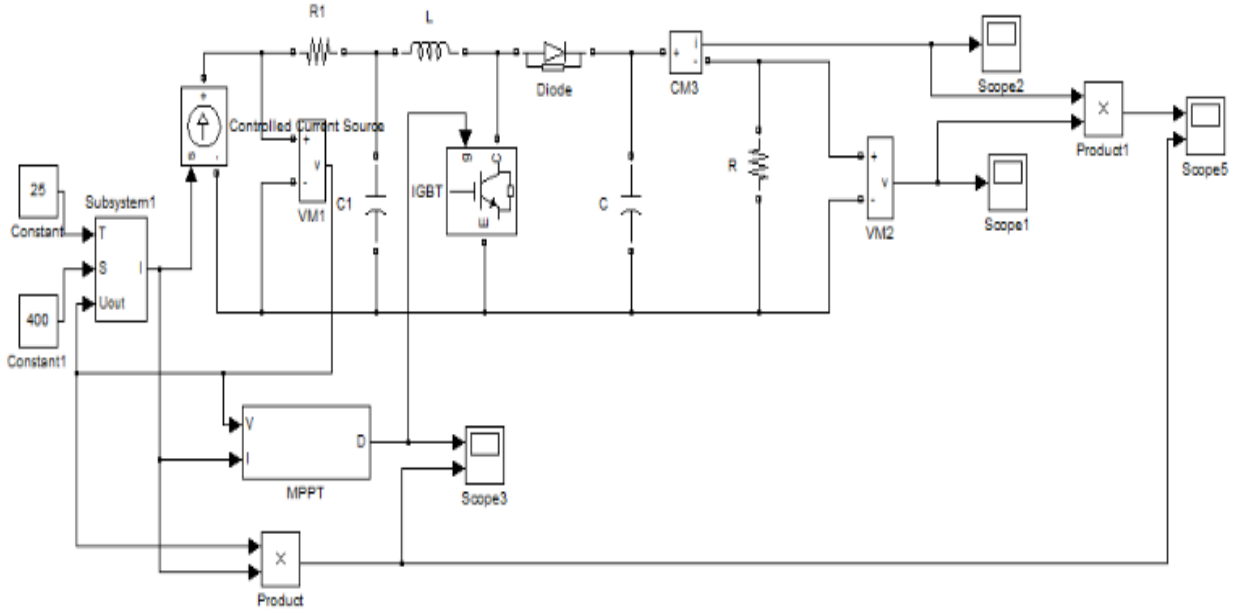

Figure 5.10: Simulink Model of the MPPT System [145].

The MPPT comparison approaches considered included (1) classical P&O; (2) IncCond; (3) CV; (4) OCV; and (5) SCC. The functionality of each MPPT method was assessed upon attaining the stable state condition. As shown in figure 5.11, simulation response results for the 5 techniques at the first phase, at 1000w/m2 irradiance have been revealed. Figure 5.11 shows the PV module's output power, having simulated the system at STC (G=1000W/m2). The P&O technique had a tracking efficiency of about 96%, with IncCond being 98.5%. Nonetheless, the level of effectiveness in CV technique above was compared to other methods under this condition, with SCC technique having the least efficiency level.

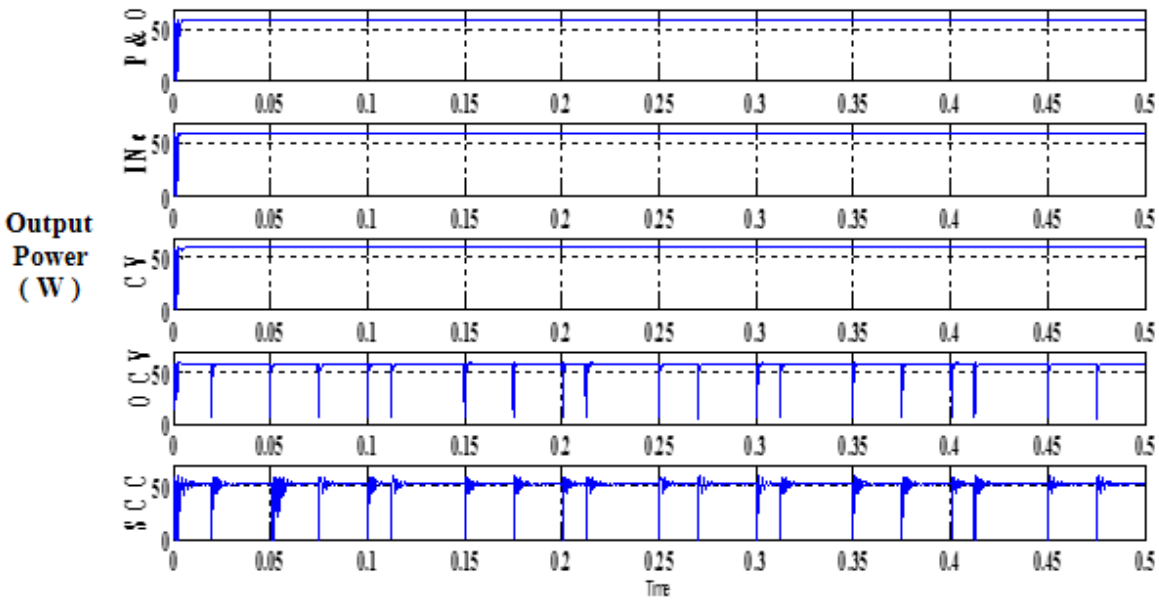

Figure 5.11: The simulation result of the system Output Power (w) at STC.

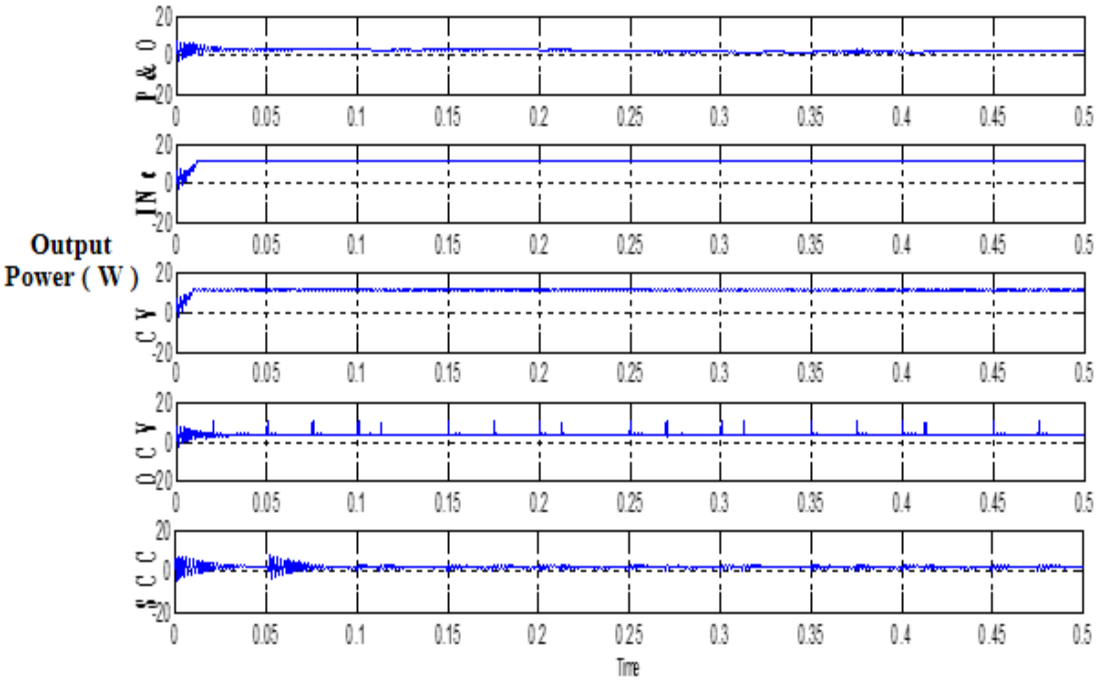

Figure 5.12: The simulation result of the system Output Power (w) under 200kw/m^2, 25°C.

Figure 5.12 shows the output of PV module, having simulated the system at low solar radiation (G=200kw/m2). The results show that P&O's MPPT tracking efficiency was lower than 70% at minimal irradiance levels. Decrease in solar radiation resulted in decrement in output power, with perturbation undergoing a directional change, while the controller held its perturbation direction until increment to irradiance. This remains among the highly popular

demerit associated with P&O algorithm. The levels of efficacy in CV (83%) and IncCond (87) were significantly higher compared to P&Q algorithm within this condition, with OCV (66%) and SCC (64%) approaches being lower. Regardless the failure of P&O to have MPP tracked at low solar radiation levels, it is able to maintain several advantages over the IncCond technique, i.e., it is less costly as well as being better in terms of dynamic response. Nonetheless, the P&Q algorithm entails several constraints in its operation, such as: (a) it results in an oscillation around MPP in its steady form; (b) it has a slower response time.

Just as evident from figure 5.13, the PV module's output power subjected to frequently varying atmospheric condition has been shown. From the results, it is evident how systems under SCC and OCV techniques had huge power loss volumes, with IncCond and CV having excellent performance. This is a clear indication that both IncCond and CV possess high efficiency levels, with identical dynamic responses and performances.

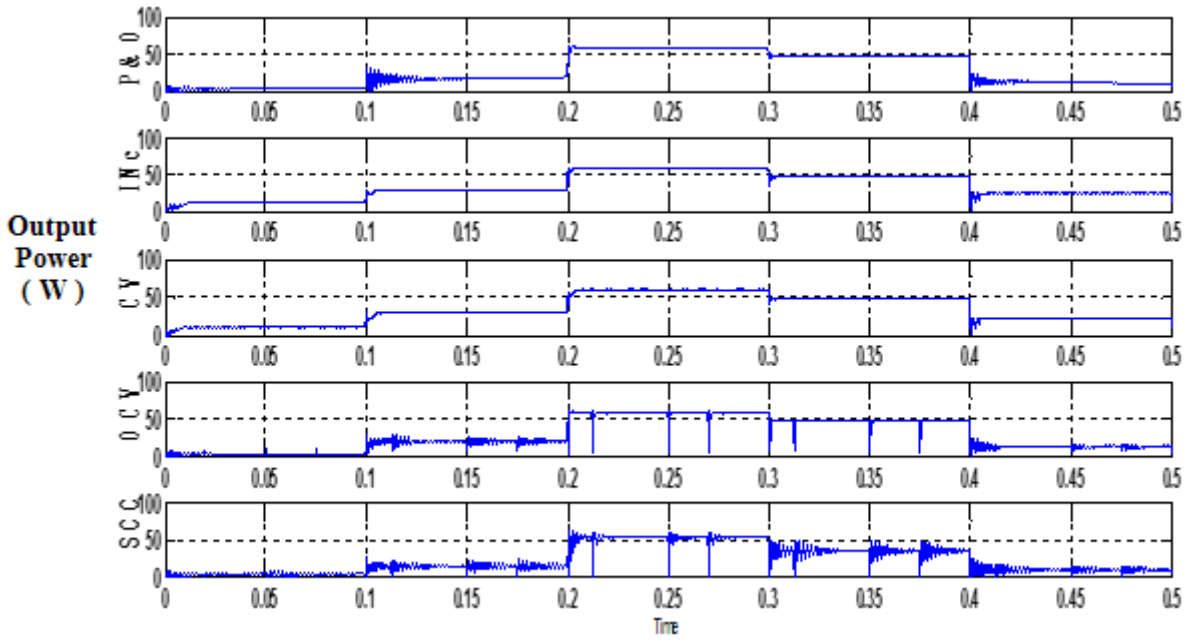

Figure 5.13: The simulation result of the system Output Power (w) under rapidly changing solar radiation, 25°C

The 5 MPPT algorithms' simulation results at a frequently varying radiation of "200 w/m^2, 600 w/m^2, 1000 w/m^2, 800 w/m^2 and 400 w/m^2," evidently show the comparatively efficient tracking effectiveness of MPP with the IncCond technique in situation of varying irradiation. The operating point of the PV module, upon which IncCond technique was instigated at G= G=600 w/m² and G=1000 w/m², (i.e., 33w and 57w, in that order), near to module's MPP at

identical conditions, the results of P&O were 22w and 58w. Although IncCond technique promotes efficient performance set under various weather conditions, its operation of PV model at MPP would not be possible. Regardless of having advanced tracking effectiveness compared to the P&O technique, it needs 4 sensor gadgets for the pertinent computing, resulting in low response duration for conversion, and eventually losing power hugely. Nonetheless, this technique is highly beneficial compared to P&O method since it offers increased efficiency levels at frequently fluctuating atmospheric conditions.

The easiest MPPT algorithm upholding the PV module's operating point close to its MPP is the CV technique. This is attained by having the module output voltage regulated to match a a fixed value of reference voltage (Vref). The value of Vref is identical to maximum output voltage of the PV module. This technique disregards the effect of solar radiation and temperature, since it considers Vref being equal to that of ideal MPP. Therefore, the module's operating point is not capable of being ideal MPP, hence the need to install data for varying geographical areas. Moreover, contrary to preceding approaches, this does not necessitate computation of the output power. As an alternative, it gauges the output voltage of the PV module needed to initiate the converter's duty cycle. The method is equally characterized by being inexpensive, with high efficiency under minimal solar radiation, besides being simple to execute when compared to the other approaches. Nonetheless, it is impossible to have MPP tracked correctly under frequently fluctuating weather conditions. As seen in figure 5.11, the significance of observing the effectiveness of the CV method's tracking procedure lies within its enhanced efficiency at low insulation compared to IncCond or the P&O technique. Due to this CV approach is capable of being highly efficient when merged with other MPPT approaches.

The efficiency of SCC technique is relatively less compared to other methods under frequently fluctuating atmospheric conditions, since it was unable to have PV module operated at its MPP. Upon adjusting solar radiation at t=200ms, the irradiance was 1000w/m² plus t=300ms, with the level of irradiance decreasing to 800 w/m2 and eventually dropped to 400w/m² at t=400ms (as illustrated in Figure 5.13). The reason behind this was the fluctuation of the duty cycle in the wrong direction up to when the new SCC measurements were gauged, hence restoring the reference current value. As a result, minimal regulation speed is capable of establishing high efficiency than high speed, more so during frequently varying atmospheric conditions. The ability to gauge SCC during the system's operation is considered as the key advantage associated with this method, since it normally needs addition

of an extra switch between the converter and the PV module. Ref [4] suggests using a boost converter and employing the converter switch to short the PV module. However, this approach results in an increase in power loss. A further drawback of this technique is that the current factor is an approximation, which will change if a PSC occurs.

Additionally, the implementation of OCV algorithm is considered uncomplicated and simple, since no input is needed. Furthermore, the PV module voltage requires being gauged in order to set the reference voltage, which needs regulating the operating point of the PV module, for the purpose of facilitating its closeness to MPP. This is attained by having the converter's duty cycle regulated to meet the module voltage with the Vmax. Regardless these advantages, this method, just like with the CV technique, ignores the effect of temperature and solar radiation on the output of PV module, resulting in decreased precision, and inability to acquire MPP constantly. This method requires OCV measurements, resulting in the need to insert a switch between the converter and the PV module. In addition, for the purposes of calculating the OCV, this OCV technique needs extra valves, as well as a capacitor between the converter and the module as a measure of facilitating power to the load during open circuit. Additionally, due to unevenness between the OCV to Vmax ratio with the ambient temperature, this method is only able to maximize the power at a single temperature. For that reason, this method is unable to facilitate the optimal efficiency achieved by IncCond and P&O methods, however it is normally highly efficient compared to the SCC technique.

5.4. Summary

This chapter has established that the MPPT algorithms employed in PV systems are among the most significant of the different variables underpinning the system's electrical efficiency. It has also identified that, in order to optimise costs, algorithm selection should be given close thought once the implementation of an MPPT system has been decided. The current study provides a comprehensive overview of the categorisation and features of the most popular MPPT algorithms. A discussion has already been extended to the operating concepts and application procedures of MPPT algorithms, including: P&O; CV and current; and IncCond. Table 1 presented the analysis findings, and determined the ranges of efficiency as well as further comparison parameters. It was noted that different algorithms are chosen based on different considerations, and that P&O and IncCond comprise the most frequently used MPPT algorithms, due to their cost-efficiency and simplicity. MPTT applications have recently been increasingly integrated with software-based artificial intelligence methods, i.e. FL, ANN and GA.

This section has offered a discussion of the functionality of five widely used MPPTs concerning their speed, performance, cost and competence. By considering the results from simulation, it is evident that the optimal performance was acquired from the IncCond technique, since it offered the optimal efficiency levels. The P&O technique equally exemplified a significant intensity of efficiency; though, it suffered low efficiency levels at decreased levels of irradiance, since its response duration is inadequate under minimal solar radiation. Therefore, the IncCond method can be used in an application where high and rapid changing weather conditions are usual, as its response time is relatively independent of the radiation level. Both IncCond and P&O methods need a high-performance microcontroller compared to the other 3 techniques (that is, OCV, CV, and SCC). Among these methods, the most satisfactory results were evident from the CV technique, with its functionality under minimal solar radiation being highly effective compared to P&O technique. Therefore, the CV technique is regarded as the easiest method and is capable of facilitating excellent performance in situations needing cost minimization. Both SCC and OCV approaches demonstrated the least efficiency, more so under frequently varying conditions. Moreover, additional valves are required in the converter for the OCV and SCC methods, resulting in lower efficiency and greater power losses.

IncCond algorithms are considered to be the most effective on-line MPPT algorithms in detecting and remaining at the MPP, requiring a control circuit of greater complexity but generating more power. As previously noted, the primary drawbacks of P&O MPPT algorithms include: insufficient response speed; fluctuation around the MPP; and tracking in an incorrect direction when atmospheric conditions undergo rapid change. Hence, the current study seeks to identify solutions to these drawbacks, in order to improve the efficiency of MPPT algorithms, as these algorithms are frequently employed in PV systems. The further analysis of the P&O and IncCond methods, along with their performance, will be investigated in detail in Section 6.4 of Chapter Six.

Chapter Six

Particle Swarm Optimisation (PSO)

6. Introduction

This chapter will: firstly, provide an overview of the PSO algorithm. Secondly, it will propose a simple technique to overcome the drawbacks of the conventional MPPT algorithms, along with their difficulty in tracking under variable conditions. Thirdly, there will an analysis of different MPPT techniques, including the issue of their tracking efficiency under fast-changing irradiance.

6.1. Overview of the Particle Swarm Optimisation Algorithm

A further optimisation technique capable of being applied in a multivariable function optimisation with many local optimal points is the PSO algorithm, as outlined by Kennedy and Eberhart in 1995 [96, 98]. The principle of the PSO algorithm has been inspired by the social behaviour observed in natural phenomena, e.g. bird flocking and fish schooling. The differences between PSO and alternative global optimisation methods consist of PSO's easy implementation and rapid convergence. As a result, PSO has received increased attention from researchers studying its use with MPPT in PV systems. Following the flocking analogy noted above, PSO models several cooperative 'birds', in the form of particles, acting together in a 'flock', otherwise known as a swarm. Each particle moving in the swarm has a fitness value mapped by an objective function and an individual velocity, which the particle uses to decide the direction and distance of its movement. Each particle exchanges the information it obtains during its respective search process [93 - 98].

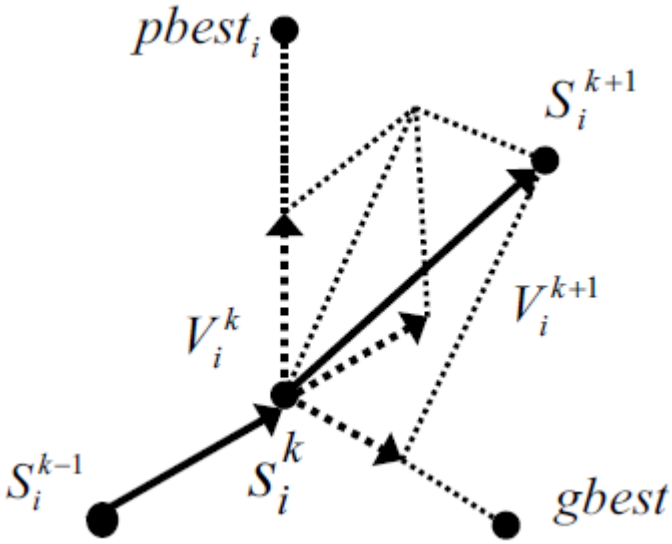

Figure 6.1.Movement of a PSO particle [16]

The position of a particle is influenced by two variables: (1) the most effective solution is identified by the particle itself (*p*best), which is stored for use as an individual best position; and (2) the best particle in a neighbourhood (*g*best), which is stored as the best position of the swarm. The particle swarm employs this method to move towards the best position and continuously revises its direction and velocity. In this manner, each particle ultimately moves to an optimal point, or close to a global optimum [16]. The standard PSO method can be defined by means of the following equations:

$$v_i(k+1) = wv_i(k) + c_1 r_1.\left(P_{best} - x_i(k)\right) + c_2 r_2.\left(g_{best} - x_i(k)\right) \quad (6\text{-}1)$$

$$x_i(k+1) = x_i(k) + v_i(k+1) \quad (6\text{-}2)$$

i=1, 2…, N

Where xi and vi are the velocity and position of particle i, respectively; k represents the iteration number; w is the inertia weight; r1 and r2 are random variables, whose values are uniformly distributed in the range (0,1); and c1 and c2 represent the cognitive and social coefficients, respectively. *P*best,i forms the individual best position of particle i, and *g*best,i is the best position of all particles in the swarm. If condition (6.4) of the initialisation has been satisfied, the method is updated as (6.3):

$$p_{besti} = x_{ik} \quad (6\text{-}3)$$

$$f(x_{ik}) > f(p_{besti}) \quad (6\text{-}4)$$

where f represents the objective function to be maximised.

The essential operating guideline for this strategy can be clarified as follows:

Stage 1 (PSO Initialisation): a random initialisation of the particles is considered by engaging a consistent allocation over the search area, or getting instigated on grid nodes within the search space with halfway points. The primary velocities are determined randomly.

Stage 2 (Fitness Evaluation): each particle's fitness value is examined by having the candidate solution supplied to the objective function.

Stage 3 (Update Individual and Global Best Data): pbest,i and gbest (individual and global best fitness values, in that order) plus the positions, are renewed via comparing the freshly computed fitness values with the preceding examples, as well as having the pbest,i and gbest replaced (in addition to their resultant positions), as required.

Stage 4 (Update Velocity and Position of Each Particle): each particle's position and velocity within the swarm is updated using (6.1) and (6.2).

Stage 5: (Convergence Determination): checking of the convergence measure is done, and, when achieved, termination of the process may occur; else, the iteration number goes up by 1 and go to stage 2.

6.1.1. Application of Practical Swarm Optimisation to Maximum Power Point Tracking

This chapter explains the application of the PSO technique in bringing solution to the intricacy entailing the MPPT controller in a PV system. The planned PSO-based MPPT algorithm's flowchart is exemplified in figure 6.2, with the key blocks of this algorithm being delineated as follows:

Step 1. *(Parameter Selection):* As far as the planned MPPT algorithm is concerned, the converter's duty cycle is described as the particle position; the derived output power being considered to operate as the fitness vale assessment function; with each particle's initial

velocity and position being initialised at random and in a consistent distribution within the search space.

Step 2. *(Fitness Evaluation):* The fitness value of particle i, is calculated subsequent to the controller issuing the duty cycle directive, symbolizing the location of particle i.

Step 3. (Update Individual and Global Best Data): pbest, i and gbest positions and values are revised by evaluating the freshly computed fitness values with those obtained previously, plus having pbest, i and gbest and their resultant positions replaced accordingly.

Step 4. *(Update Individual and Global Best Data):* updating fitness values, gbest (global best fitness values) and pbest (individual best positions), of each particle is achieved by having the fresh computed fitness values with the preceding examples as well as substituting the gbest and pbest equivalent to their positions as needed.

Step 5. *(Update Velocity and Position of Each Particle):* by engaging the assessment of all particles, each particle's positions and velocities in the swarm are updated via engaging PSO equations (6.1) and (6.2).

Step 6. *(Convergence Determination):* The converge criterion are located either to the optimal solution or reach the maximum number of iterations. If the convergence criterion is met, the process will terminate; otherwise, rerun Steps 2 through to 7.

Step 7: *(Reinitialisation)*; by considering the PSO technique, the convergence technique is either to establish the most favourable solution, or attain the maximum number of iterations. However, the fitness value in PV systems does not remain constant, since it varies respective of the applied load as well as the atmospheric conditions. For that reason, there is the need to reinitialise PSO while a search recommenced for a novel method of identifying the novel MPP upon having the output of the PV module varied. In the present utilization, reinitialisation of the planned PSO algorithm is met upon satisfying the below functions:

$$\frac{p_i(k+1)-p_i(k)}{p_i(k)} > \Delta p \qquad (6\text{-}5)$$

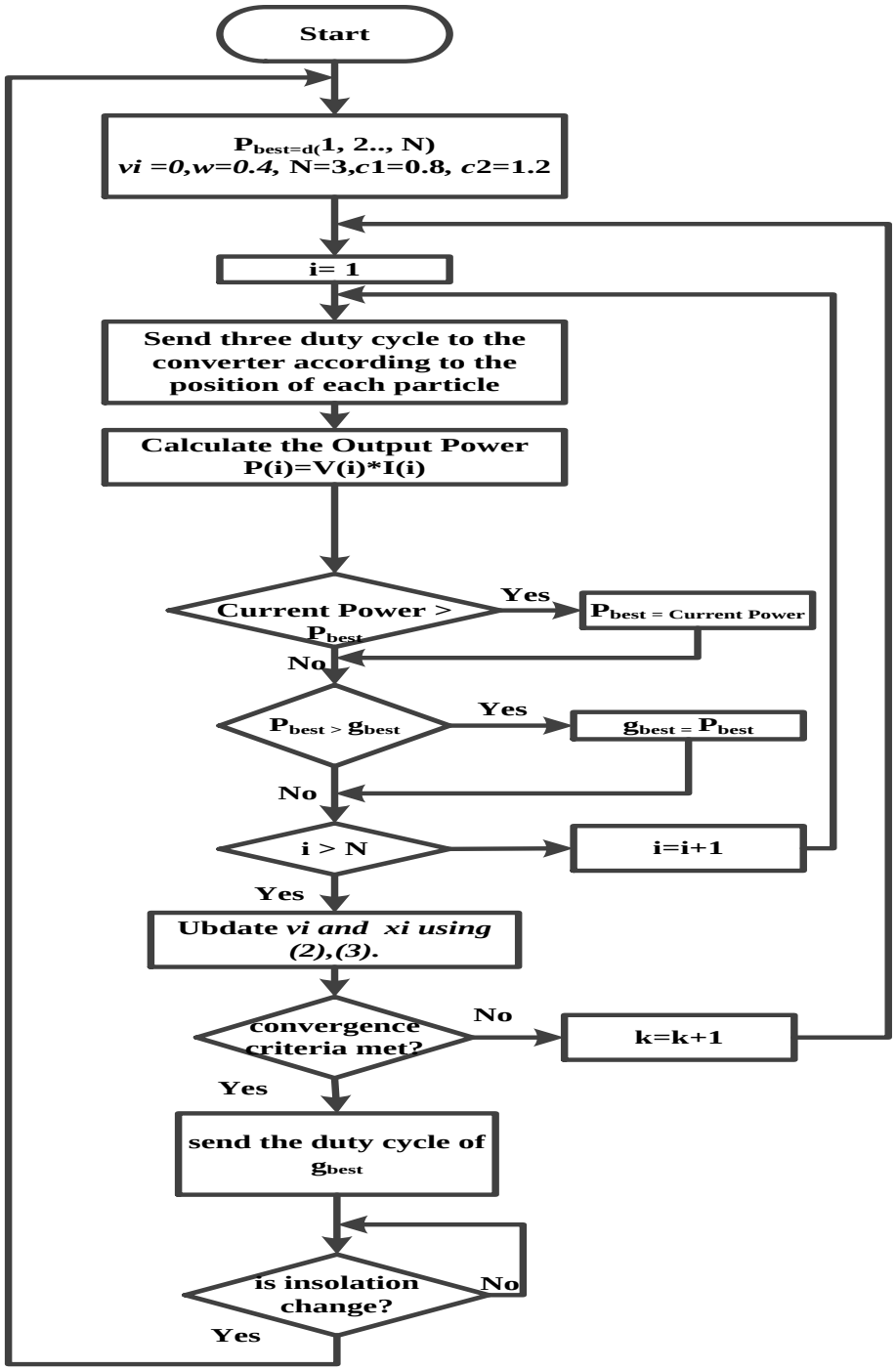

Figure 6.2. PSO Method flowchart [146]

6.2. Analysis of Maximum Power Point Procedures

6.2.1. Dynamic Behaviour of Perturbation and Observation and Incremental Conductance methods

Chapter 5 described the ways in which the P&O technique is able to develop a number of inaccuracies in a situation in which the level of irradiance undergoes a succession of rapid changes. The INC technique also contains the same issue. MPPT will not function correctly

when the fluctuation in the level of intensity leads to a considerable variation in power (i.e. more than the variation caused by the change in the value of voltage), since it will presume that the variation in power has been produced due to its action. The entire sequence of events is depicted in the following figure:

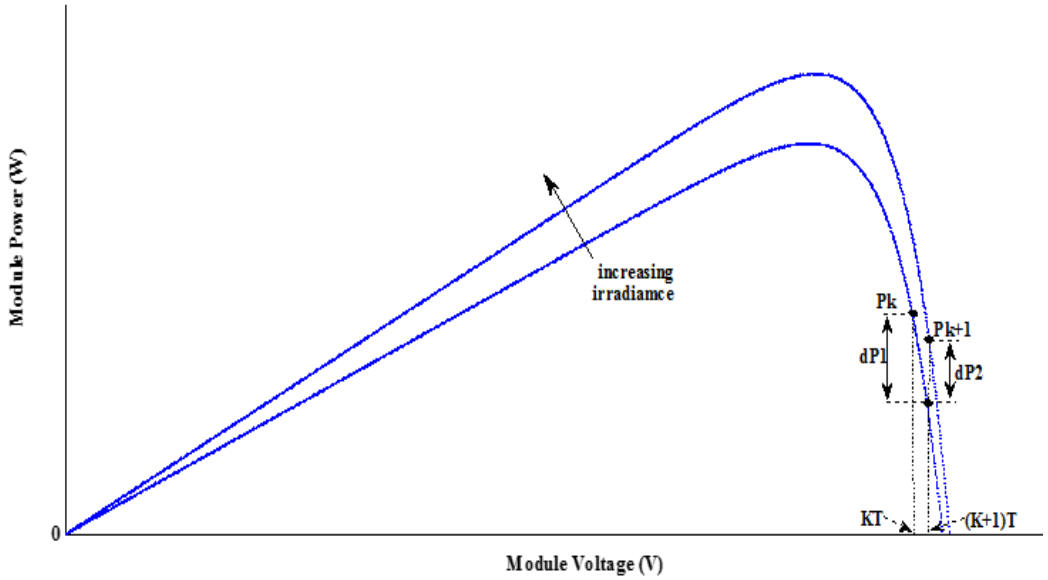

Figure 6.3: When the change in level of irradiation is gradual then both the INC and the P&O techniques function properly and follow the tracking path accurately.

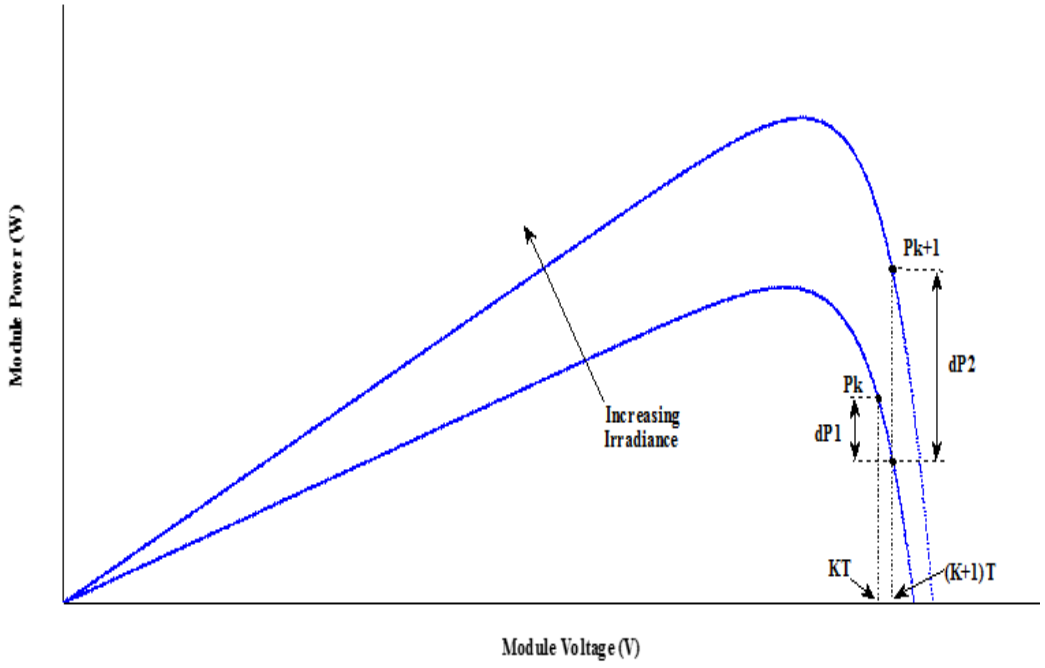

Figure 6.4: When the change in level of irradiation is quick then both the INC and the P&O techniques are unable to follow the tracking path accurately.

In relation to Figure 6.3 and 6.4:

T Stands for the duration for which MTT is measured;

P_k, P_{k+1} denotes the amount of power at k and k+1 sampling intervals;

dP_1 denotes the effect of disturbance in MPPT on the value of power; and

dP_2 stands for the variation in value of power due to a rise in irradiation.

The calculation of a change in power with reference to any two sampling points is accurately undertaken by MPPT when the dP2 is less than dP1, since the variation in power will have the ability to depict the impact of the disturbance, as demonstrated in Fig. 6.3. Where the dP1 is less than dP2, P_{k+1}-P_k (depicted in Figure 6.4) will always remain positive, irrespective of the change in the direction of MPPT, and MPPT will be unable to correctly pinpoint the tracking direction.

6.2.2. Tracking of Particle Swarm Optimisation for Maximum Power Point

Fig. 6.5 demonstrates the behaviour of PSO under a uniform of solar radiation levels. The red points in Figure 6.5 denote duty cycle d1, i.e. the pink points stand for duty cycle d2, and duty cycle d3 is represented by blue points.

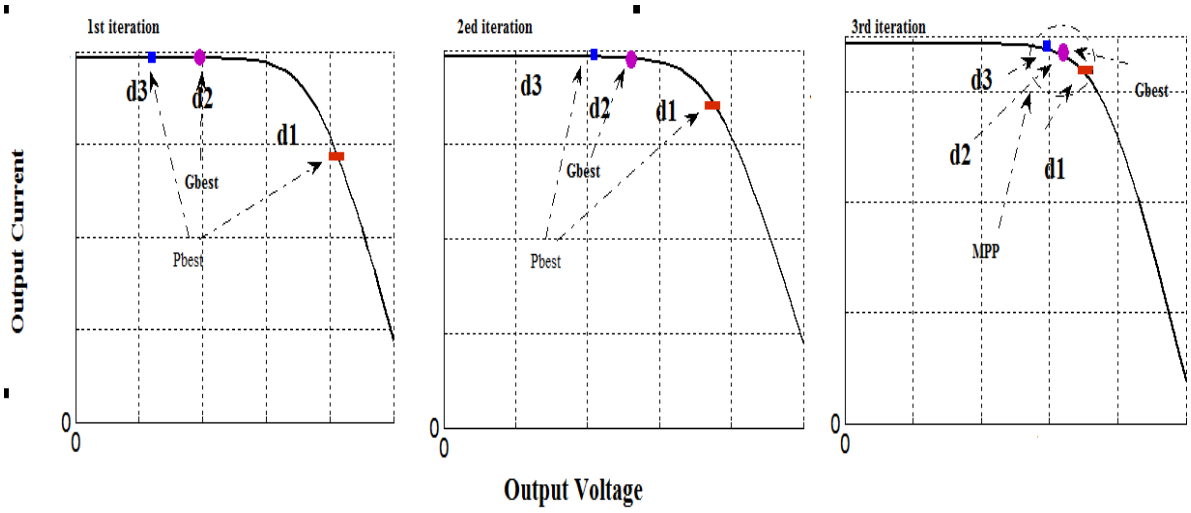

Figure 6.5. The tracking principle of PSO in searching for the MPP.

In relation to the initial cycle, the duty cycle plays the role of *p*best*i*. As demonstrated in Figure 6.5 (a), the title of *g*best goes to d2, as it is from this that the most accurate fitness value is achieved (i.e. this provides the value of array power). The total velocity is dependent

solely on *g*best in case of the second cycle. Since the value of (*p*best*i* −*d* (*i*)) results as null (6.2), the value of *g*best velocity (denoted by d2) also results as null. Hence, the duty cycle experiences no change, and velocity remains 0. Therefore, the process of exploration will not be influenced by this particle. Figure 6.5 (b) depicts the strategy employed in practical situations where a minor amount of change in the duty cycle is created, so that the fitness value also undergoes a measure of change. Figure 6.5 (c) depicts the movement of particles in the third cycle. The particles related to previous cycles continue to progress toward *g*best in the same direction as their fitness value is in a good form. As far as the third cycle is concerned, the velocity value is at the minimum in case of all duty cycles (*di*, *i* = 1, 2, 3). The velocity further decreases in the next cycle and ultimately the duty cycle reach a fixed value. The oscillations around MPP subsequently decrease and there is no change in the operating point.

6.2.3. Effect of Partial Shading Conditions

The solar cells in the practical system are connected in a series of parallel configurations to form the modules/arrays to generate the desired value of the voltage. However, the PV module output voltage is determined by the generated output current. This depends primarily on the solar radiation conditions, as it is directly proportional to the irradiance. This will result in an opportunity to have different maximum output power points instead of one MPP in an application such as multiple PV modules working at different irradiance conditions. This may result in a substantial reduction of the output power of the complete system, as its controller is unable to establish the true operating point at MPP. This condition can occur due to a PSC [16–19]. Figure 6.6 demonstrates I-V-P curves used to test the performance of LI-PSO and studied techniques under PSCs.

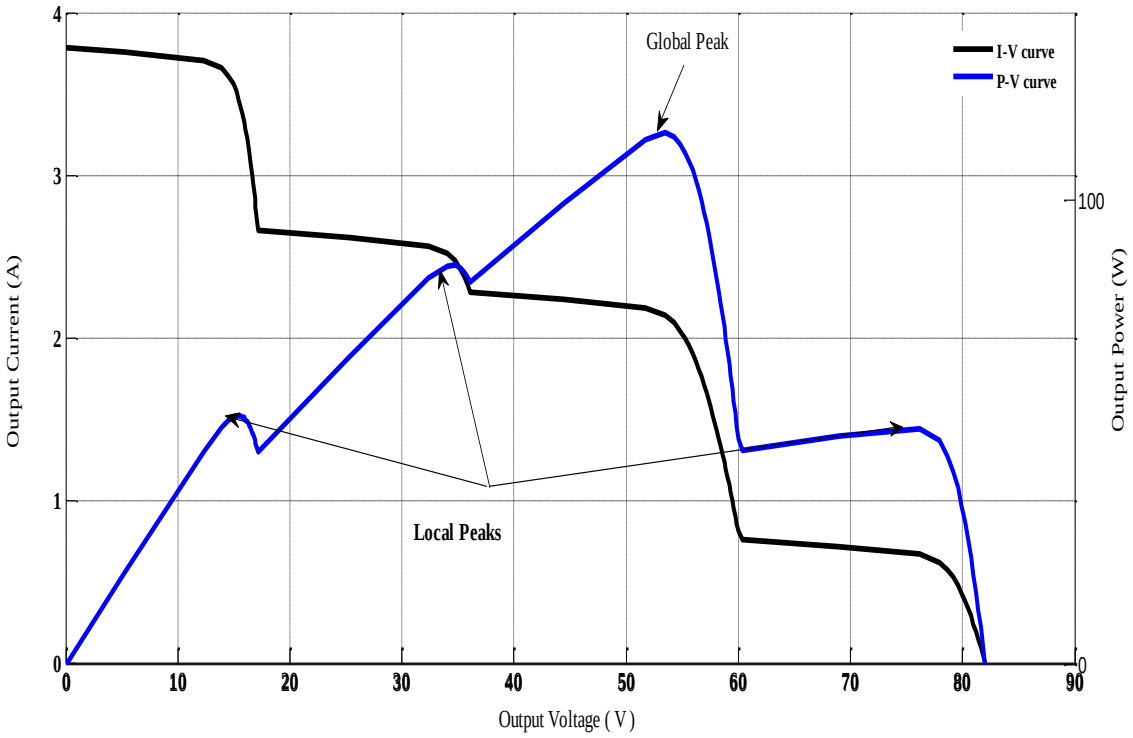

Figure 6.6. I-V-P curves used to test the performance of the LI-PSO and studied techniques under PSCs.

6.2.4. Dynamic Behaviour of Perturbation and Observation and Incremental Conductance under Partial Shading Conditions

The efficiencies of conventional P&O and IncCond MPPT methods, are above 92%. However, their efficiencies are reduced under PSC, during which the PV array exhibits multiple MPP, leading to the potential for conventional methods to lose the direction of tracking the true MPP. As described in Chapter 5, conventional MPPT methods are based on the slope and sign value power to voltage dP/*dV*. Therefore, the MPPT controller will be unable to differentiate the true MPP and local MPP, and will force the PV module operating point into the local MPP, causing a reduction in the system output power. Fig. 6.7 demonstrates the tracking principle of conventional MPPTs under PSC, and the reasons it can fail to track the true MPP.

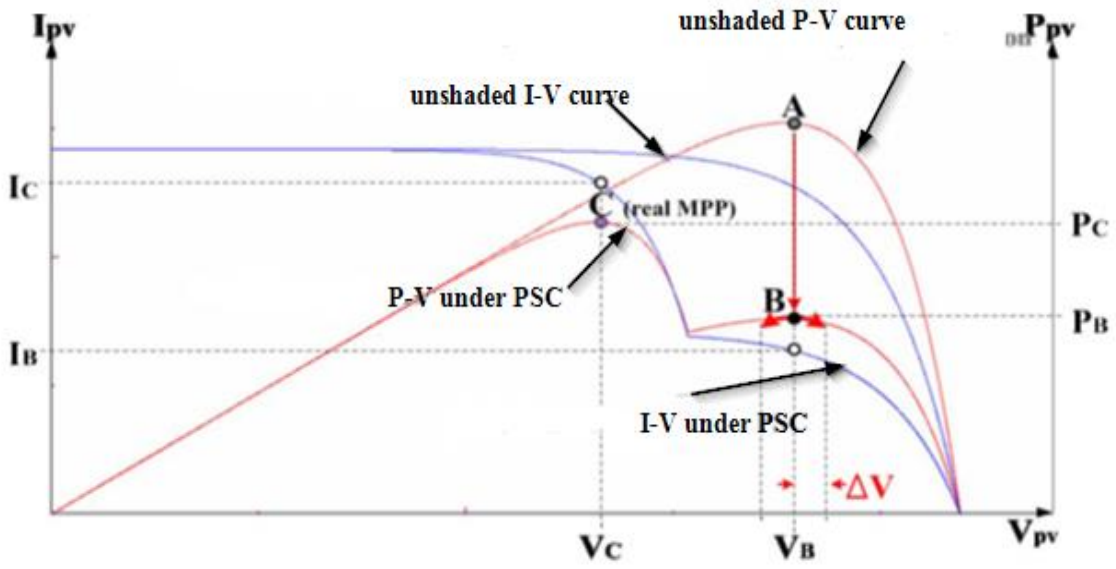

Figure 6.7: The tracking principle of conventional MPPTs under PSC

As seen in Figure 6.7, prior to the occurrence of the PSC, the operating point of the PV module was at point A. When PSC occurred, the operating point of the PV module moved to point B instead of the true MPP (which, in this case, is C). As a result of the conventional method principle, the PV operating point oscillates around point B, due to the predetermined voltage reference step (ΔV). Therefore, the PV module will be operated at PB instead of PC, which is the true MPP. The operating point needs to move to point C to increase power. A number of improvements to increase the conventional methods of efficiency under PSC have been proposed in the literature, by adding adaptive perturbation. However, these techniques remain relatively ineffective.

6.2.5. Tracking of Particle Swarm Optimisation during Partial Shading

Where the solar irradiation is identical for the complete PV array, the resultant PV curve has a unique MPP value. However, many peaks are present in the PV curve in situations of partial shading, including one GP and many local peaks, as demonstrated in Figure 6.8.

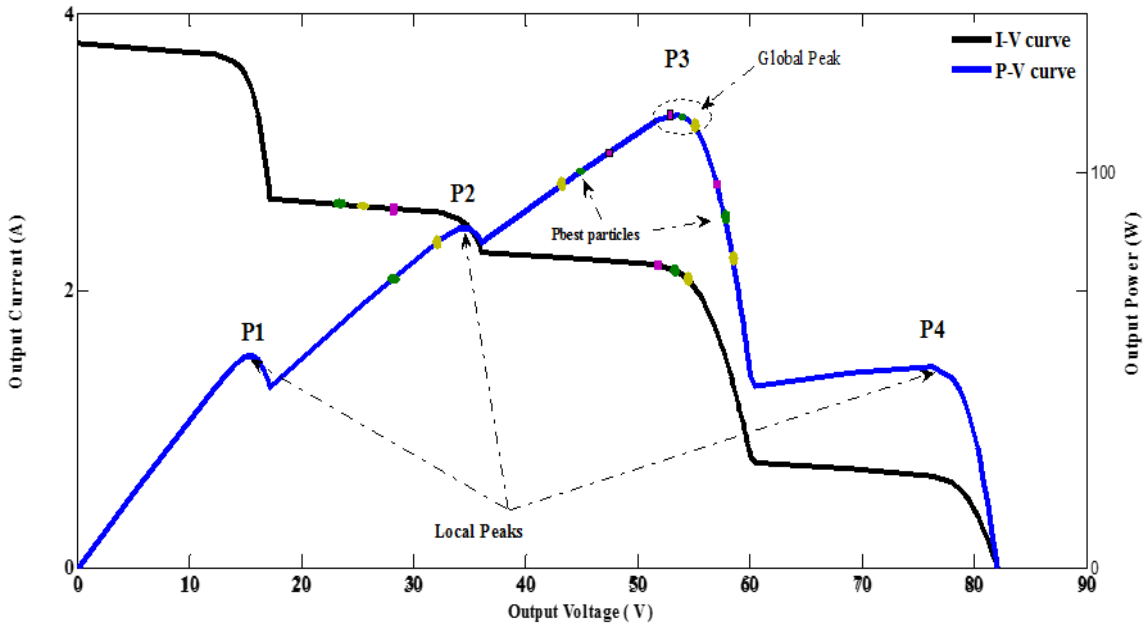

Figure 6.8. MPPT tracking by PSO during partial shading.

In the given graph, there are four stairs in the I-V curve and four peaks in the P-V curve, the latter being denoted by P_1, P_2, P_3, and P_4. Both the local and GPs have 0 as their time derivative dP/dV. The given procedure was unable to differentiate between global (P_3) and local (P_1, P_2, P_4) in an accurate manner, due to the majority of methods related to MPPT employing the slope and sign value of dP/dV. There is a greater likelihood that MPPT is inadvertently tapping into the local peak, causing a decrease in output, and subsequently leading to a poor result from the entire PV assembly. Correct demarcation of GP takes place in the case of the P&O technique, as the technique is based on use of search methods. The expertise of P&O in tracking in situations of partial shading is demonstrated in Figure 6. As in the previously demonstrated curve (i.e. Figure 6.8), three duty cycles are also present in this method, playing the role of *p*best particles. Both the current and voltage values lay away from the GP (P_3) during the initial stage, gradually reaching the GP (P_3) with the progression of cycles.

6.3. An improved Particle Swarm Optimisation based Maximum Power Point Tracking

"The difference between the PSO algorithm and conventional techniques is that the updating of the duty cycle based on the particle velocity is not fixed in the PSO method, while in other techniques the duty cycle is perturbed by a fixed value. This results in oscillations around the MPP under a steady state [93 - 99]. The particles are generally initialised in a

random manner in a standard PSO, following a uniform distribution over the search space. This requires long time delays, in order for the particles to converge towards the MPP, thus leading to lengthy computation times [93, 95]. However, a proper initialisation of the particles can improve PSO efficiency and detect superior solutions with a more rapid convergence" [147].

In the proposed PSO algorithms in Section 6.1.1, the three basic parameters (i.e. inertia factor and acceleration coefficients) need to be tuned in order to accelerate convergence. However, the selection of PSO parameters has a considerable influence on its performance, and there is no rule for determining the optimum of its value during its practical application. A common issue with the PSO algorithm is that the change of the duty cycle must be minimal under slow variation in solar radiation, in order to track the MPP correctly. However, this causes a certain amount of energy to be wasted in the exploration process, leading to a slow convergence towards the MPP. By contrast, a sizeable change in the duty cycle does not permit the duty cycles to correctly locate the new MPP [94, 96].

"In view of these drawbacks, a new MPPT method for the PV system is proposed, based on the LI formula and PSO methods. Initially, the LI method is employed to determine the optimum value of the duty cycle in the case of the MPP according to the operating point. Starting from this point, the PSO method is used to search for the true GP. The proposed MPPT controller essentially initialises the particles around the MPP, thus providing the initial swarm with information concerning the most effective position. This can improve PSO efficiency, and lead to a more rapid convergence with zero steady-state oscillations. Additionally, there is no need to place a restriction on the particle velocity, due to the initial values being closer to the MPP" [147].

6.3.1. Lagrange Interpolation Polynomial

The task of polynomial interpolation is to find a polynomial P(x) such that P (xi) = yi for i with $1 \leq i \leq n$. The polynomial interpolation problem was first solved by Newton, with a different elegant solution subsequently identified by Lagrange the Lagrangian method of interpolation can be defined as a method used to find a polynomial of order n that passes through the $n+1$ data points $(x_1, y_1 = f(x_1)), (x_2, y_2 = f(x_2)), \ldots, (x_n, y_n = f(x_n))$, the polynomial P(x) being defined as:

$$P(x) = \sum_{j=1}^{n} P_j(x), \tag{6.6}$$

Where

$$P_j(x) = y_j \prod_{\substack{k=1 \\ k \neq j}}^{n} \frac{x - x_k}{x_j - x_k}. \tag{6.7}$$

Thus, the polynomial P(x) can be written as:

$$\begin{aligned} P(x) = {} & \frac{(x-x_2)(x-x_3)\cdots(x-x_n)}{(x_1-x_2)(x_1-x_3)\cdots(x_1-x_n)} y_1 + \frac{(x-x_1)(x-x_3)\cdots(x-x_n)}{(x_2-x_1)(x_2-x_3)\cdots(x_2-x_n)} \\ & y_2 + \cdots + \frac{(x-x_1)(x-x_2)\cdots(x-x_{n-1})}{(x_n-x_1)(x_n-x_2)\cdots(x_n-x_{n-1})} y_n. \end{aligned} \tag{6.8}$$

For $n = 3$, $p(x)$ the quadratic polynomial that passes through three data points:

$$p(x) = y_1 \frac{(x-x_2)(x-x_3)}{(x_1-x_2)(x_1-x_3)} + y_2 \frac{(x-x_1)(x-x_3)}{(x_2-x_1)(x_2-x_3)} + y_3 \frac{(x-x_1)(x-x_2)}{(x_3-x_1)(x_3-x_2)} \tag{6-9}$$

The function $P(x)$ passes through the points (x_i, y_i), as can be seen for the case $n = 3$,

$$P(x_1) = \frac{(x_1-x_2)(x_1-x_3)}{(x_1-x_2)(x_1-x_3)} y_1 + \frac{(x_1-x_1)(x_1-x_3)}{(x_2-x_1)(x_2-x_3)} y_2 + \frac{(x_1-x_1)(x_1-x_2)}{(x_3-x_1)(x_3-x_2)} y_3 = y_1 \tag{6-10}$$

$$P(x_2) = \frac{(x_2-x_2)(x_2-x_3)}{(x_1-x_2)(x_1-x_3)} y_1 + \frac{(x_2-x_1)(x_2-x_3)}{(x_2-x_1)(x_2-x_3)} y_2 + \frac{(x_2-x_1)(x_2-x_2)}{(x_3-x_1)(x_3-x_2)} y_3 = y_2 \tag{6-11}$$

$$P(x_3) = \frac{(x_3-x_2)(x_3-x_3)}{(x_1-x_2)(x_1-x_3)} y_1 + \frac{(x_3-x_1)(x_3-x_3)}{(x_2-x_1)(x_2-x_3)} y_2 + \frac{(x_3-x_1)(x_3-x_2)}{(x_3-x_1)(x_3-x_2)} y_3 = y_3. \tag{6-12}$$

The use of the LIM has the advantage of having no requirements for the data points to be in order, or arranged in a particular order. Moreover, the Lagrange polynomial is simple, and

does not require uniform spacing, as it can be fitted to both equally or unequally spaced data [136,137].

6.3.2. Maximum Power Point Tracking algorithm based on numerical calculation

Due to its effective start-up features, the (CV) method is employed to ensure the MPPT algorithm is more rapid and precise. The suggested control mechanism is characterised by a simple control policy with sample arithmetic facilitating its implementation in hardware, and therefore contributing to the enhancement of the speed, stability and precision of MPPT. Moreover, the three sampling point design can prevent erroneous interpretations influenced by rapid transformations in environmental conditions.

"A novel MPP tracking controller based on the LI and a PSO method is proposed to rapidly identify MPP, and overcome the issues posed by the conventional MPPT algorithms of speed, stability and accuracy. The scheme proposed in this study estimates the value of the voltage (V_{MPP}) of the PV module I–V characteristic in the first step using the CV method approximation. As illustrated in Figure 6.9, the voltages of the MPPs (V_{MPP}) near a CV value at a particular degree of temperature of the solar radiation. The control concept underpinning the CV method is that the operating point will always function close to the MPP, provided that the output voltage of the solar arrays remain at the CV close to V_{MPP}. As outlined in Chapter 5, the V_{MPP} in this method is established to be 0.78 times that of open-circuit voltage, since modifications in irradiations have no significant influence on the open-circuit voltage of the PV modules" [147].

The value of V_{MPP} is equal to the measured PV module maximum output voltage at standard test conditions (STC), present on the PV module data sheet. This technique assumes that the value of V_{MPP} is approximately equal at different irradiance, as demonstrated in Figure 6.9 [47,48].

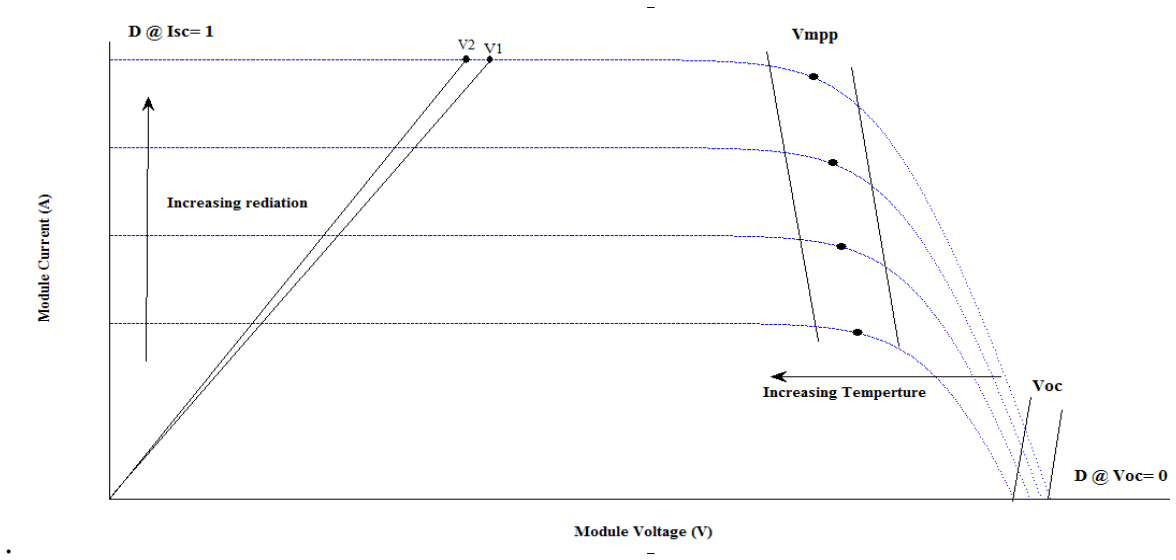

Figure 6.9: I-V Characteristic of a PV cell [147]

Where Voc represents the open circuit voltage of the PV panel, the ratio between the PV module maximum output voltage and its open circuit voltage is equal to constant K.

$$V_{mpp} / V_{oc} = K \qquad (6\text{-}13)$$

The working principle of the algorithm is shown as follows:

"The algorithm begins by obtaining the present value of *V(k)* and using previous values stored at the end of the preceding cycle, *V(k-1)*. The value of the duty cycle d_{mpp}at (V_{mpp}) is then estimated, using the LIM, employing four selecting points from the (I-V) characteristic. Figure 6.9 represents the PV module (I-V) curve described by a quadratic interpolation function. The interpolation nodes x_1 and x_2 represent the voltage values of two sampling points (V_1 andV_2), while x_0 represents the voltage V_0 at the short circuit current (i.e. equal to zero) and x_3 represents the open circuit voltage provided by the PV module data sheet. The function values y_1 and y_2 correspond to the voltage values representing the duty cycle (d_1 , d_2) values of the sampling points, and y_0 and y_3 represent the duty cycle ($d|_{I_{sc}}$ and $d|_{V_{oc}}$) at the I_{sc} and V_{oc} points, i.e. equal to 1 and 0, respectively. With the values of V_0 ,V_1, V_2 and V_{oc}obtained via the aforementioned process, the value of the duty cycle at MPP d_{mpp} at

(V_{mpp}) is estimated employing LI. Eq 6.14 (below) gives the interpolation formula for d_{mpp}corresponding toV_{mpp}:

$$y(x) = \frac{(x-x_1)(x-x_2)(x-x_3)}{(x_0-x_1)(x_0-x_2)(x_0-x_3)}y_0 + .. + \frac{(x-x_0)(x-x_1)(x-x_2)}{(x_3-x_0)(x_3-x_1)(x_3-x_2)}y_3 \quad (6\text{-}14)$$

Where x is the value of V_{mpp}.

By using the above principle, the algorithm for determining the value of d_{mpp}corresponds to V_{mpp}. Therefore, the PSO algorithm will start the optimisation with the initial value close to MPP"[147.

6.3.2.1. The proposed algorithm

"Unlike conventional techniques, where perturbing and observing the power is a means of tracking the PV MPP, resulting in long computation times, the proposed algorithm computes the value of initial particles' d_{MPP} (duty cycle at MPP) based on the voltage at maximum power, ensuring the algorithm will begin the optimisation with the initial value close to MPP" [147].

The initial value of particles can be defined as:

$$d_i^k = [d1, d\,2, d3, ..., dN\,] \quad (6\text{-}15)$$

Where *N* is the number of particles and *k* is the number of iterations.

To begin the process, the algorithm transmits three duty cycles (*d*1, *d*2, and *d*3) to the Cùk converter. These values will be taken as the *p*best in the first iteration, and the value closer to the MPP (fitness value) will be taken as the *g*best value. The duty cycle velocity and position will be updated according to the *p*best and *g*best values. Consequently, according to the PSO principle, the duty cycle will be perturbed by a small value in the following iteration as a result of comparing the present with the previous fitness value. This process continues until all particles reach MPP (i.e. a best fitness value), where the velocity is near to zero.

Since the value of *d*2 is estimated (i.e. computed using 6.14), *d*1 and *d*3 are calculated by adding and subtracting a value of *d*x from *d*2 to obtain the upper and lower boundaries,

leading to a rapid dynamic response with accurate tracking. Therefore, a new set of duty cycles can be defined as:

$$d\,i\,new = [d2 - dx,\ d2,\ d2 + dx] \tag{6-16}$$

Where dx is chosen to be equal to velocity.

Thus, the duty cycles $d2$ computed using (6.14) will be very close to the final best duty cycle. Additionally, due to the PSO exploration, one of di (i = 1, 2, 3) will remain very close to the best duty cycle. This thus allows the PSO to very rapidly track the new GP. The two particles ($d1$ and $d3$), which represent *p*best, are too close to *g*best ($d2$), and there is no need for any considerable change in their velocity to reach closer to $d2$. In the case of any sudden change in weather conditions, the duty cycle is re-initialised, using (6.16) to set a new duty cycle capable of correctly tracking a new MPP.

The complete flowchart of the proposed method is shown in Figure 6 and the main building blocks of the proposed algorithm can be summarised as follows:

Step 1. Parameter selection: For the proposed MPPT algorithm, the calculated duty cycle of the converter in (6.16) is defined as the particle position, and the PV module output power is chosen as the fitness value evaluation function.

Step 2. PSO initialisation: In standard initialisation, PSO particles are generally randomly initialised. However, for the proposed MPPT algorithm, the particles are initialised at fixed, equidistant points, positioned around the GP.

Step 3. Fitness evaluation: The fitness evaluation of particle *i* will be conducted after the digital controller sends the PWM command, according to the duty cycle representing the position of particle *i*.

Step 4. Determination of individual and global best fitness: The new calculated *p*best and *g*best of each particle value will be compared against the previous examples. They will then be replaced according to their positions, as necessary.

Step 5. Updating the velocity and position of each particle: The velocity and position of each particle in the swarm are updated according to (6.1) and (6.2).

Step 6. Convergence determination: The convergence criterion is checked. If the end criterion is met, computation will terminate, if not, the iteration is increased by one rerun of Steps 2 through to 6.

Step 7. Reinitialisation: The convergence criteria in the standard PSO algorithm are to find the optimal solution, or the success of the maximum number of iterations. However, in a PV system, the optimum point is not constant, due to its dependence on weather conditions and load impedance. Therefore, the proposed LI-PSO algorithm will reinitialise and search for the new MPP whenever the following conditions are satisfied:

$$|v_{i+1}| < \Delta v \tag{6-17}$$

$$\frac{p_i(k+1)-p_i(k)}{p_i(k)} > \Delta p \tag{6-18}$$

Where $p_i(k+1)$ is the new PV power, $p_i(k)$ is the previous PV power at its maximum point, and Δp (%) is set to 1%.

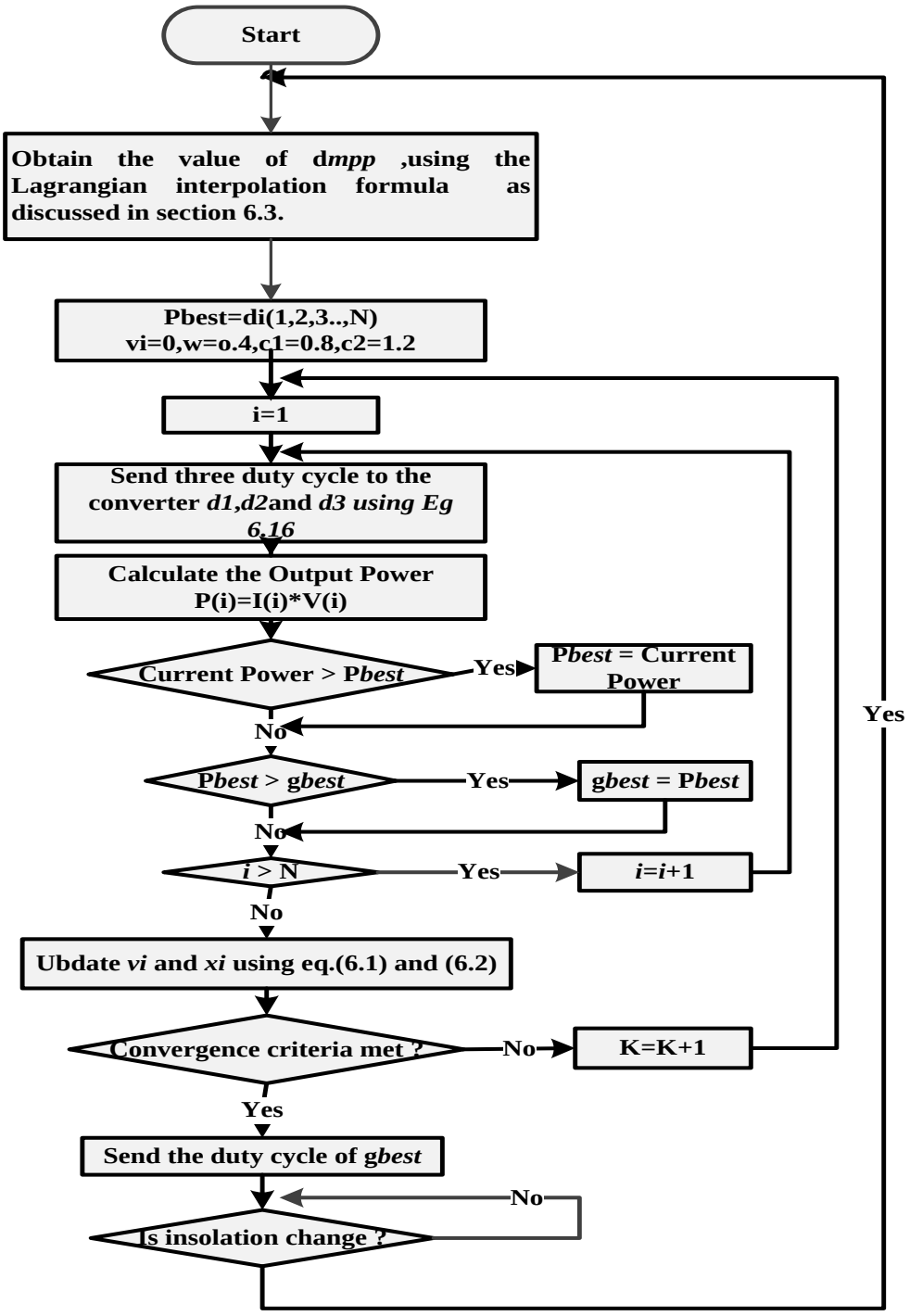

Figure 6.10: LI-PSO algorithm flowchart [147].

Where p_i (k+1) is the new PV power, p_i (k) is the previous PV power at its maximum point. The equations (10) and (11) stand for agent's convergence detection and abrupt alteration of insolation, correspondingly. Like already accounted in [27], there are two matters in ΔV choice: 1) lesser values lead to better MPPT firmness but poor tracking reaction and 2) superior values result in faster tracking reaction at the cost of greater oscillations. Therefore, a balanced rate must be selected. Nevertheless, when ΔP is great the subsequent constraint (11)

might not be contented on account of lesser variations in real power, and therefore the agents' rate of initialization is minor. In line with ref [27] real-time investigational explorations, so as to conquer these restrictions and to attain better tracking performance, the employ of excessive values for ΔV and ΔP must be evaded to warrant MPPT stability.

6.4. Summary

This chapter has: firstly, presented an overview of the PSO and the ways in which it can be applied to track MPP; secondly, it has discussed the dynamic behaviour of existing MPPT methods; thirdly, it has discussed their behaviour in the event of partial shadowing, where the conventional methods tracker can stop at local MPP instead of global MPP; fourthly, there has been an examination of a new MPPT algorithm based on PSO, which can overcome confusion under rapidly changing irradiance. The analyses have revealed that accurate tracking of MPP by means of the PSO technique is not affected by varying conditions. The strength of this method consists of it being efficient in tracking, easy to implement, and has a simple framework. However, in a normal PSO, optimisation performance is influenced by the choice of parameters, since the particles undergo a random initialisation through an even distribution over the search area. This takes considerably more time for them to come together around the MPP, and hence the delayed computation.

However, an effective initialisation of the particles can improve PSO efficiency and detect more effective solutions with faster convergence. Thus, an improved MPPT algorithm has been proposed, based on a simple numerical calculation for determining the values of the duty cycle in the case of MPP, and by which particles can be initialised efficiently around the MPP to avoid both unnecessarily redundant searching and a situation in which the area being actively searched by the swarm becomes too small.

The following chapter will examine the simulation results of the proposed MPPT controller, followed by a comparison with the P&O, IncCond and PSO techniques in terms of their tracking efficiency, convergence speed, and performance.

Chapter Seven

Simulation results

7. Simulation System

A Canadian company named Opal-RT has developed RT-LAB which actually a platform set of test application on the basis of modelling and has the ability to conduct hardware within loop and rapid control prototyping. It employs a special technique to segregate a complicated model into multiple subsystems which will operate simultaneously. Afterwards, a simulation system of changeable distributed parallel real time will be composed from distributing those subsystems to multiple CPU nodes. Fig. 7.1 illustrates the system structure.

A programmable FPGA is installed within the target machine and 10ns is the frequency of digital I/O channel, pulse resolution. One simulation step can obtain or generate multiple pulse events in the platform of RT-LAB simulation system. In this way, the IGBT switch in the electric inverter can be provided with highly précised timing. If the events of FPGA can be combined through identifying unique real time algorithm and function of RE-EVENTs, then 10μs can be obtained as the simulation step [137-143].

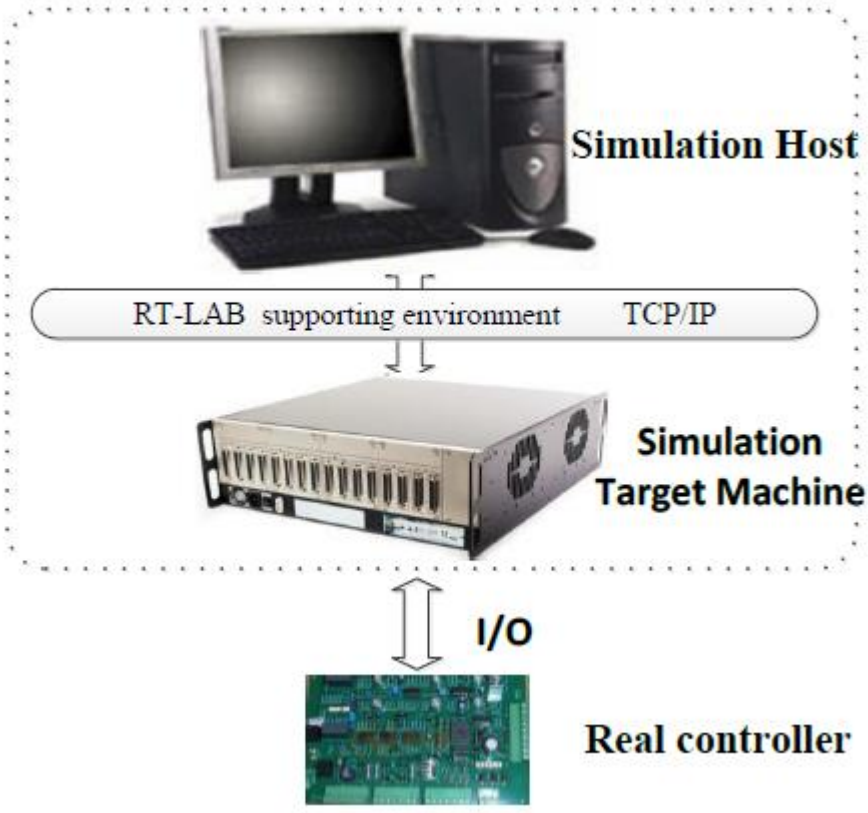

Figure 7.1: Diagram of RT-LAB

7.1. Modelling Standard of RT-LAB

The models that are installed by Simulink are to be compacted out of the apex and SM, SS, and SC should be used to name RT-LAB so that functions of various parts can be ensured. Curve within the simulation system, data communication among the main parameters and real time observation are performed by SC subsystem. Data are gathered and displayed with the help of fundamental module found in programs. SM subsystem takes over the responsibility of network synchronization and real time observation. SS subsystem normally belongs to the system models involved in simulation. Segregated model comprises one SM subsystem, one SC subsystem and SS subsystem. There are only switch, oscilloscope and logic selection and no calculating parts in the SC susbsystem. Opcomm synchronous communication module holds significant part in simulation and each signal has to reach subsystem above via undergoing the Opcomm module [140- 143].

7.2. Testing Program

Fig.7.2 illustrates testing main program. 10μs is the simulation step. Fig. 7.3illustrates SM subsystem. It has the purpose of completing simulation calculation along with synchronous communication of MPPT. A type of advanced conductance increment technique is implemented in the experiment. The modules vulnerable to the events are replaced by RTEVENTS modules. PWM signal is giving accurate output. The digital output module of RT-LAB is the OP5110-5120 Digital Out that has the ability of carrying out output of PWM signal. The analogue input module is the Analog In that also has the ability of carrying out input of current and voltage of photovoltaic cell. FPGA has been blended with the synchronous drive module that is the OP5110- 5120 Opsync.

Fig.7.4 illustrates SC subsystem. It has the ability of performing current, system information, voltage and power of photovoltaic cell. Due to same sampling rate of four signals, only one Opcomm module is required.

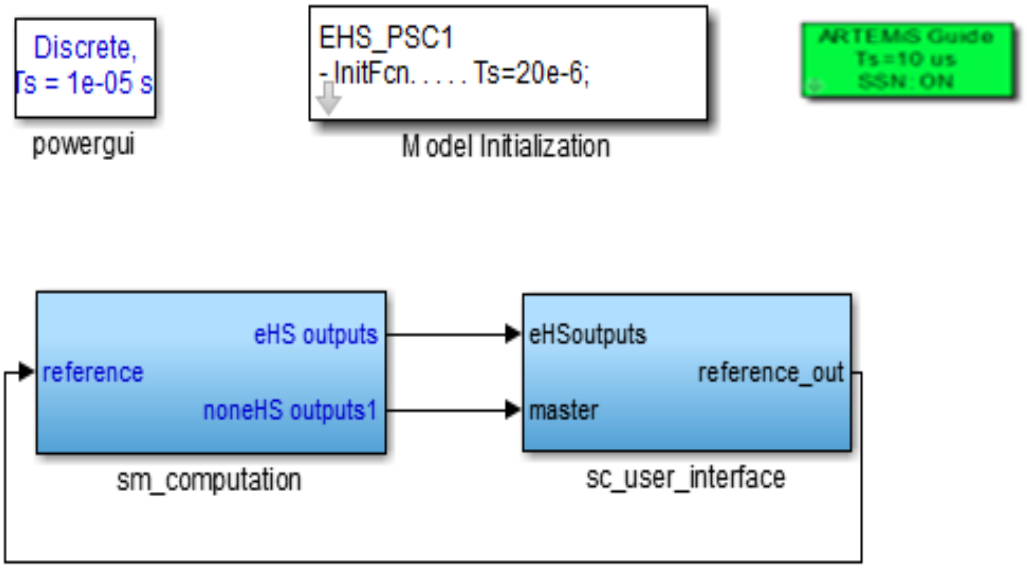

Figure 7.2: Experiment Circuit

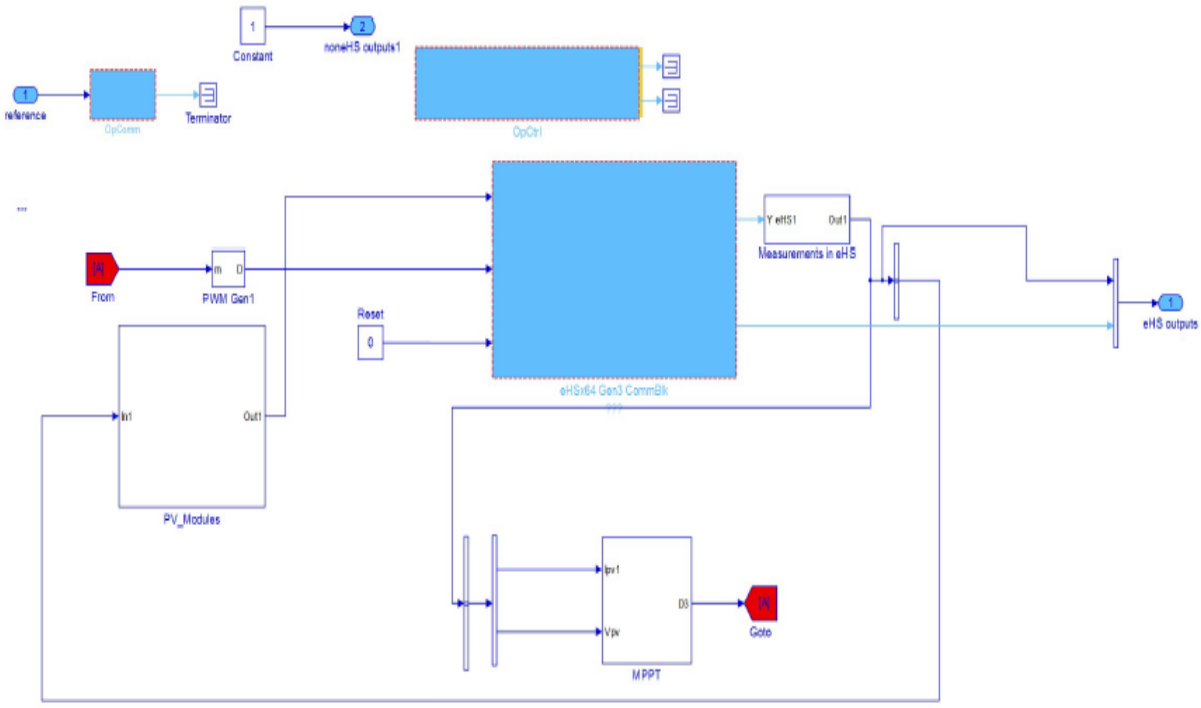

Figure 7.3: SM Subsystem

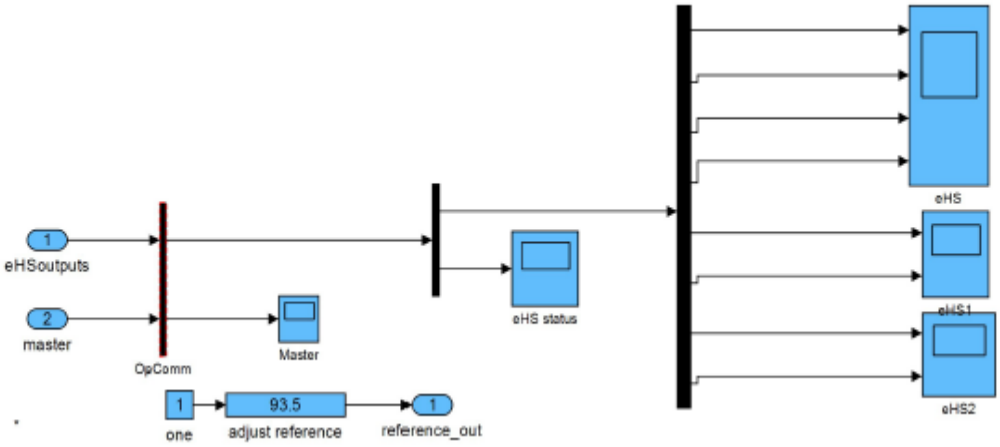

Figure 7.4: SC Subsystem

7.2.1. Testing Results

Fig. 7.5, 7.6 and 7.7 illustrate the waveforms of testing real time simulation. The model was run in real-time with a time-step of 10μs for the proposed control, and 135ns for the electrical circuit, while the PWM pulse was generated at 50 kHz. Section 6.1 accounts the development of proposed MPPT controller. There are three cases that are considered while testing its operation under RT simulation:

Case 1: (Test under STC with insolation of 1000 W/m2 and temperature of 25∘ C)

Case 2: (Test under Climatic Conditions with insolation of 500 W/m2 and temperature of 25∘ C)

Case 3: (Test under PSC where isolation and temperature variations from partial shading)

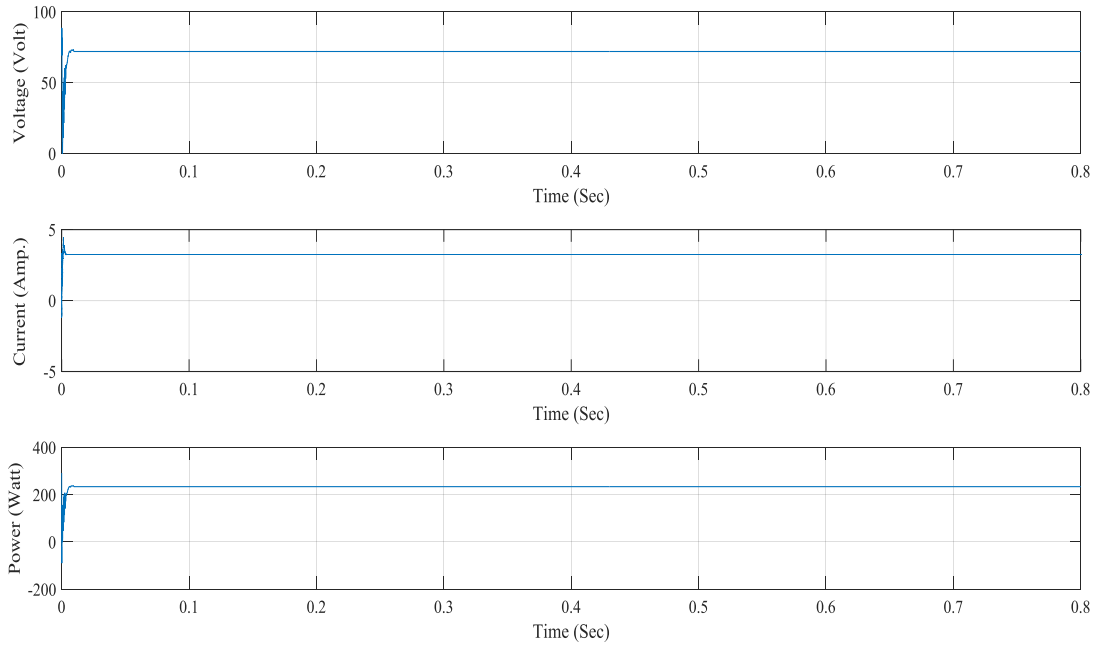

Figure 7.5: OPAL-RT results of LI-PSO MPPT controller (current, voltage, and power) case1 [147].

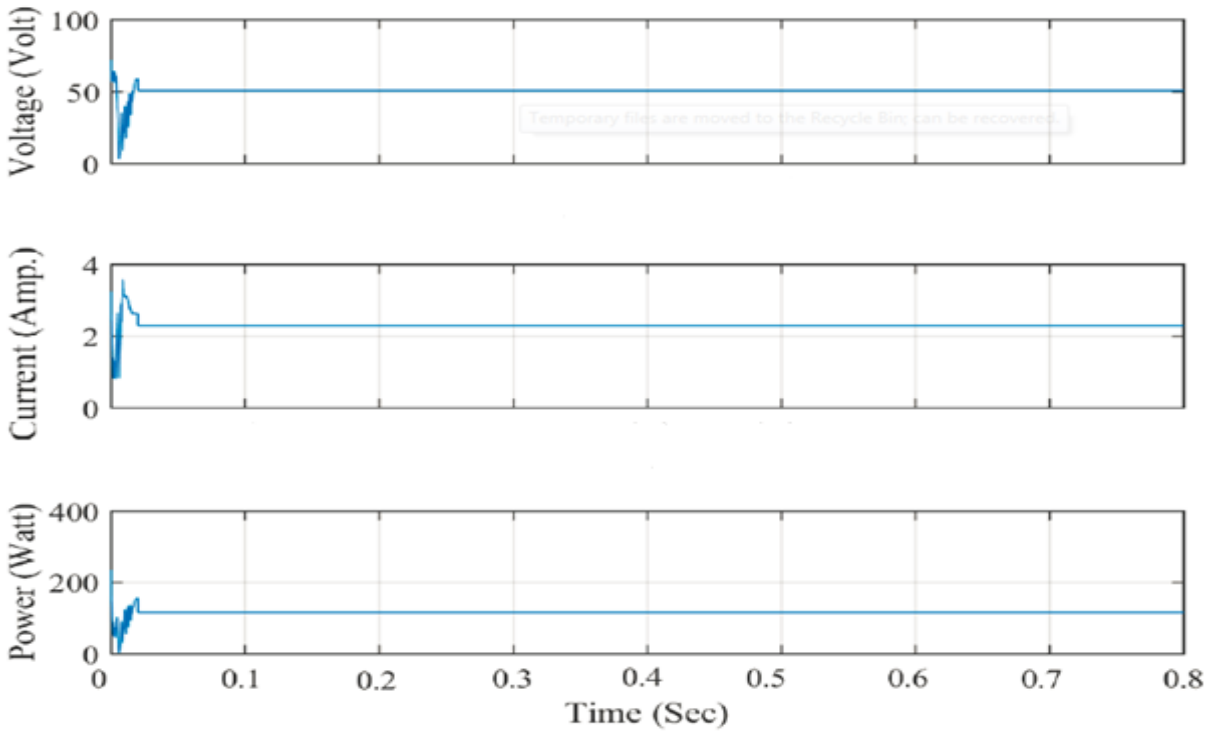

Figure 7.6: OPAL-RT results of LI-PSO MPPT controller (current, voltage, and power) case2.

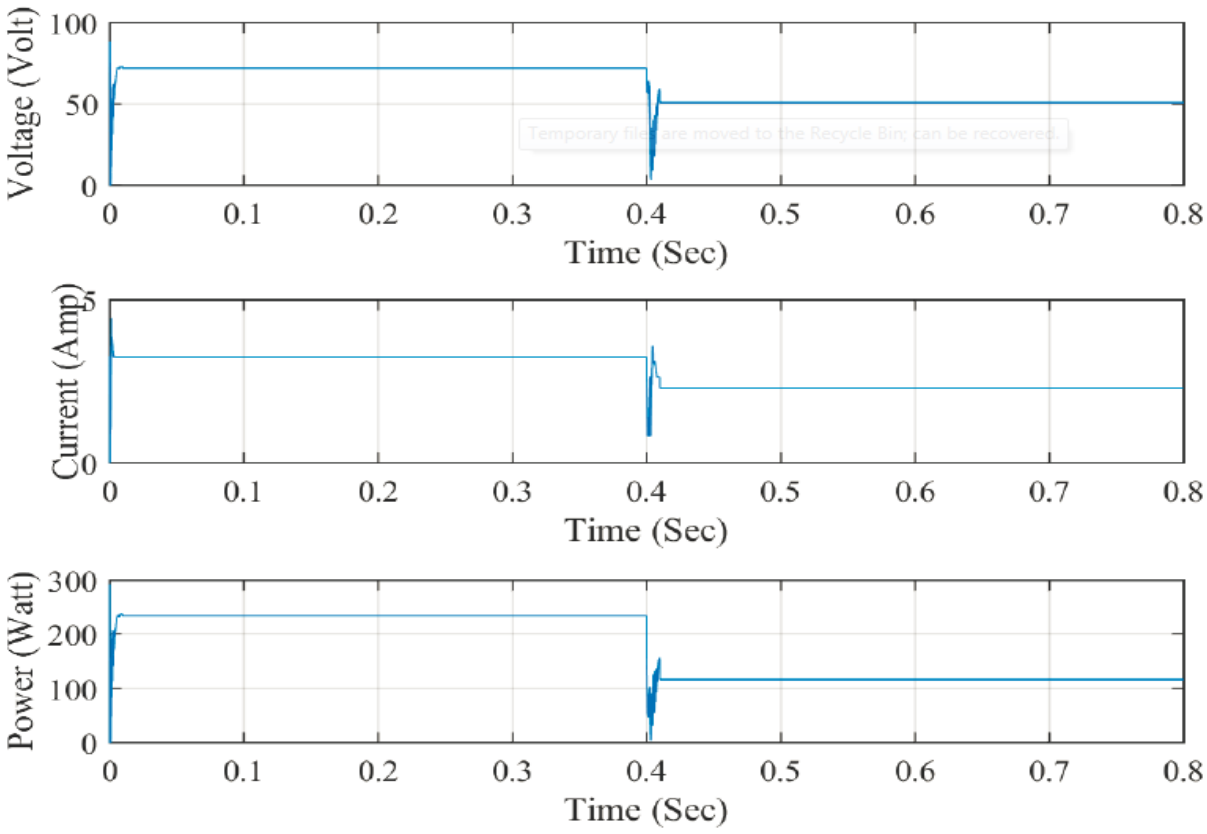

Figure 7.7: OPAL-RT results of LI-PSO MPPT controller (current, voltage, and power) case3.

Fig.7.7 shows that the MPP value being accompanied with the proposed algorithm is 342.64 W whereas for the selected PV module is 340 W. The latter was optimized less than 2

ms with a very fast convergence speed as the LI-PSO brings operating point and optimal point close to each other through a single step.

The system behaviour under the 500 W/m^2 solar radiation level at a fixed temperature of 25°C for the PV modules is shown in Fig.7.6. was 115.67 W is the theoretical value of the MPP especially in these cases where the selected PV can generate that theoretical value of MPP.

Fig.7.5and 7.6 can be referred while observing that the proposed controller acquired the response curves replied more promptly with no oscillation near the MPP compared to the conventional methods. As suggested in the results, MPPT method comprises faster speed and gets rid of oscillation near MPP and usually detects the global MPP in each case.

The output power of the methods investigated and proposed under PSC is depicted in Fig.7.7. Primarily, the maximum power of operating PV was at 240 W when t = 0.4 s. Some of the PV modules from the array were covered, which results four peaks P_1, P_2, P_3, *and* P_4 and P_4 defines the GP. Moreover, this figure illustrates that new global GP is detected by the proposed method at the occurrence of PSC. The proposed method has only one-time restart solving the problem of frequent restarting in dynamic case. The cumulative change of voltage and power is considered as dependable variables to assess environmental change. The proposed MPPT method has the capability of detecting global MPP within dynamic as well as static environment. Thus, its positive qualities in brief will be:

The method is able to detect the global MPP in dynamic and static environment.

Compared to the existing technique, this method is much advanced in detecting speed with no stable oscillation in static environment.

7.3. Simulation of the proposed Maximum Power Point Tracking method

The proposed system has been developed on Matlab/Simulink (Fig.7.8) and consists of a PV module, with the Ćuk converter being selected as the power interface. The MPPT controller (in which the output voltage and current of the PV module are fed to the MPPT algorithm, and subsequently to the output of the PWM signal) is used to drive the switch of the Ćuk converter to execute the MPPT from the PV module. There are a number of benefits to this system: (1) the complete control mechanism is simplified; (2) the time required to perform calculations is decreased; and (3) there is no requirement to tune PI gains, which enables the system to achieve a fast, dynamic response, and considerably reduces its complexity.

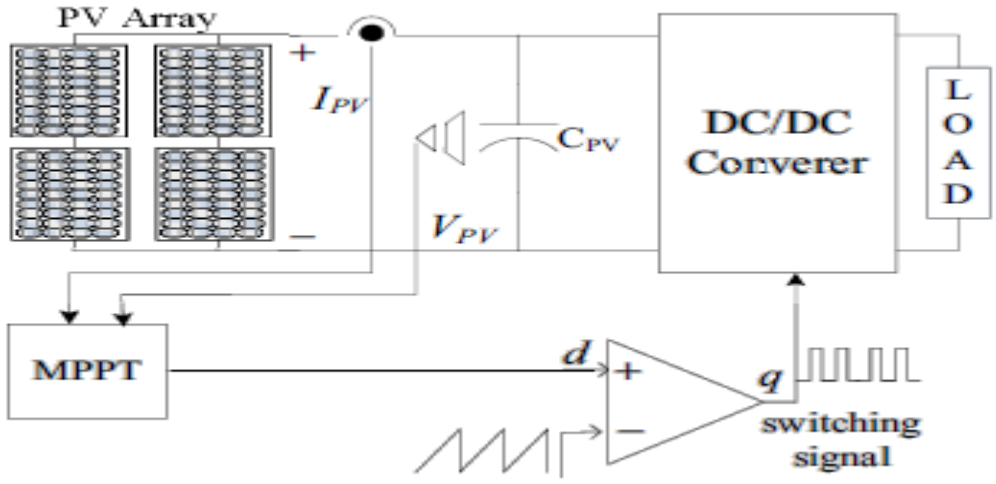

Figure 7.8: Simulink model of the MPPT System

The proposed system was simulated in Matlab to verify the effectiveness of the tracking algorithm and its response time. At the same time, the response time of the proposed algorithm was analysed and compared to P&O and IncCond methods and the conventional PSO-based MPPT (PSO-MPPT) algorithm. P&O and IncCond periodically update the duty cycle *d* (*k*) by a fixed step-size of (0.02). The converter parameters were calculated as described in Chapter 5, and the parameters tabulated in Table 7.1 were used.

Table 7.1: Simulation parameters of cuk converter

L1	L2	C1	C2
1.5mH	2.5mH	10 uF	5 uF
f	50KHz	Rload	10 Ω

The parameters formulated in table 7.1 were employed to implement the PSO algorithm and the proposed scheme.

Table 7.2: The PSO parameters

PSO agents			
M	3	**N**	2
PSO Coefficients			
***C*1**	1.2	***w***	
***C*2**	0.8	0.4	
Condition of initialisation			
Δ*P*	1%	**ΔV**	0.4

"Firstly, the proposed system was simulated with the Matlab model under constant weather conditions at (1000 W/m^2, 25 °C) and (200 W/m^2, 25 °C); secondly, when the PV array was partially shaded (as demonstrated in Figure 6.6); and finally, the dynamic performance of the system was studied according to the test conditions addressed in European Standard EN 50530[22]. The performance of each MPPT technique was evaluated when the steady state condition was reached" [147].

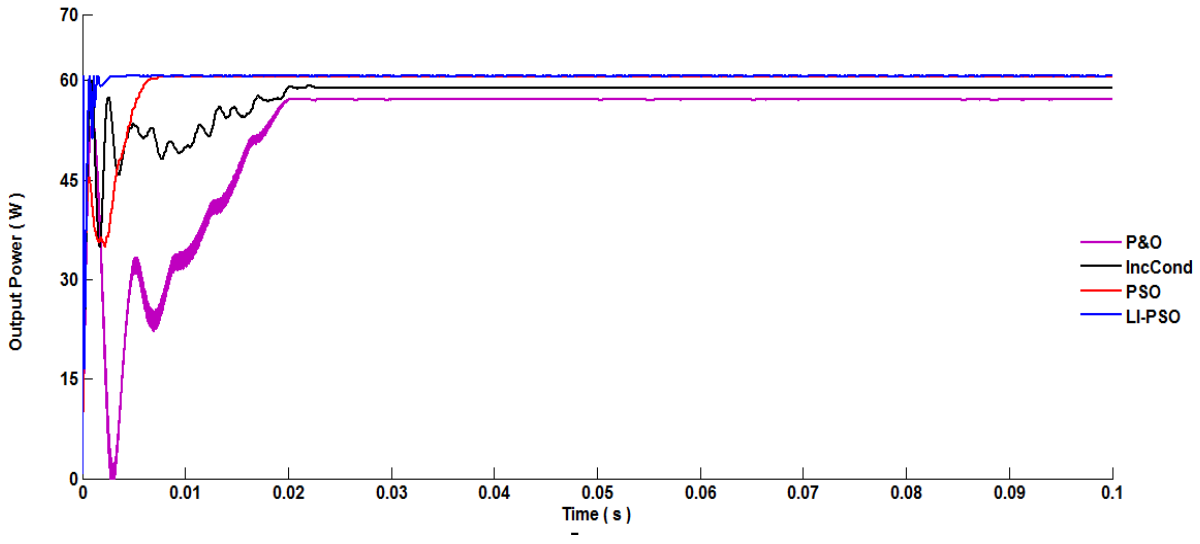

Figure 7.9: The dynamic response of the output power (w) at STC [147].

"It can be observed in Figure 7.9, that the MPP value of the selected PV module is 60 W, while it is 60.57 W with the LI-PSO algorithm. The optimisation time of the latter was less

than 2 ms and the convergence speed was also very fast, due to the LI-PSO moving the operating point close to the optimal point in one step. This is unlike conventional techniques, where P&O of the PV module output power are used to track MPP. By contrast, the conventional PSO yielded 60.5 W and required 24 ms to settle to a new MPP. At this point, the P&O and IncCond methods yielded values of only 58.78 W and 59.45 W, respectively. It is clear from the simulation result that the proposed algorithm set the operating point at MPP with zero oscillation at the steady state after three iterations" [147].

Figure 7.10 demonstrates the behaviour of the system under low solar radiation (G = 200 W/m^2, T = 25 °C). It can be seen that the MPP value of the selected PV panel is 11.5 W, while it is 11.64 W with the LI-PSO algorithm, and the convergence speed is very fast. The conventional PSO was 11.53 W and its optimisation time was 35 ms. In that time, the P&O and IncCond methods yielded values of only 10.04 and 10.85 W, respectively. When it comes to convergence speed, the proposed method is faster than the conventional PSO algorithm, as the conventional method requires a comprehensive search to be completed to set a new MPP.

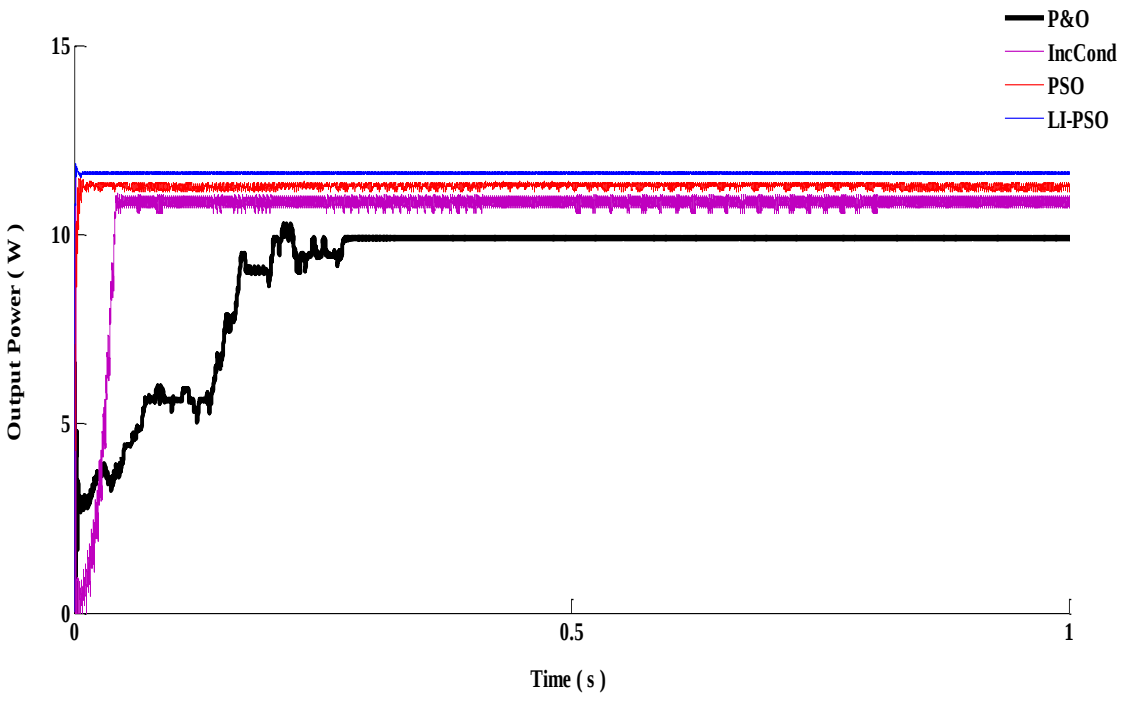

Figure 7.10: The dynamic response of the output power (w) at G = 200 W/m^2 and constant T = 25 °C [147].

Fig. 7.11 demonstrates the behaviour of the system when solar radiation levels for the PV modules were changed from 300 W/m^2 up to 500 W/m^2 at a constant temperature of 25°C. The theoretical value of the potential MPP generated from the selected PV module in these

cases is 16.56 W and 30.92 W, respectively. The change in the solar irradiation was at 0.03 s, and Figure 7.12 demonstrates the output power of the system when the radiation has been reduced from 800 W/m^2 to 500 W/m^2.

In Figures 7.11 and 7.12, it can be seen that PSO has an unsuitable response for short periods when there is a gradual change in radiation, which is a common issue with the original PSO algorithm. From Figure 7.11, it is clear that all techniques reach the MPP within 30 ms, and that the proposed method has proven to be the most rapid, and to demonstrate the most effective tracking efficiency. The oscillation around MPP was zero, with its starting time to reach the MPP for 300 W/m^2 of radiation being less than 2 ms, while P&O was the slowest technique. The conventional PSO provided improved performance in comparison to the P&O and IncCond techniques in both dynamic and steady-state responses as it reached MPP at 14 ms. However, its performance was lower than the proposed technique, and it took longer to reach MPP. This has proved to be one of the common disadvantages of the PSO algorithm, as it typically takes a considerable length of time to track the MPP for large search spaces. The proposed technique has provided excellent performance in comparison to alternative methods, both in terms of dynamic and steady-state responses.

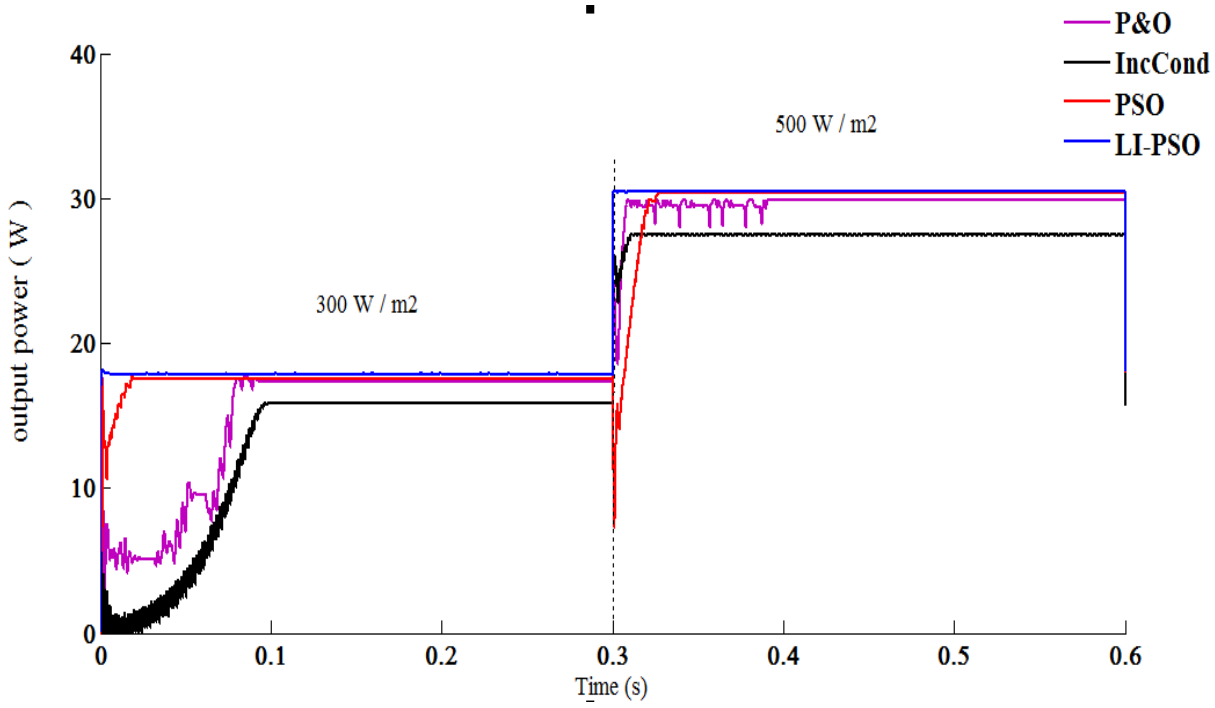

Figure 7.11: The dynamic response of the output power (w) during rapidly increasing radiation levels [147].

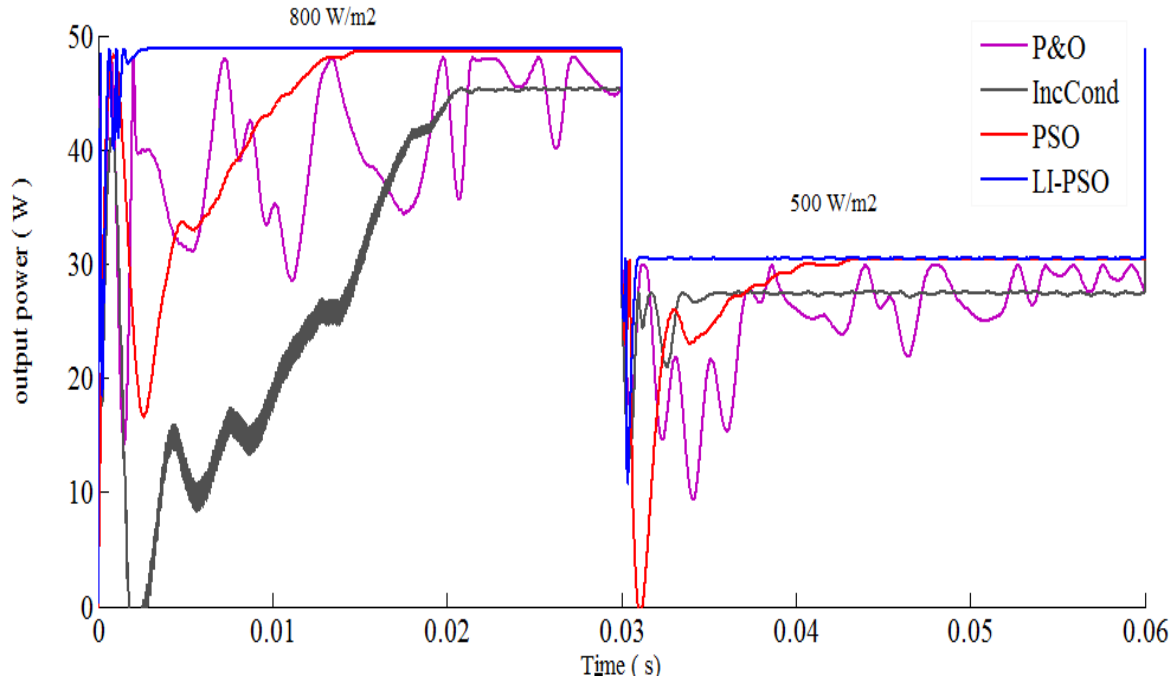

Figure 7.12: The dynamic response of the output power (w) during rapidly decreasing radiation levels [147].

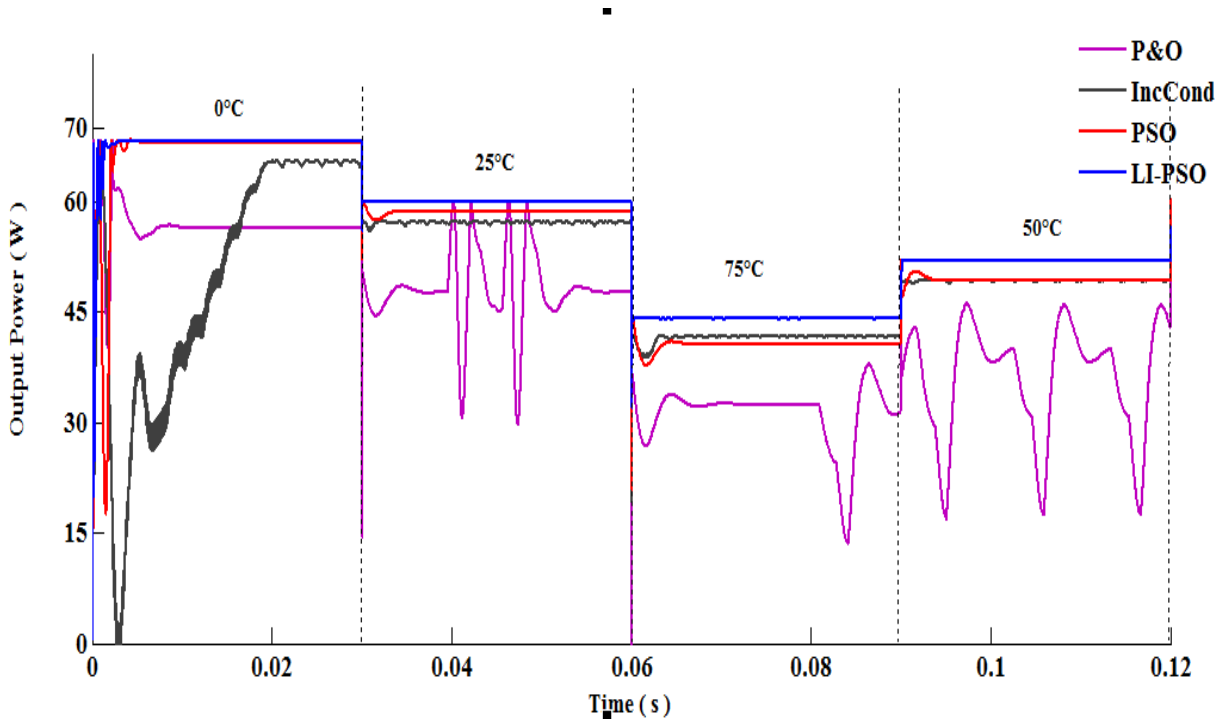

Figure 7.13: The dynamic response of the output power (w) during rapidly changing temperature, G = 1000 W/m^2[147].

"Figure 7.13 demonstrates the dynamic response of the system output power under varying temperatures of 0°C, 25°C, 70°C, and 50°C. It is clear that in the LI-PSO MPPT technique, the time taken to set the operating point of the system at its MPP was less than 2 ms, and that its tracking efficiencies were higher than 97.98% in all test conditions, while the conventional

PSO was at 0.004 s. The IncCond technique displays an improved performance in comparison to the P&O in the steady-state response. The IncCond algorithm has provided an improved performance under rapid solar irradiance and had fewer oscillations around MPP. The only advantages of the P&O algorithm in comparison to its P&O technique consist of its low cost, and simplicity to implement" [147].

Table 7.1 summarises the simulation result of the tracked power in (W) between the studied MPPT for different temperatures. It is clear that the generated power when using the proposed algorithm is above 98% under all test conditions.

Table 7.3: Comparison of the studied methods for different temperatures

T	**P&O**	**INC**	**PSO**	**MR_PSO**	**Theoretical value of PV**
0	56.32	62.95	67.88	68.22	66.45
25	57.76	59.21	60.52	60.64	60.5
50	42.65	48.85	49.52	52.84	53.08
75	35.59	41.68	41.04	45.62	46.18

According to the findings attained, it cannot be said that higher efficiency is promoted by either the P&O or the IncCond technique, both of which contain a fixed step perturbation structure. Nevertheless, by comparison with P&O, IncCond produced a slightly higher rate of efficiency (98.3% vs. 98.5%). However, at low levels of insolation, both techniques performed rather poorly, particularly IncCond, which yielded an efficiency below 95% on a large number of occasions. Hence, to increase efficiency to 100%, it is necessary to employ adaptive MPPT techniques that are faster and have minimal fluctuation around the MPP.

Figure 7.14 demonstrates the output power of the system under rapidly changing atmospheric conditions. The simulation results of the studied methods under varying weather conditions of 200 W/m^2, 600 W/m^2, 1000 W/m^2, 800 W/m^2, and 400 W/m^2 clearly demonstrate that the proposed MPPT tracks MPP in a relatively short time. Whereas, the standard PSO algorithm was faster than the P&O and IncCond methods with less power losses under varying weather conditions. The dynamic response of the system output power using IncCond was higher than P&O in this case, while P&O has proved to be the least

effective method, due to its high oscillation around MPP, which reduces the generated output power, as its response time is limited under low solar radiation. This is the most common issue with the P&O technique under rapidly changing radiation levels, as it requires higher values of the duty cycle to increase its tracking of the MPP. Neither the P&O nor the IncCond techniques are the most effective choice in the case of rapidly changing radiation levels, as they require a greater length of time to track the MPP, which, in turn, results in a reduction in the amount of generated power. An increase in the step size of the duty cycle may assist in increasing their efficiency in these conditions; however, this will result in a hard oscillation in the steady-state that reduces the output power of the system.

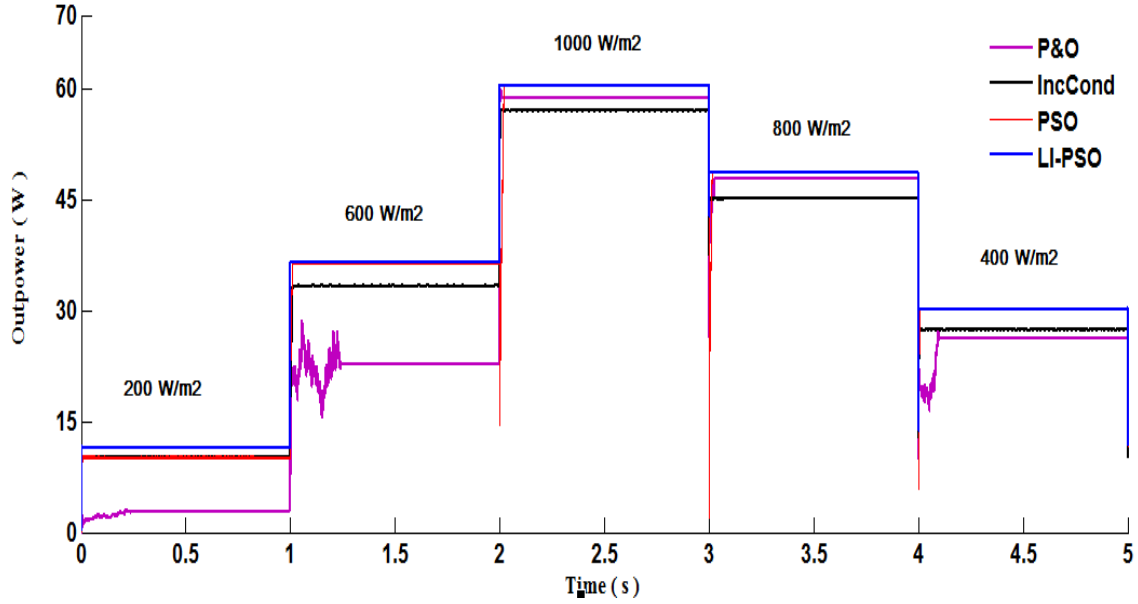

Figure 7.14: The dynamic response of the output power (w) under rapidly changing solar radiation, T =25°C.

The following table provides a comparison of the tracked power in (W) between the theoretical value of PV module and studied MPPT for high and low solar radiation. It clarifies that the yield energy by of proposed algorithm is above 99.5 % under all test conditions.

Table 7.4: Comparison of the studied methods [147].

G	P&O	INC	PSO	LI-PSO	Theoretical value of PV
200	10.04	10.85	11.18	11.67	11.5
400	14.22	19.78	24.16	24.29	24.26
600	33.62	33.68	36.51	36.58	36.52

800	42.6	43.35	48.05	48.76	48.68
1000	57.76	59.21	60.22	60.64	60.5

Figure 6.6 illustrates the output power under PSCs of both (1) the studied techniques and (2) the proposed technique. The simulated PV module is the MSX60 connected in the Series-parallel (4×1) configuration, and the electrical specifications of the PV module are demonstrated in Table 3.1. The resulting *I-V and P-V* curves when a number of the modules in the PV array are shaded are shown in Figure 6.6. It can be observed that the *P-V* curve of the PV array exhibits multiple MPPs under this condition. Initially, the PV was operated at the maximum power of 240 W, and at t = 0.03 s, while some of the PV modules in the array were shaded, resulting in four peaks, i.e. P_1, P_2, P_3, *and* P_4, where P_4 (118 W) is the GP.

Figure 7.15 clarifies that, when partial shading occurs, the operating point of P&O was at P_2 (53 W) as the MPP, while both PSO and IncCond trap to the local peak P_3 (98 W). Yet, LI-PSO was tracked the true GP P_4 (118 W), due to the first particle being set to the converged value from the first step, thereby allowing the particles to converge more rapidly to the GP. In addition, the conventional PSO-MPPT algorithm proving to be rapid, and setting the operating point of the system at an accurate point, it has a disadvantage when searching for MPP with multiple peaks. In this case, this occurred when some of the modules were shaded, resulting in tracking the local MPPs and enabling the particles to track the global MPP. In the traditional PSO algorithms, the three basic parameters (w, $c1$ and $c2$) need to be toned to accelerate convergence.

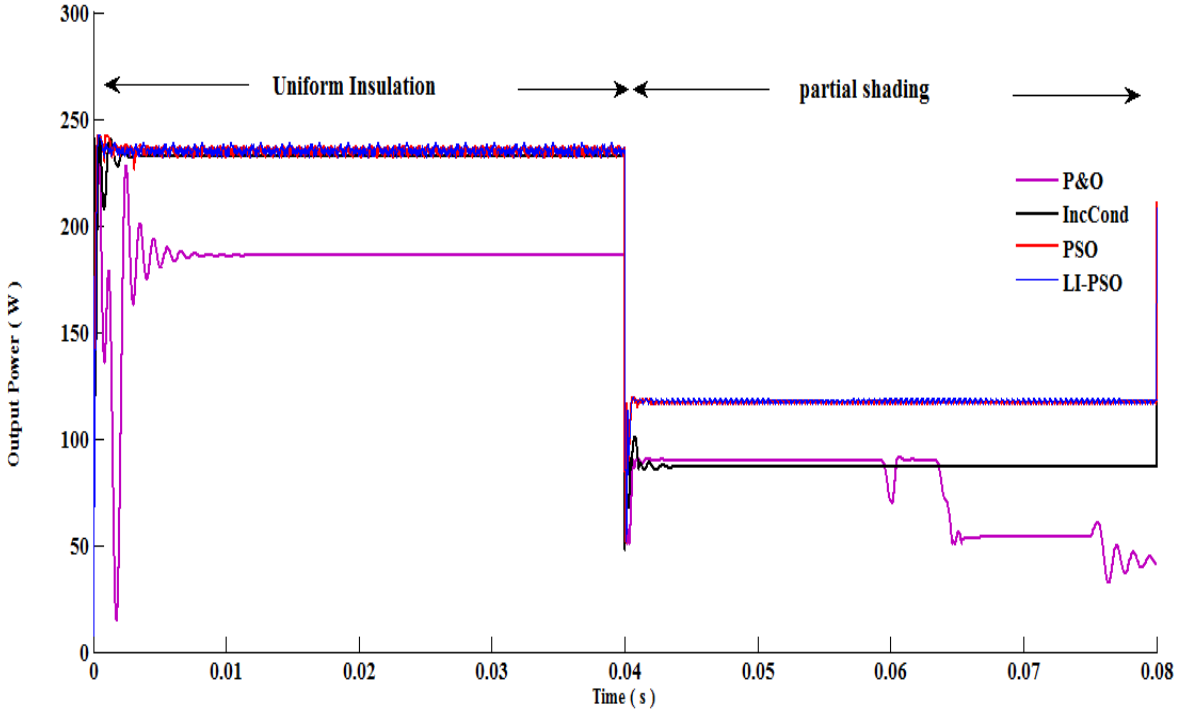

Figure 7.15: The dynamic response of the output power (w) under PSCs[147].

The following table sets out a comparison between the theoretical value of the PV module and the PV module operating points with a PSO_MPPT and LI_PSO algorithm.

Table 7.5: Comparison between the theoretical value of the PV module and the PV module operating points with PSO and LI-PSO algorithm [147].

G(w/m2)	The PV module operating points PSO-MPPT			The PV module operating points LI-PSO			The theoretical value of PV module		
	I_{mpp}	V_{mpp}	P_{mpp}	V_{mpp}	I_{mpp}	P_{mpp}	V_{mpp}	I_{mpp}	P_{mpp}
100	0.319	16.96	5.42	17.03	0.322	5.48	16.02	0.358	5.74
200	0.668	17.23	11.52	17.26	0.674	11.63	16.4	0.721	11.84
300	1.07	17.38	17.67	17.46	1.017	17.76	16.7	1.077	18
400	1.4	17.2	24.08	17.2	1.41	24.25	16.9	1.431	24.2
500	1.77	17.08	30.35	17.13	1.78	30.49	17	1.785	30.36
600	2.148	17	36.51	17.04	2.152	36.68	17.02	1.145	36.5

									2
700	2.47	17.23	42.54	17.25	2.476	42.73	17	2.507	42.63
800	2.856	17.04	48.67	17.13	2.581	48.84	17	2.863	48.68
900	3.24	16.87	54.65	16.95	3.236	54.85	16.95	3.225	54.67
1000	3.616	16.76	60.52	16.77	3.62	60.72	16.8	3.607	60.6

Figure 7.16 demonstrates the operating point of the system when the value of *w* has been changed, and it is evident that both the proposed scheme and the conventional PSO were able to operate the system at the exact GP when w = 0.7, while the conventional PSO was tracked at the local peak instead of GP when w =0.4. This is due to the inertia weight being used to control the velocity in the standard PSO by the use of a constant value of *w*. However, choosing its value is an important parameter in PSO, as a large value facilitates a GP, while a small value facilitates a local optimum.

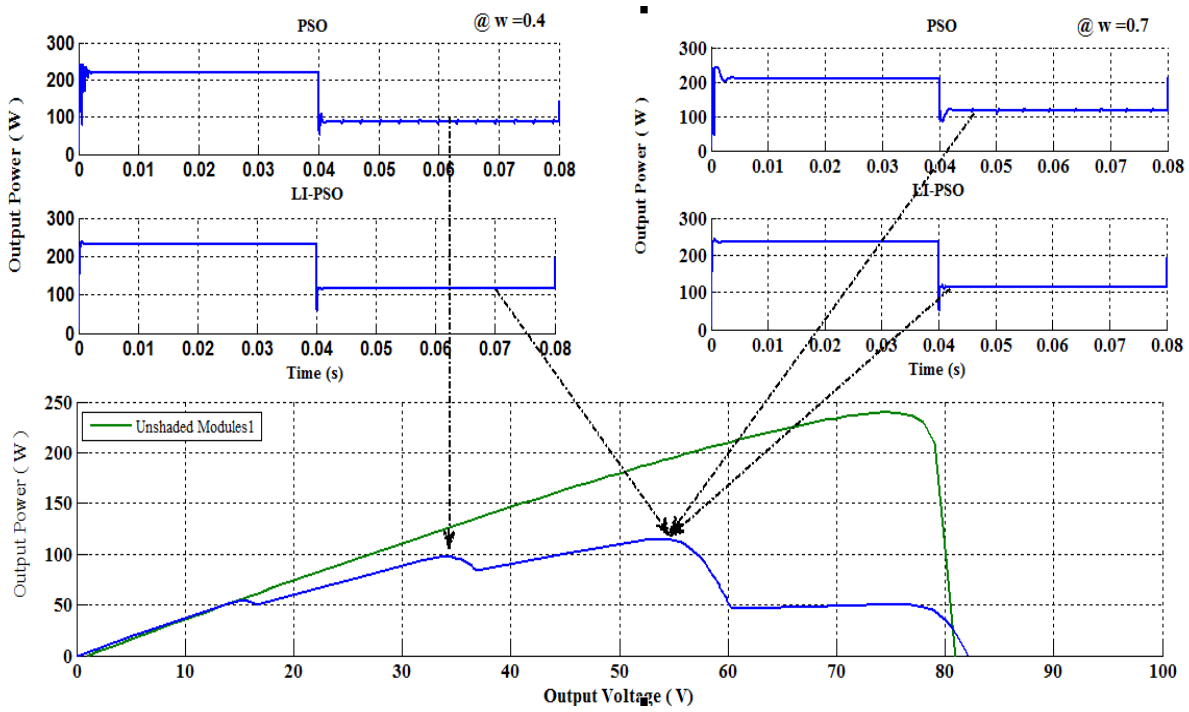

Figure 7.16: Tracking performance of PSO and LI-PSO under PSCs at (w=0.4 and w=0.7) [147].

"Figure 7.16 demonstrates that, when the weight (w) was set to a low value, the operating point of the system using the conventional PSO was at local P_3 (98 W). This is because a low

value of w might cause the particle to cause convergence issues and track the local optimum instead of GP. Thus, additional iteration is required to reach the final solution, as a result of the distance to GP. However, as the number of iterations increase, the value of w gradually decreases. This, in turn, decreases the movement of the particles, as well as leading to a low tracking speed, or instead tracking the local optimum for GP. Therefore, the value of w in conventional PSO needs to be set to a higher value during the initial search for an effective exploration, and then to be gradually reduced in order to obtain an accurate optimisation, while large values of c1, and c2 may cause convergence problems and increased tracking time. Therefore, the learning factors and inertia weight in the conventional PSO must be modified when a PSC occurs. However, there are difficulties in choosing its values, and it is generally tuned by means of experiments. By contrast, when the PV characteristic is changed, the proposed algorithm sets the duty cycle close to the optimum in the first step, and then PSO locates the GP in the following step, resulting in a shorter tracking time" [147].

7.3.1. The EN 50530 test sequence

The use of the dynamic test EN 50530 enables a standard method to be derived for calculating the performance given by PV systems connected to grid using a PV array simulator, which produces the same kind of output as a PV source. Inverters form the instrument in which the test is most commonly employed, but DC-DC convertors can also be evaluated by its use, since the test provides an assessment of the MPPT algorithm, rather than the effectiveness of conversion [28].

The test used to calculate the dynamic efficiency of MPPT in different environmental conditions involves employing different ramp profiles in a fixed time interval. The test is based on an insolation ramp with varied values of insolation and slopes, enabling all possible conditions to be simulated, allowing an assessment of whether the MPPT algorithm can function in accordance with the changes in insolation.

Three varieties of insolation regions are employed throughout the duration of the test, in order to create three varieties of insolation levels with 1000 W/m2 taken as the reference value: (1) insolation in range of low to medium (100-500 W/m2); (2) insolation in the range of medium to high (300-1000 W/m2); and (3) insolation during the start and closure of operations. In the low- medium and medium-high scenario, the ramp sequence with the value of slopes varying from 0.5 W/m2/s up to 100 W/m2/s are employed. In the case of the start and closure of operations, a slope of one ramp profile (2-100W/m2) is used [28]. In the best

conditions, the I-V module technique (i.e. thin film and crystalline silicon) is employed to set up two electrical circuits. When the I-V curve is used within a PV simulation, the circuit functions in a manner in which insolation G is approximately equal to PMPP, but the value of VMPP differs on the basis of the G value.

In order to evaluate the performance of the MPPT algorithms, the simulation was undertaken according to the test conditions addressed in European Standard EN 50530 [28]. The test used to calculate the dynamic efficiency of MPPT in different environmental conditions involves using different ramp profiles in a fixed time interval. Figure 7.17 demonstrates the insolation in a range of low to medium (100-500 W/m2).

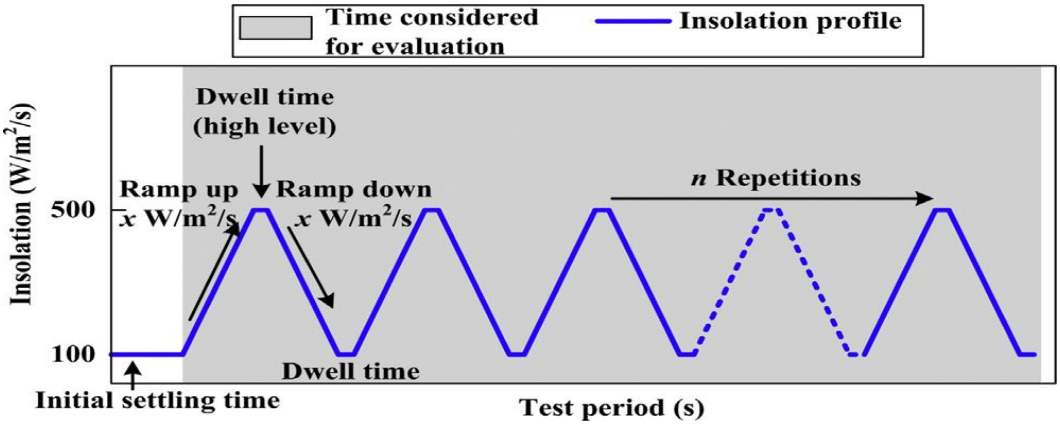

Figure 7.17: Test sequence (low–medium insolation) for the characterisation of MPPT efficiency under changing insolation conditions [22].

Figure 7.18 (below) demonstrates the insolation in the range of medium to high (300-1000 W/m2), and insolation during the start and closure of operations.

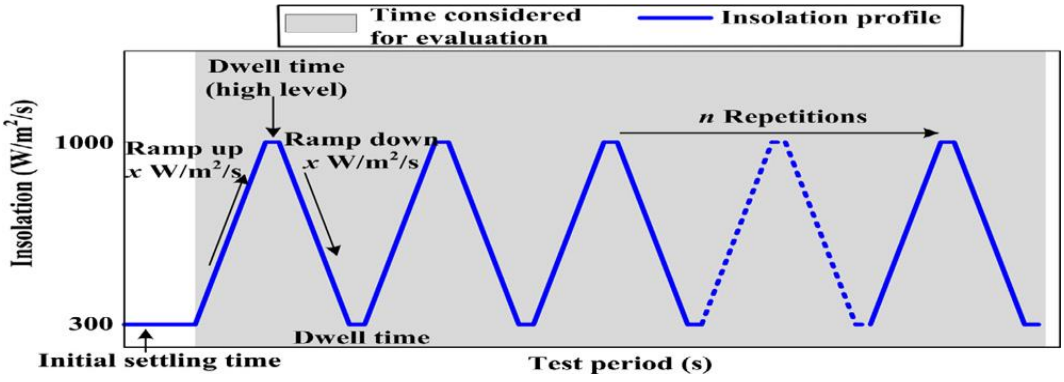

Figure 7.18: Ramp test sequence (medium–high insolation) for the characterisation of MPPT efficiency under changing insolation conditions [22].

In the low-medium and medium-high scenario, the ramp sequence with the value of slopes varying from 0.5 w/m^2/s up to 100 w/m^2/s is employed. In the case of start and closure of

operations, a slope of one ramp profile (2-100 w/m^2) is used [28]. Table 7.6 demonstrates the slopes proposed for irradiance levels from 300 to 1000 w/m^2.

Table 7.6: Slope (W/m2/s) Rise time (s) Dwell time Total Simulation time

Slope (W/m^2/s)	Rise time (s)	Dwell time	Total Simulation time
10.00	70.00	10.00	170.00
14.00	50.00	10.00	130.00
20.00	35.00	10.00	100.00
30.00	23.33	10.00	76.67
50.00	14.00	10.00	58.00
100.00	7.00	10.00	44.00

Five different slopes are chosen from Table 7.6: 14,20,30,50 and 100 w/m^2/s, which covered low to medium (100-500) and medium-high irradiance (300–1000 W/m²). Figure 7.19 reveals that the dynamic performance under two tests (20 and 100 W/m2/s), and confirms that the proposed scheme demonstrates the most effective performance in terms of stability and time response, while the conventional PSO gave an improved performance in comparison with P&O and IncCond methods. The lowest performance was by the P&O method, due to its fixed step size value. The IncCond algorithm demonstrates a more effective performance than the P&O algorithm. However, it has a slow time response, is highly sensitive to the perturbation size under low radiation levels, and, in comparison to the LI-PSO and conventional PSO algorithms, is unstable, and suffers with the steady state fluctuations, as reported in several works [69, 102]. Both P&O and IncCond MPPT algorithms demonstrate that they are slow in extracting MPP in comparison to PSO and LI-PSO, with their tracking efficiency being 94.09% and 95.67%, respectively.

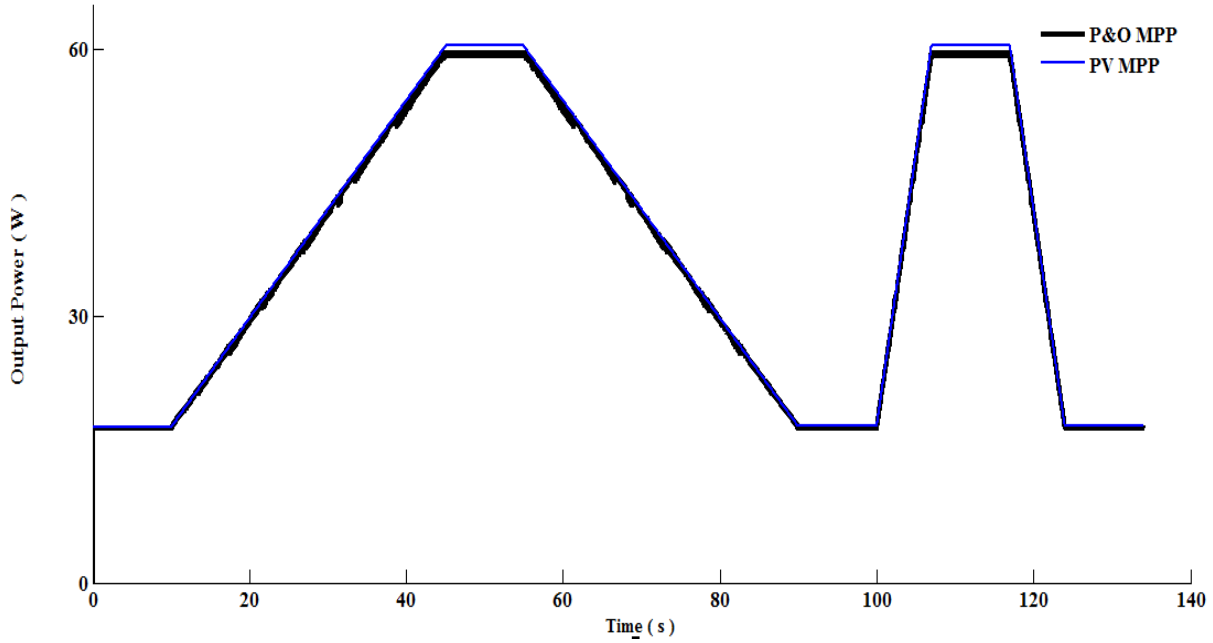
P&O MPP
PV MPP
Output Power (W)
60
30
0
0
20
40
60
80
100
120
140
Time (s)

(a)

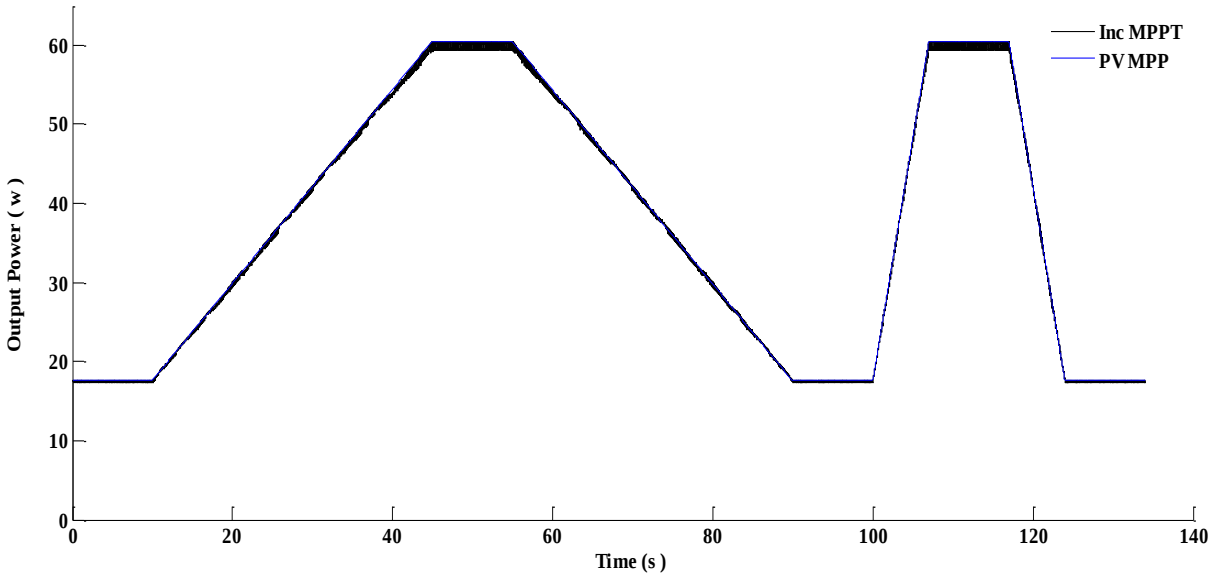
Inc MPPT
PV MPP
Output Power (w)
60
50
40
30
20
10
0
0
20
40
60
80
100
120
140
Time (s)

(b)

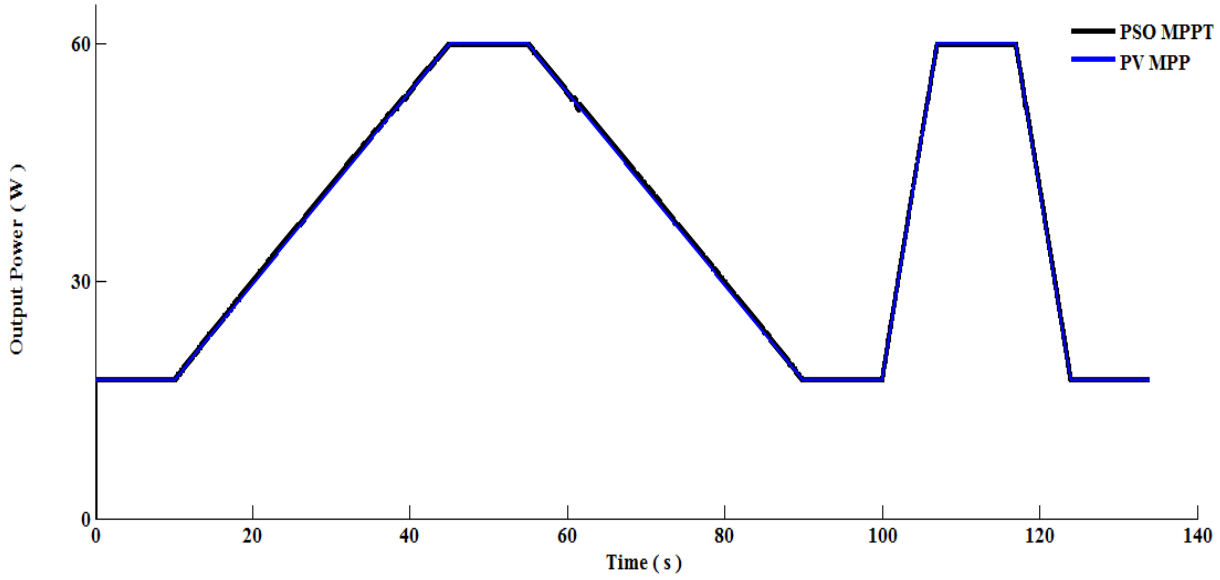

(c)

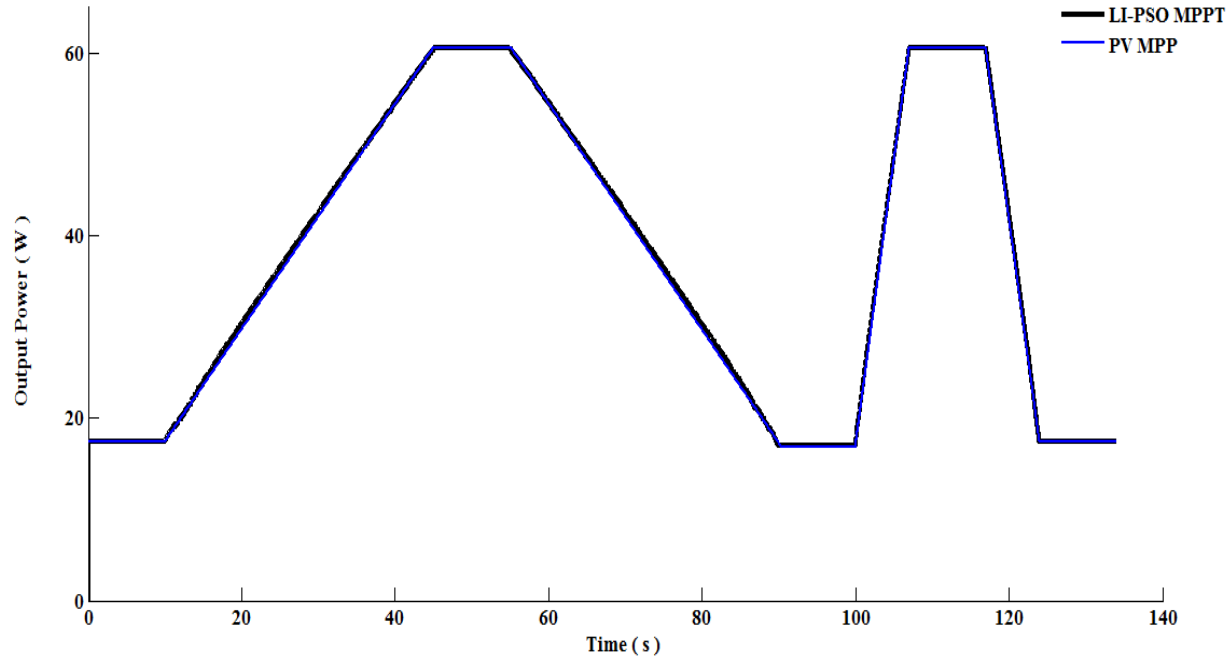

(d)

Figure 7.19: Dynamic MPPT performances from 20% to 100% irradiance. (a) P&O method. (b) IncCond method. (c) PSO method. (d) LI-PSO method [147].

According to the outcome of the experiment under the irradiation slope chosen from Table 7.6, it is evident that both algorithms P&O and IncCond give power from the PV panel that is not close to MPP. Additionally, the algorithms may tend to incorrectly direct the DC voltage. Again, the current can intently track the MPP current and in the right direction.

This can be attributed to the direct proportionality of the PV array current to the irradiation. Consequently, the PV current behaves in an identical manner to when the irradiation changes following a slope. In theory, for specific examining frequency, there should be a particular ideal current increase when the current varies linearly. At the same, the power varies in the same direction as the current. However, neither the current, nor the power, vary smoothly, particularly when the algorithm is disturbed. Despite this, both can be utilised to decide the direction of MPP variation. Moreover, at the point at which there is a rise of irradiation as a result of a slope, there is a rise of both power and current, while when irradiation reduces, both power and the current also diminish.

The dynamic efficiency of the proposed algorithm (along with that of other methods) was tested according to the irradiation slopes detailed in Table 7.6. Figure 7.20 and Figure 7.21 represent the performance of the proposed algorithms and other techniques under irradiation slopes of 14 and 30, 50 W/m2/s, respectively.

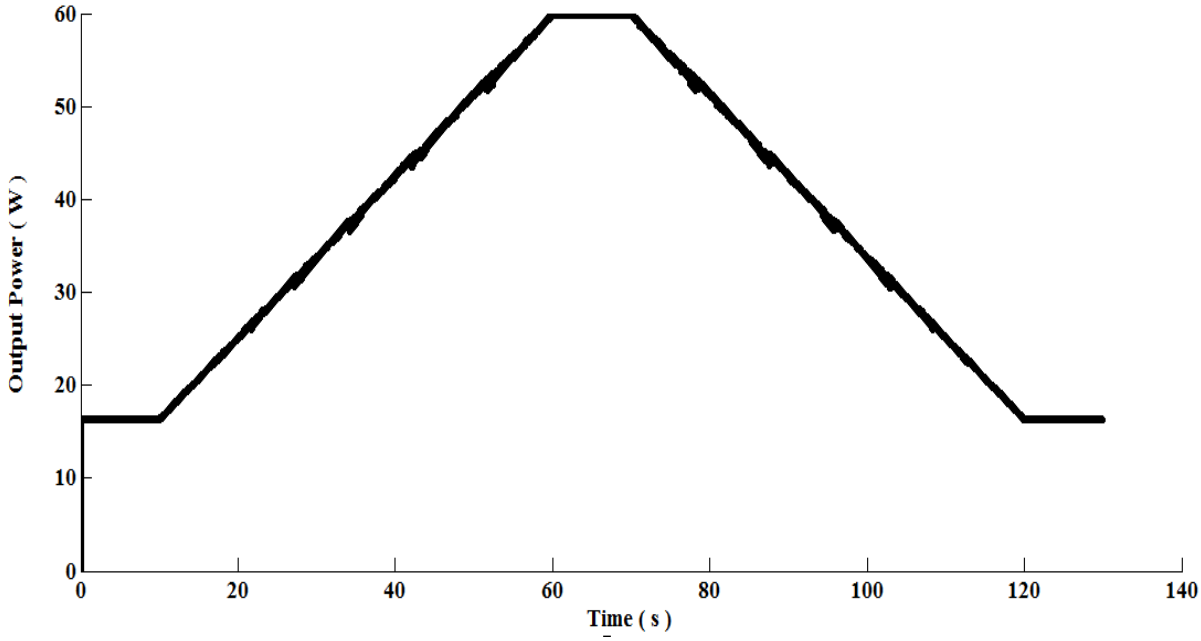

(a) P&O method.

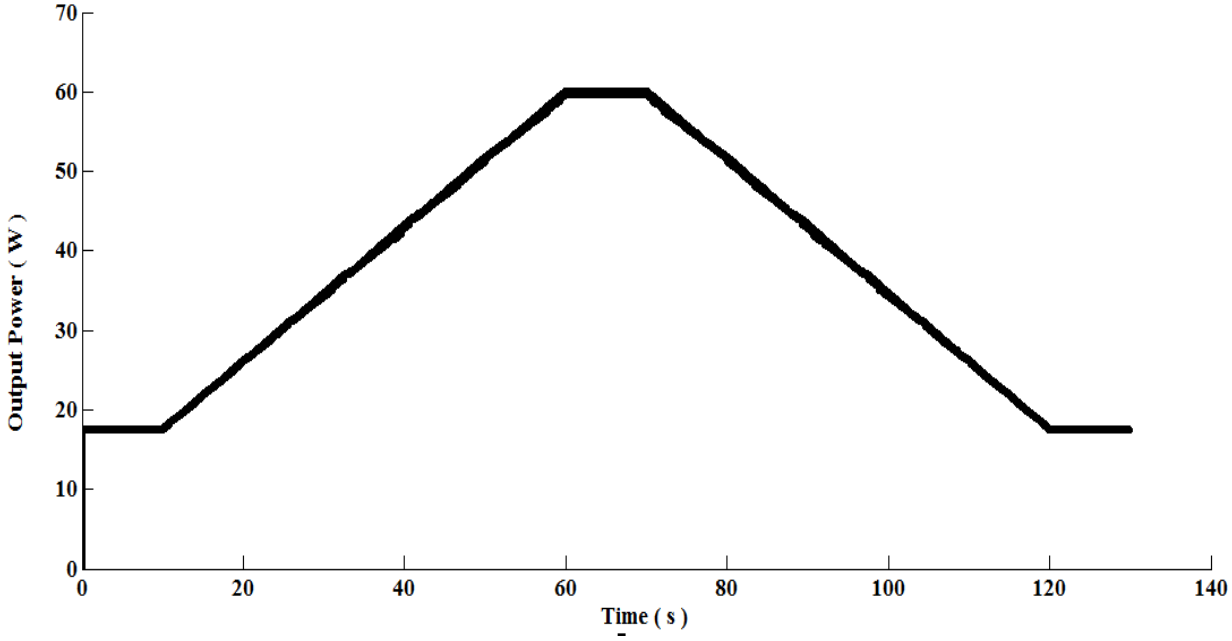

(b) IncCond method

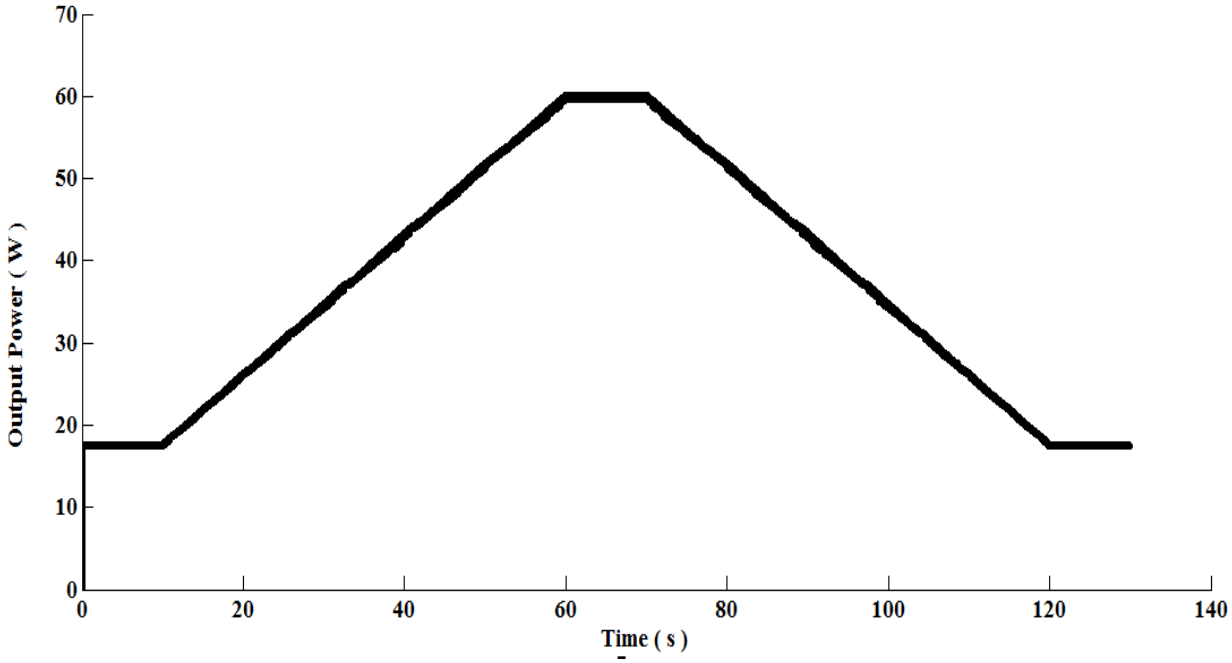

(c) PSO method.

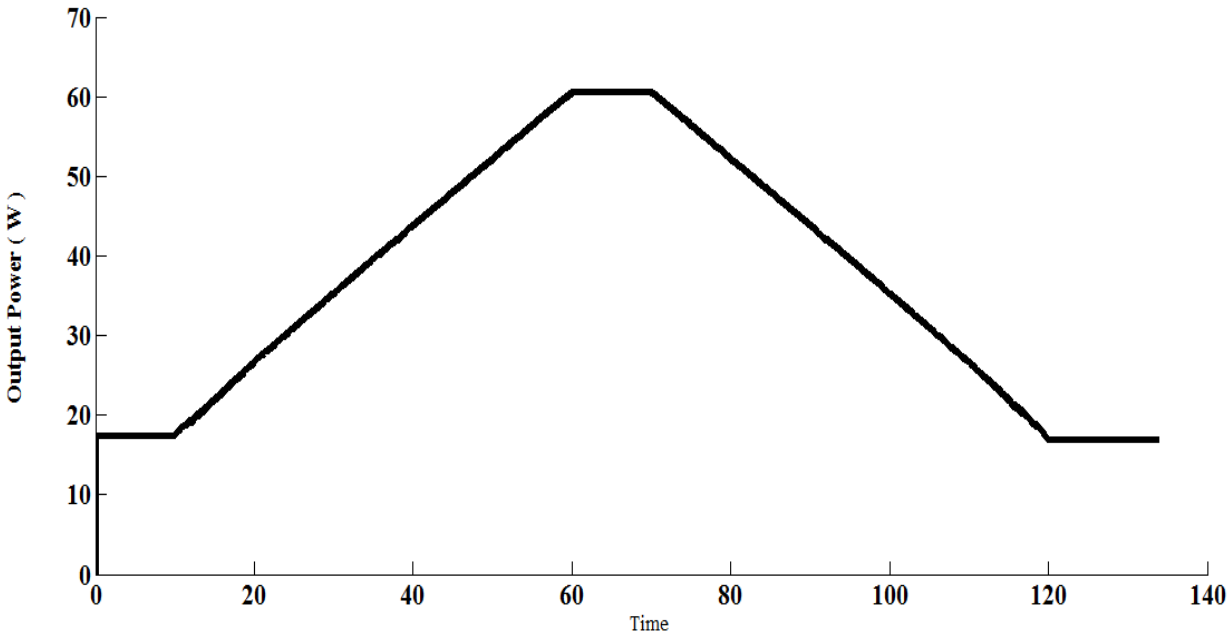

(d) LI-PSO method

Figure 7.20: Dynamic MPPT performances of 14% irradiance. (a) P&O method. (b) IncCond method. (c) PSO method. (d) LI-PSO method

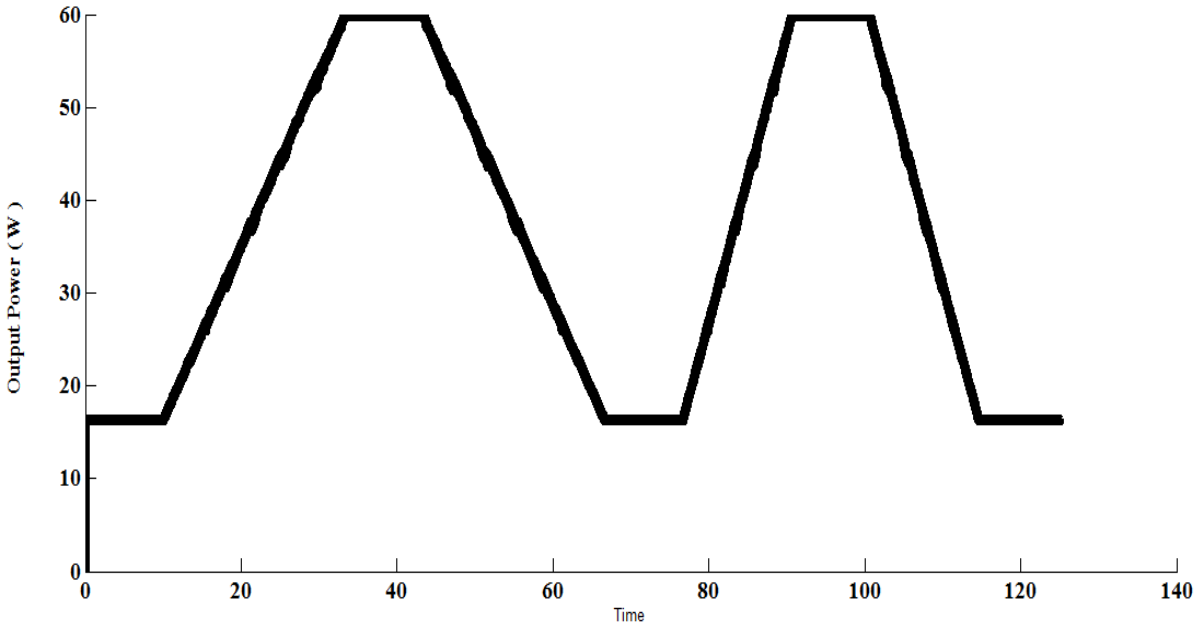

. (a) P&O method

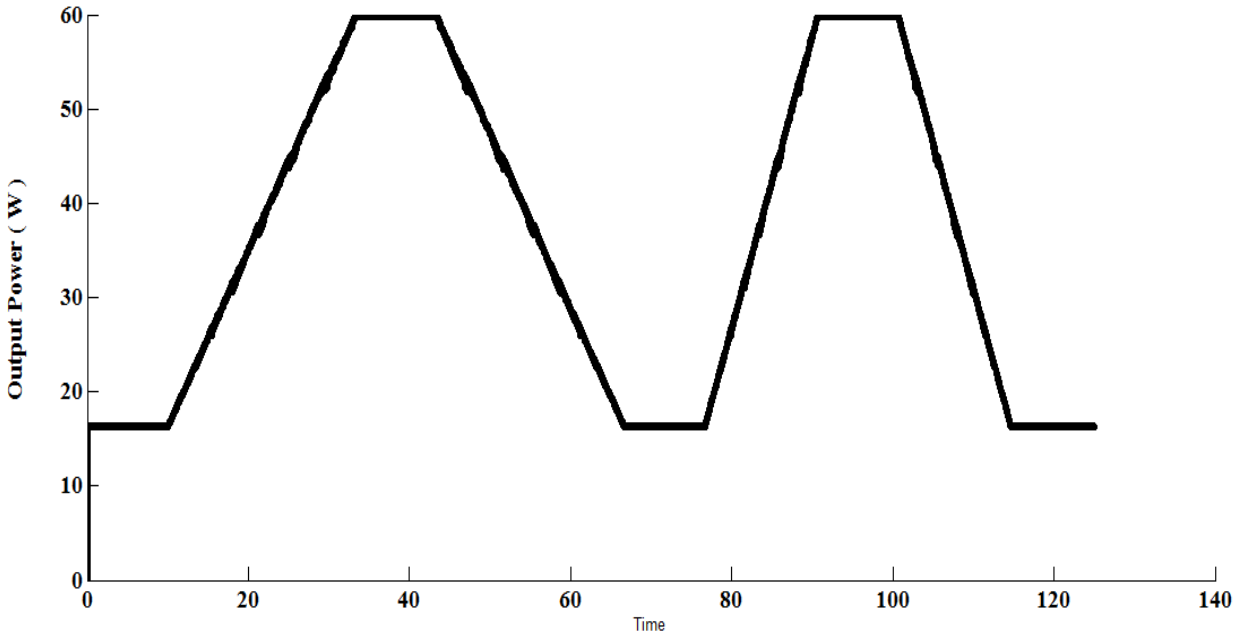

(b) IncCond method

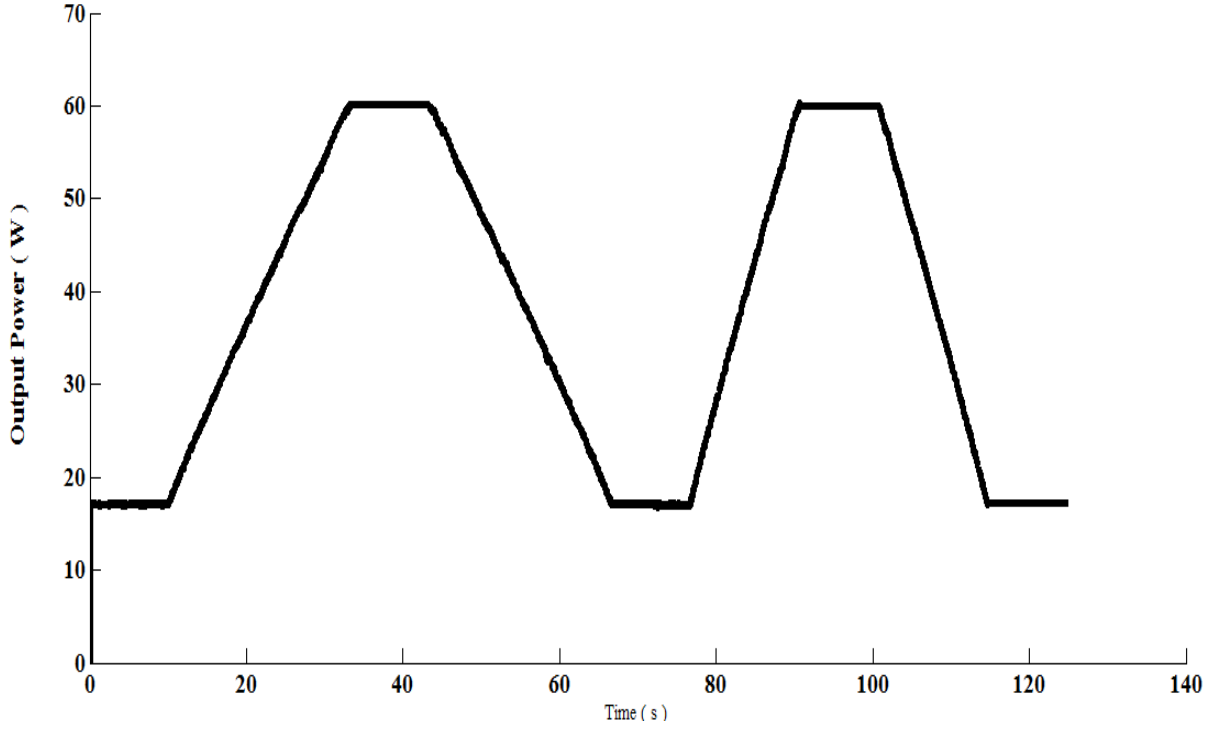

(c) PSO method.

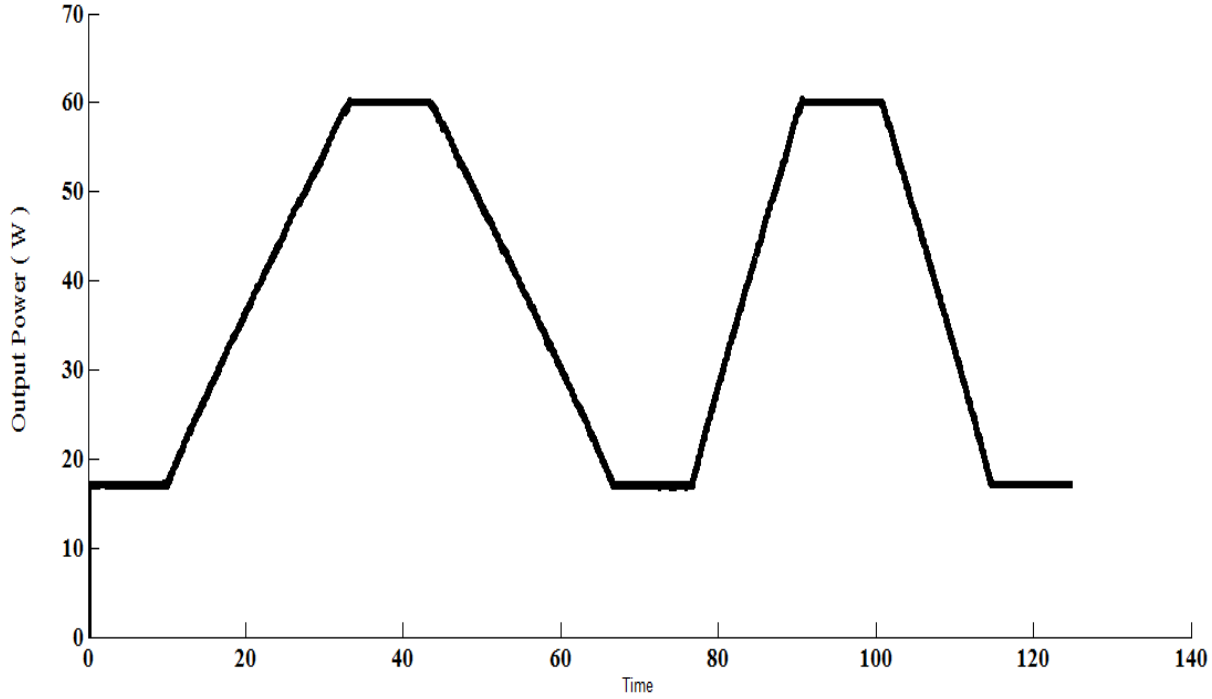

(d) LI-PSO method

Figure 7.21 : Dynamic MPPT performances from 30 % to 50% irradiance. (a) P&O method. (b) IncCond method. (c) PSO method. (d) LI-PSO method

The above figure clarifies that the efficiency of the IncCond and P&O algorithms are low and cause oscillations around MPP in the steady state, due to the dynamics of the IncCond and P&O algorithms, and the perturbation step size which is not sufficiently large to follow the ramp, as reported in [69,102]. Therefore, adaptive MPPT methods with faster tracking speeds should be adopted to improve their efficiency. However, the tracking becomes highly ineffective due to the lack of a controller to recognise the variation of irradiation, in particular when slopes are smaller and the reference voltage is constantly maintained. This prompts a serious drop in the power acquired from the PV array following the failure to track MPP.

It is indicated that the MPP tracking is of high quality comparable to all slopes. However, there exists a little slack in each of these cases that is rather worthy as an algorithm to establish the way in which the irradiance changes first, followed with the setting of a reference as required. The dynamic efficiency of each method was calculated as follows:

$$n_{MPPT} = \frac{P_{PV}}{P_{MPP}} \tag{7.1}$$

Therefore, thirty points each second were utilised to ascertain the dynamic effectiveness. Table 7.7 demonstrates the effectiveness under the suggested slopes in Table 7.6.

Table 7.7: Dynamic efficiency [147].

Efficiency (%)		MPPT			
		P&O	IncCond	PSO	LI-PSO
Slope [W/m2s]	14	89.90	92.12	98.78	99.15
	20	89.96	93.43	98.87	99. 07
	30	91.95	93.35	99.52	99.61
	50	94.09	95.78	99.50	99.75
	100	94.25	95.78	99.73	99.84

As indicated in Table 7.7, the efficiency of PSO is somewhat lower than with improved LI-PSO algorithms. Therefore, this study affirms that the most effective outcomes have been acquired with improved LI-PSO and PSO techniques. In addition, it is significant to note that 99.95 % of dynamic efficiency has been achieved utilising irradiation slopes.

From the simulation result, it is apparent that the conventional PSO is fast and accurate when searching for single peak values. Nonetheless, when PSC occurs, conventional PSO tracking efficiency is low, due to the weight (w) that needs to be correctly readjusted. A greater step size in weighting equation leads to an increase in the particle velocity, while a decrease in w causes the particle movements to shrink, thus enabling the controller to locate the operating point at the accurate MPP. Therefore, the parameters of a conventional PSO need to be modified when a partial shedding condition occurs. The difference between the proposed algorithm and the standard PSO is that the particles (i.e. the duty cycle) are initialised to the optimal value in relation to the MPP.

The P&O method has revealed a considerable power loss and resulted in oscillation around the MPP, thus proving to be the least effective performer in terms of efficiency, particularly under rapidly changing conditions. This is due to the possibility of this algorithm becoming

confused and dependent on the perturbation direction under rapidly changing weather conditions. Thus, if the duty ratio is decreasing and radiation increasing, increases in output power will be influence by the voltage perturbation, as the algorithm continues to decrease the voltage, so moving the operating point away from the true MPP. This will continue until the change of irradiance is halted. This is in contrast to the tracking efficiencies of systems containing the conventional PSO and the IncCond method, of which the latter demonstrated the more effective performance. The IncCond method has higher efficiency and less confusion when sudden changes in weather conditions occur in comparison to the P&O method, as its time response is independent of solar radiation. However, its implementation is more complex than that of the P&O method, and requires a more rapid controller with high sampling accuracy. This increases the system cost, while its tracking speed is considerably slower in comparison with the conventional PSO method.

7.4. Summary

This chapter has established that the algorithm put forward in this current study has been verified with the OPAL-RT real time simulator and Matlab Simulink tool, with a number of simulations being undertaken and compared to: (1) the P&O method: (2) the IncCond method; and (3) the conventional PSO based algorithm. The simulation results demonstrate that the proposed LI-PSO method has a more rapid response speed than other methods, due to particles automatically migrating to the best (or close to the best) position when weather conditions change. This thus significantly reduces the time wasted by particle tracking in incorrect areas, thereby substantially enhancing the system tracking speed, while also reducing the steady-state oscillation (i.e. to practically zero) once MPP is located. This represents a considerable improvement in relation to the conventional PSO method, in which the new operating point is at too great a distance from the MPP, and additional iterations are required to reach the new MPP.

As demonstrated in Figures 7.14, 7.15 and 7.16, the LI-PSO and PSO produced satisfactory results when the slope gradients were higher than 10 $W/m^2/s$. Comparison of the performance of the various algorithms addressed in this thesis suggests that the LI-PSO and PSO techniques yield optimal results. As demonstrated in Table 7.7, the use of irradiation slopes produced a dynamic efficiency of over 99.4%. Moreover, under all ramps indicated in Table 7.6, the LI-PSO algorithms tracked the MPP in a highly efficient manner (Figure 7.19). On the other hand, despite being effective with the slopes from Table 7.6, the IncCond algorithm exhibited a lower tracking performance in conditions with smaller gradients, because the

irradiation change went undetected by the controller, and hence an identical reference voltage was maintained. Consequently, no tracking of MPP was conducted, and therefore the power level derived from the PV array decreased significantly. Thus, it can be concluded that MPP is not successfully tracked by P&O and IncCond with all the slopes suggested by the protocol.

The P&O and IncCond algorithms were found to share a close similarity in terms of performance. Hence, the selection of one over the other is solely for purposes of simplicity. A comparison of the flowcharts of these two algorithms (see Figures 5.5 and 5.6) reveal that IncCond exhibits greater complexity, as it necessitates the power increments to be divided by those of the voltage (current), and the result compared to zero. By contrast, the P&O technique can be argued to be a less complex algorithm, as it requires only a straightforward comparison of the increments to zero.

The findings obtained, and the analyses performed in this study, all indicate that the proposed LI-PSO technique is the most suitable MPPT algorithm. Detection of the nearest local maximum renders the P&O and IncCond techniques disadvantageous, particularly as more than one maximum may occur in the V-P characteristic curve during partial shading of the PV array. One solution to this issue is to integrate the two techniques with a further method capable of detecting the global maximum. However, global MPPT techniques are significantly ineffective and therefore not widely employed. Their primary function is to verify the proximity of the operating point to the real MPP at regular intervals. Once this verification is completed, the most effective MPPT algorithm is used by the controller.

The present study has discussed the majority of MPPT algorithms capable of identifying the real MPP; however, a more detailed investigation has been undertaken on the P&O and IncCond techniques alone, since they possess the advantage of simplicity and effectiveness. The European Standard EN 50530 was followed in the analysis of their performance and dynamic MPPT efficiencies. The assessments corroborated the findings of other studies regarding the limitations of these two techniques.

This leads to the conclusion that the LI-PSO algorithms perform more effectively in comparison to other techniques, on the basis of the comparative analysis of the performances of the LI-PSO, PSO, P&O and IncCond algorithms, as well as the results obtained from the testing of dynamic efficiency. In consideration of all these different aspects, the LI-PSO algorithm can be said to be the optimal algorithm, as standard-based measurement revealed that it had a dynamic efficiency of more than 99.4%.

Chapter Eight

Conclusion and Future Work

8. Conclusion

This chapter discusses the main conclusions of this thesis, followed by an examination of proposed areas for future work. This thesis has highlighted the issues related to MPPT in relation to tracking techniques for optimum and stability control in PV systems. A new MPPT, based on the PSO algorithm, has been presented, to enhance the most extreme power point tracking in PV systems. Moreover, there has also been an introduction of an improved principle for reinitialising the duty-cycle.

This proposed algorithm has included new plans for overcoming the difficulties connected with rapidly-changing insolation levels and the impact of PSC. The results have been validated by simulation, i.e. MATLAB/Simulink and RT-real time simulation experiments under a number of differing operational conditions. The proposed LI-PSO achieved superior performance in comparison to the conventional PSO algorithm. Comparisons were undertaken by observing the response of each algorithm under different conditions in terms of convergence speed and performance, to reach the optimum point.

Chapter One gave a brief introduction to the importance of the MPPT controller, along with the aim, objectives, and outlines of this thesis. Chapter Two took the form of a literature review, including information concerning different MPPT algorithms obtained from books and journals. Chapter Three gave an introduction to PV panels and their electrical attributes, including an examination of the yield power of PV modules in relation to their yield voltage and yield current. These attributes demonstrated the significance of MPPT units, together with resolving a number of recurrent issues impacting on MPPT. Chapter Four compared four basic non-isolated DC-DC converters under a number of different atmospheric conditions, in order to determine the most effective DC-DC converter for the PV system. Four topologies were presented: (1) buck converter (step down); (2) boost converter (step up); (3) buck-boost converter; and (4) Cùk converter. Chapter Five examined existing MPPT algorithms (e.g. P&O, IncCond, open-circuit voltage, short circuit current and CV), together with a number of chosen works concerning MPPT algorithms providing the enhancement undertaken in this field. Chapter Six proposed a more effective algorithm, including strategies to resolve drawbacks resulting from rapidly changing climatic conditions and PSC. The proposed MPPT system with PSO in this study is configured to adjust the diverse prerequisites elements of the PV system, including fast tracking in distinctive natural conditions, high exactness, stability

and high effectiveness. Section 6.3 of Chapter Six presented and actualised an improved PSO MPPT algorithm based on a simple numerical calculation for determining the values of the duty cycle in the case of MPP, capable of overwhelming the difficulties related to rapidly changing insolation levels and the influence of PSC. It was established that this can be easily understood, and is capable of being executed on commercial micro-controllers. Moreover, it was established that the proposed LI-PSO MPPT algorithm increases PV efficiency under uniform irradiance and PSC, without the addition of any additional complexity in comparison to the traditional MPTT algorithm. At the same time, it was confirmed that this algorithm has been configured to allow it to be appropriate for actualisation on commercial microcontrollers, with an introduction of an advanced principle for reinitialising the (duty-cycle). Therefore, this form of methodology can establish the working point with greater accuracy prompting to a precise step-size update.

Chapter Seven included a comparison between traditional MPPT algorithms for PV systems and the proposed LI-PSO MPPT algorithm systems. The suggested algorithm also considered the issue of PSC (i.e. multiple peaks in the power function). Again, simulation and exploratory results were established that confirmed the performance and usefulness of the proposed algorithm. The simulation has been undertaken utilising SIMULINK, in which the diverse aspects of the model configuration and parameters have been described. The efficiency of the proposed LI- PSO has been tested using MATLAB/Simulink and RT-real time simulation, and compared to the existing MPPT algorithm, the P&O, IncCond and PSO algorithm. A comparison took place of the proposed algorithm output to that of the P&O, IncCond and PSO based MPPT algorithm, and these comparison figures were presented together with a table summarising the change in effectiveness in both transient and unfaltering state reactions. The results in Chapter Seven illustrate the efficiency of supervisory controller, which achieved an improved performance under all conditions without oscillation around the MPP, whereby leading to the osculation being practically zero.

The results from the simulation having revealed that the novel duty cycles will be altered in the condition of any variation in atmospheric state, respective of variation in working power, but its value holds its position near the novel best duty cycle. Due to this, duty cycles' initialisation fails to bring about an unneeded examination of the P-V curve, hence permitting the fresh MPP to be employed swiftly. In addition, it is worthy arguing that despite the likelihood that the duty cycle computed via (6.14) fails to confirm its nearness to the final last superlative duty cycle, because of the perturbation factor K2, at minimum one of di (i = 1, 2,

3) will equally be near to the best duty cycle. As a result, both 6.14 and 6.16 dependably guarantee fast tracking.

In this work, a mechanism was proposed by which particles can be initialized efficiently around the MPP to avoid both unnecessarily redundant searching and a situation in which the area being actively searched by the swarm becomes too small. The simulation results show that the proposed LI-PSO method has a faster response speed than other methods. This is because the particles automatically migrate to the best position or close to it when the weather conditions change. As a result, this significantly reduces the time wasted by particle tracking in incorrect areas, thereby substantially enhancing the system tracking speed while also reducing the steady-state oscillation (practically to zero) once the MPP is located. This is a great improvement upon the conventional PSO method, in which the new operating point is too far from the MPP and more iterations are required to reach the new MPP.

The proposed scheme contains a number of advantages over other MPPT techniques.

1) In the proposed scheme, the controller tracks two points at the same time (*p*best*i* and *g*best), as the perturbation of duty cycle is computed by two terms: as can be seen from Eq (6.16). This allows the proposed PSO to track the new GP with great rapidity, thus improving its dynamic response and efficiency in comparison with the traditional PSO algorithm.
2) The new technique of updating the particles' position, can improve the operability of the algorithm and reduce its dependence on parameters.
3) The proposed method can effectively avoid the disadvantages of conventional MPPT methods, which can easily fall into local MPP instead of GMPP.
4) If a sudden change in weather conditions occurs, the controller will work on the correct direction towards the GMPP, as its information is obtained through the use of three duty cycles, unlike the conventional MPPT, which can be perturbed in the wrong direction.
5) In the case of partial shading, when the PV array exhibits multiple peaks on its $P-V$ characteristic, the proposed MPPT controller can track the true MPP correctly, as it is based on a searching scheme. In conventional methods, however, the controller is likely to trap the operating point at local MPP instead of the GMPP.
6) The proposed method is simple and easy to implement, using a low-cost microcontroller, having excellent rates of accuracy with fast speed without any oscillation, being practically zero on the steady state.

8.1. Recommendations for further work

This study has focussed on the MPPT operation of the PV array, rather than the working states of the electric loads. More significantly, a new investigation managing renewable scattered energy system would incorporate a number of different sources energy (e.g. wind, diesel, and fuel cell) to upgrade energy usage. However, the primary reason for the use of readily available renewable PV energy, along with wind, a small amount of hydro, fuel cell, and hydrogen innovation as a storage media, will be to encourage a means of establishing clean, ecological friendly energy to replace fossil fuel that lead to exhausted resources.

The results of the simulations undertaken in this work have identified a number of areas for future work, including improving and expanding a number of aspects of the current study, as outlined below:

Modelling and simulation of PV systems. The dynamic displaying of the PV module has been undertaken with consideration of both the vulnerabilities and the parametric changes, but with no consideration of the factor of the aging of PV panels. However, the execution assessment identified with the investigation of the materials on the PV board is required to incorporate the maturing aspect of PV panels in the created model. Therefore, this study will assist in the expectation of a long-term execution of stand-alone PV systems.

At the same time, this work can, to a greater extent, be expanded, in particular through the creation of a complex MPPT algorithm for both charger and inverter, to enhance productivity. Moreover, a number of different MPPT based control algorithms can be produced, considering the distinctive source and load combinations. Again, the electronic capacity of the qualities of all modules in standard arrangement encourages a less demanding controller outline and its configuration. At the same time, the establishment of an automatic changeover to different operation modes will remove the need for manual operation.

9. References

[1] A. N. A. Ali, M. H. Saied, M. Mostafa and T. Abdel-Moneim, "A survey of maximum PPT techniques of PV systems," *Proceedings of the IEEE Energytech,* pp. 1-17, 2012.

[2] A. Zbeeb, V. Devabhaktuni, A. Sebak, and L. Maheshwari, "A new microcontroller-based MPPT algorithm for photovoltaic applications", *Int. Conference on Energy and Environment*, Chandigarh, India, March 2009.

[3] Akihiro Oi, "*Design and Simulation of Photovoltaic Water Pumping System*", Master of Science Thesis, California Polytechnic State University, 2005.

[4] E. Koutroulis, K. Kalaitzakis and N. C. Voulgaris, "Development of a microcontroller-based, photovoltaic maximum power point tracking control system," *IEEE Transactions on Power Electronics*, vol. 16, 2001pp. 46-54.

[5] W. Xiao, N. Ozog and W. G. Dunford, "Topology study of photovoltaic interface for maximum power point tracking", IEEE *Trans. Ind. Electron.*, vol. 54, no. 3, 2007, pp.1696 - 1704.

[6] Y. Jung, J. So, G. Yu and J. Choi, "Improved perturbation and observation method (IP&O) of MPPT control for photovoltaic power systems," in *Conference Record of the Thirty-First IEEE Photovoltaic Specialists Conference, 2005.* 2005, pp. 1788-1791.

[7] W. Xiao and W. G. Dunford, "A modified adaptive hill climbing MPPT method for photovoltaic power systems," in *Power Electronics Specialists Conference, 2004. PESC 04. 2004 IEEE 35th Annual,* 2004, pp. 1957-1963.

[8] A. Mahmoud, H. Mashaly, S. Kandil, H. El Khashab and M. Nashed, "Fuzzy logic implementation for photovoltaic maximum power tracking," in *Industrial Electronics Society, 2000. IECON 2000. 26th Annual Confjerence of the IEEE,* 2000, pp. 735-740.

[9] A. Yazdani and P. P. Dash, "A control methodology and characterization of dynamics for a photovoltaic (PV) system interfaced with a distribution network," *IEEE Trans. Power Del.*, vol. 24, 2009, pp. 1538-1551.

[10] A. Safari and S. Mekhilef, "Incremental conductance mppt method for pv systems," *in 2011 24th Canadian Conference on Electrical and Computer Engineering (CCECE)*, 2011, pp. 345-347.

[11] H. Abouobaida and M. Cherkaoui, "Comparative study of maximum power point trackers for fast changing environmental conditions," in *Multimedia Computing and Systems (ICMCS), 2012 International Conference on*, 2012, pp. 1131-1136.

[12] C. Hua and C. Shen, "Comparative study of peak power tracking techniques for solar storage system," in *Applied Power Electronics Conference and Exposition, 1998. APEC'98. Conference Proceedings 1998., Thirteenth Annual*, 1998, pp. 679-685.

[13] J. J. Nedumgatt, K. Jayakrishnan, S. Umashankar, D. Vijayakumar and D. Kothari, "Perturb and observe MPPT algorithm for solar PV systems-modeling and simulation," in *2011 Annual IEEE India Conference*, 2011, pp. 1-6.

[14] D. Hohm and M. Ropp, "Comparative study of maximum power point tracking algorithms using an experimental, programmable, maximum power point tracking test bed," in *Photovoltaic Specialists Conference, 2000. Conference Record of the Twenty-Eighth IEEE*, 2000, pp. 1699-1702.

[15] S. Park, G. Cha, Y. Jung and C. Won, "Design and application for PV generation system using a soft-switching boost converter with SARC," *IEEE Trans. Ind. Electron.*, vol. 57, pp. 515-522, 2010. [16] R. Kadri, J. Gaubert and G. Champenois, "An improved maximum power point tracking for photovoltaic grid-connected inverter based on voltage-oriented control," *IEEE Trans. Ind. Electron.*, vol. 58, 2011pp. 66-75.

[17] H. Abidi, A. B. B. Abdelghani and D. Montesinos-Miracle, "MPPT algorithm and photovoltaic array emulator using DC/DC converters," in *2012 16th IEEE Mediterranean Electro Technical Conference*, 2012, pp. 567-572.

[18] T. Hiyama and K. Kitabayashi, "Neural network based estimation of maximum power generation from PV module using environmental information," *IEEE Trans. Energy Convers.*, vol. 12, 1997. pp. 241-247.

[19] C. Hua and C. Shen, "Study of maximum power tracking techniques and control of DC/DC converters for photovoltaic power system," in *Power Electronics Specialists Conference, 1998. PESC 98 Record. 29th Annual IEEE,* 1998, pp. 86-93.

[20] Y. LIU, "*Advance control of photovoltaic converters*," Ph. D. dissertation, Dept. of Engg. University of Leicester, UK, April 2009.

[21] E. V. Paraskevadaki and S. A. Papathanassiou, "Evaluation of MPP voltage and power of mc-Si PV modules in partial shading conditions," *IEEE Trans. Energy Convers.,* vol. 26, 2011pp. 923-932.

[22] E. Karatepe and T. Hiyama, "Simple and high-efficiency photovoltaic system under non-uniform operating conditions," *IET Renewable Power Generation,* vol. 4, 2010pp. 354-368.

[23] Q. Zhang, X. Sun, Y. Zhong and M. Matsui, "A novel topology for solving the partial shading problem in photovoltaic power generation system," in *Power Electronics and Motion Control Conference, 2009. IPEMC'09. IEEE 6th International,* 2009, pp. 2130-2135.

[24] H. Patel and V. Agarwal, "Maximum power point tracking scheme for PV systems operating under partially shaded conditions," *IEEE Trans. Ind. Electron.,* vol. 55, 2008pp. 1689-1698.

[25] S. Jain and V. Agarwal, "A new algorithm for rapid tracking of approximate maximum power point in photovoltaic systems," *IEEE Power Electronics Letters,* vol. 2, 2004,. pp. 16-19.

[26] K. Ishaque and Z. Salam, "A deterministic particle swarm optimization maximum power point tracker for photovoltaic system under partial shading condition," *IEEE Trans. Ind. Electron.,* vol. 60, 2013. pp. 3195-3206.

[27] M. Miyatake, M. Veerachary, F. Toriumi, N. Fujii and H. Ko, "Maximum power point tracking of multiple photovoltaic arrays: a PSO approach," *IEEE Trans. Aerospace Electron. Syst.,* vol. 47, 2011, pp. 367-380.

[28] Bründlinger R et al. prEN 50530 – The new European standard for performance characterisation of PV inverters. In: 24th Eur Photovoltaic Solar Energy Conf, 2009.

[29] K. Hussein, I. Muta, T. Hoshino and M. Osakada, "Maximum photovoltaic power tracking: an algorithm for rapidly changing atmospheric conditions," *IEE Proceedings-Generation, Transmission and Distribution,* vol. 142, 1995, pp. 59-64,

[30] Z. Salameh and D. Taylor, "Step-up maximum power point tracker for photovoltaic arrays," *Solar Energy,* vol. 44, 1990, pp. 57-61.

[31] C. Hua and C. Shen, "Comparative study of peak power tracking techniques for solar storage system," in *Applied Power Electronics Conference and Exposition, 1998. APEC'98. Conference Proceedings 1998., Thirteenth Annual,* 1998, pp. 679-685.

[32] Y. Liu, J. Chen and J. Huang, "A review of maximum power point tracking techniques for use in partially shaded conditions," *Renewable and Sustainable Energy Reviews,* vol. 41, 2015, pp. 436-453.

[33] T. Wu, C. Chang and Y. Chen, "A fuzzy-logic-controlled single-stage converter for PV-powered lighting system applications," *IEEE Trans. Ind. Electron.,* vol. 47, 2000,pp. 287-296.

[34] C. Hua, J. Lin and C. Shen, "Implementation of a DSP-controlled photovoltaic system with peak power tracking," *IEEE Trans. Ind. Electron.,* vol. 45, 1998, pp. 99-107.

[35] C. Hua and C. Shen, "Control of DC/DC converters for solar energy system with maximum power tracking," in *Industrial Electronics, Control and Instrumentation, 1997. IECON 97. 23rd International Conference on,* 1997, pp. 827-832.

[35] M. Berrera, A. Dolara, R. Faranda and S. Leva, "Experimental test of seven widely-adopted MPPT algorithms," *in PowerTech, 2009 IEEE Bucharest,* 2009, pp. 1-8.

[36] G. Farivar, B. Asaei and S. Mehrnami, "An analytical solution for tracking photovoltaic module MPP," *IEEE Journal of Photovoltaics,* vol. 3, 2013,pp. 1053-1061.

[37] A. Brambilla, M. Gambarara, A. Garutti and F. Ronchi, "New approach to photovoltaic arrays maximum power point tracking," in *Power Electronics Specialists Conference, 1999. PESC 99. 30th Annual IEEE,* 1999, pp. 632-637.

[38] S. M. R. Kazmi, H. Goto, O. Ichinokura and H. Guo, "An improved and very efficient MPPT controller for PV systems subjected to rapidly varying atmospheric conditions and

partial shading," in *Power Engineering Conference, 2009. AUPEC 2009. Australasian Universities*, 2009, pp. 1-6.

[39] K. Irisawa, T. Saito, I. Takano and Y. Sawada, "Maximum power point tracking control of photovoltaic generation system under non-uniform insolation by means of monitoring cells," in *Photovoltaic Specialists Conference, 2000. Conference Record of the Twenty-Eighth IEEE*, 2000, pp. 1707-1710.

[40] Y. Kuo, T. Liang and J. Chen, "Novel maximum-power-point-tracking controller for photovoltaic energy conversion system," *IEEE Trans. Ind. Electron.*, vol. 48, 2001,pp. 594-601,.

[41] R. Faranda and S. Leva, "Energy comparison of MPPT techniques for PV Systems," *WSEAS Transactions on Power Systems*, vol. 3, 2008,.pp. 446-455,

[42] Z. Liang, R. Guo, J. Li and A. Q. Huang, "A high-efficiency PV module integrated dc/dc converter for PV energy harvest in freedom systems", IEEE *Trans. Power Electron*., vol. 26, no. 3, 2011,pp.897 -909.

[43] R. Kadri, J. Gaubert and G. Champenois, "An improved maximum power point tracking for photovoltaic grid-connected inverter based on voltage-oriented control," *IEEE Trans. Ind. Electron.*, vol. 58, 2011,pp. 66-75.

[44] M. Miyatake, F. Toriumi, T. Endo and N. Fujii, "A novel maximum power point tracker controlling several converters connected to photovoltaic arrays with particle swarm optimization technique," in *Power Electronics and Applications, 2007 European Conference on*, 2007, pp. 1-

[45] B. N. Alajmi, K. H. Ahmed, G. P. Adam and B. W. Williams, "Single-phase single-stage transformer less grid-connected PV system," *IEEE Transactions on Power Electronics*, vol. 28, 2013, pp. 2664-2676.

[46] V. Phimmasone, Y. Kondo, T. Kamejima and M. Miyatake, "Evaluation of extracted energy from PV with PSO-based MPPT against various types of solar irradiation changes," in *Electrical Machines and Systems (ICEMS), 2010 International Conference on*, 2010, pp. 487-492.

[47] J. Ahmad, "A fractional open circuit voltage based maximum power point tracker for photovoltaic arrays," in *Software Technology and Engineering (ICSTE), 2010 2nd International Conference on*, 2010, pp. V1-247-V1-250.

[48] S. Hadji, J. Gaubert and F. Krim, "Maximum power point tracking (MPPT) for photovoltaic systems using open circuit voltage and short circuit current," in *3rd International Conference on Systems and Control*, 2013, pp. 87-92.

[49] S. R. Potnuru, D. Pattabiraman, S. I. Ganesan and N. Chilakapati, "Positioning of PV panels for reduction in line losses and mismatch losses in PV array," Renewable Energy, vol. 78, , 2015, pp. 264-275.

[50] T. L. Kottas, Y. S. Boutalis and A. D. Karlis, "New maximum power point tracker for PV arrays using fuzzy controller in close cooperation with fuzzy cognitive networks," *IEEE Trans. Energy Convers.*, vol. 21, 2006, pp. 793-803.

[51] Senjyu, T. Uezato and K. (1994Maximum power point tracker using fuzzy control for photovoltaic arrays", *Proceedings of the IEEE International Conference on Industrial Technology*, 5-9 Dec, pp. 143-147.

[52] C. Won, D. Kim, S. Kim, W. Kim and H. Kim, "A new maximum power point tracker of photovoltaic arrays using fuzzy controller," *in Power Electronics Specialists Conference, PESC'94 Record., 25th Annual IEEE*, 1994, pp. 396-403.

[53] N. Khaehintung, P. Sirisuk and W. Kurutach, "A novel ANFIS controller for maximum power point tracking in photovoltaic systems," *in Power Electronics and Drive Systems, 2003. PEDS 2003. the Fifth International Conference on*, 2003, pp. 833-836.

[54] M. Abdulaziz, S. Aldobhani and R. John, "Maximum power point tracking of PV system using ANFIS prediction and fuzzy logic tracking," 2008.

[55] Mashaly, H.M.; Sharaf, A.M.; Mansour, M.M.; El-Sattar, A.A. "Fuzzy logic controller for photovoltaic-utility interfacing scheme “, Electro technical *Conference, 1994. Proceedings., 7th Mediterranean*, On page(s): 715 - 718 vol.2N.Femia, G. Petrone, G.

[56] Spagnuolo, and M. Vitelli, “Perturb and observe MPPT technique robustness improved,” *in Proc. IEEE Int. Symp. Ind. Electron*., May 2004, vol. 3, no. 1, pp. 845–850.

[57] Y. Hsiao and C. Chen, "Maximum power tracking for photovoltaic power system," in *Industry Applications Conference, 2002. 37th IAS Annual Meeting. Conference Record of the*, 2002, pp. 1035-1040.

[58] N. Kasa, T. lida and H. Lwamoto (2000), "Maximum power point tracking with capacitor identifier for PV power system", *IEEE Procd-Electr. Power application*, Nov., Vol. 147, no 6.

[59] T. Esram and P. L. Chapman, "Comparison of photovoltaic array maximum power point tracking techniques," *IEEE Transactions on Energy Conversion EC*, vol. 22, 2007,pp. 439.

[60] X. Liu and L. A. Lopes, "An improved perturbation and observation maximum power point tracking algorithm for PV arrays," in *Power Electronics Specialists Conference, 2004. PESC 04. 2004 IEEE 35th Annual*, 2004, pp. 2005-2010.

[61] N. Femia, D. Granozio, G. Petrone, G. Spagnuolo and M. Vitelli, "Predictive & adaptive MPPT perturb and observe method," *IEEE Trans. Aerospace Electron. Syst.*, vol. 43, 2007, pp. 934-950.

[62] F. Liu, S. Duan, F. Liu, B. Liu and Y. Kang, "A variable step size INC MPPT method for PV systems," *IEEE Trans. Ind. Electron.*, vol. 55, 2008, pp. 2622-2628.

[63] T. Noguchi, S. Togashi, and R. Nakamoto, “Short-current pulse-based maximum-power-point tracking method for multiple photovoltaic-and converter module system,” *IEEE Trans. Ind. Electron.*, vol. 49, no. 1, Feb. 2002¸pp.217–223.

[64] T. Tafticht, K. Agbossou, M. L. Doumbia, and A. Ch´eritia, “An improved maximum power point tracking method for photovoltaic systems,” *Renew. Energy*, vol. 33, Jul. 2008 no. 7, pp. 1508–1516.

[65] B. Subudhi and R. Pradhan, "A comparative study on maximum power point tracking techniques for photovoltaic power systems," *IEEE Transactions on Sustainable Energy*, vol. 4, 2013pp. 89-98.

[66] H. N. Zainudin and S. Mekhilef, "Comparison study of maximum power point tracker techniques for PV systems," in *Proceedings of the 14th International Middle East Power Systems Conference (MEPCON'10), Cairo University, Egypt,* 2010, pp. 750-755.

[67] Syafaruddin, E. Karatepe and T. Hiyama, "Artificial neural network-polar coordinated fuzzy controller based maximum power point tracking control under partially shaded conditions," *IET Renewable Power Generation*, vol. 3, no. 2 Jun. 2009, pp. 239–253.

[68] M. A. S. Masoum, H. Dehbonei, and E. F. Fuchs, "Theoretical and experimental analyses of photovoltaic systems with voltage and current based maximum power-point tracking," *IEEE Trans. Energy Convers.*vol. 17, no. 4, pp. 514–522, Dec. 2002.

[69] K. Ishaque, Z. Salam and G. Lauss, "The performance of perturb and observe and incremental conductance maximum power point tracking method under dynamic weather conditions," *Appl. Energy,* vol. 119, pp. 228-236, 2014.

[70] N. Femia, G. Petrone, G. Spagnuolo and M. Vitelli, "Optimization of perturb and observe maximum power point tracking method", *IEEE Trans. Power Electron.*, vol. 20 no. 4, pp.963 -973, 2005.

[71] N. Khaehintung and P. Sirisuk, "Application of maximum power point tracker with self-organizing fuzzy logic controller for solar-powered traffic lights," in *2007 7th International Conference on Power Electronics and Drive Systems,* 2007, pp. 642-646.

[72] E. Koutroulis and F. Blaabjerg, "A new technique for tracking the global maximum power point of PV arrays operating under partial-shading conditions," *IEEE J. Photovoltaics*, vol. 2, no. 2, pp. 184–190, Apr. 2012.

[73] Ran, Li. "Perturbation parameters design for hill climbing MPPT techniques." *2012 IEEE International Symposium on Industrial Electronics*. 2012.

[74] M. Lokanadham and K. V. Bhaskar, "Incremental conductance based maximum power point tracking (MPPT) for photovoltaic system," *International Journal of Engineering Research and Applications (IJERA),* vol. 2, pp. 1420-1424, 2012.

[75] Rezk, Hegazy, and Ali M. Eltamaly. "A comprehensive comparison of different MPPT techniques for photovoltaic systems." *Solar Energy 112 (2015):* 1-11.

[76] Sera, Dezso, et al. "On the perturb-and-observe and incremental conductance MPPT methods for PV systems." *Photovoltaics, IEEE Journal of 3.3 (2013):* 1070-1078.

[77] Chen, Yie-Tone, Zhi-Hao Lai, and Ruey-Hsun Liang. "A novel auto-scaling variable step-size MPPT method for a PV system." *Solar Energy 102 (2014):* 247-256.

[78] K. Kobayashi, I. Takano, andY. Sawada, "A study on a two stage maximum power point tracking control of a photovoltaic system under partially shaded insolation conditions," *in Proc. IEEE Power Eng. Soc. General Meeting,* , vol. 4, Jul. 2003,pp. 2612–2617.

[79] Y.-H. Liu, S.-C. Huang, J.-W. Huang and W.-C. Liang, "A particle swarm optimization-based maximum power point tracking algorithm for PV systems operating under partially shaded conditions", IEEE *Trans. Energy Conver.* vol. 27, no. 4, 2012.pp.1027 -1035,.

[80] C. Rodriguez and G. A. J. Amaratunga, "Analytic solution to the photovoltaic maximum power point problem," *IEEE Trans. Circuits Syst. I, Reg. Papers*, vol. 54, no. 9 Sep. 2007, pp. 2054–2060.

[81] M. Sheraz and M. A. Abido, "An efficient MPPT controller using differential evolution and neural network," in *Power and Energy (PECon), 2012 IEEE International Conference on*, 2012, pp. 378-383.

[82] N. Femia, G. Petrone, G. Spagnuolo, and M. Vitelli, "A technique for improving p and o MPPT performances of double-stage grid-connected photovoltaic systems," *IEEE Trans. Ind. Electron.*, vol. 56, Nov. 2009 no. 11, pp. 4473– 4482.

[83] Chin, Chia Seet, et al. "Optimization of partially shaded PV array using fuzzy MPPT." *Humanities, Science and Engineering (CHUSER), 2011 IEEE Colloquium on*. IEEE, 2011.

[84] C. Larbes, S.M. A¨ıt Cheikh, T. Obeidi, and A. Zerguerras, "Genetic algorithms optimized fuzzy logic control for the maximum power point tracking in photovoltaic system," Renew. Energy, vol. 34, no. Oct. 200910, pp. 2093– 2100.

[85] D. Nguyen and B. Lehman, "An adaptive solar photovoltaic array using model-based reconfiguration algorithm," *IEEE Trans. Ind.Electron.*, ol. 55, no. 7, Jul. 2008.pp. 2644–2654.

[86] Sheraz, Muhammad, and Mohammed A. Abido. "An efficient MPPT controller using differential evolution and neural network." *Power and Energy (PECon), 2012 IEEE International Conference on*. IEEE, 2012.

[87] P. Sharma and V. Agarwal, “Maximum power extraction from a partially shaded PV array using shunt-series compensation,” IEEE J. Photovolt., vol. 4, no. 4, 2014 Jul., pp. 1128–1137.

[88] K. L. Lian, J. H. Jhang, and I. S. Tian, “A maximum power point tracking method based on perturb-and-observe combined with particle swarm optimisation,” IEEE J. Photovolt., vol. 4, no. 2 ,Mar. 2014, pp. 626–633.

[89] L. Gao, R. A. Dougal, S. Liu and A. P. Iotova, "Parallel-connected solar PV system to address partial and rapidly fluctuating shadow conditions”, IEEE *Trans. Ind. Electron*., vol. 56, no. 5, 2009, pp.1548 -1556.

[90] Y.H. Ji, D.Y. Jung, J.G. Kim, J.H. Kim, T.W. Lee, and C.Y. Won, “A real maxi-mum power point tracking method for mismatching compensation in PV array under par-tially shaded conditions,” *IEEE Trans. Power Electron*., vol. 26, no. 4, Apr. 2011, pp. 1001–1009.

[91] Y. J. Wang and P. C. Hsu, "Analytical modelling of partial shading and different orientation of photovoltaic modules”, IET Renew. Power Gener., vol. 4, no. 3,2010, pp.272 - 282.

[92] K. Ishaque, Z. Salam, M. Amjad, and S. Mekhilef, “An improved particle swarm optimization (PSO)-based MPPT for PV with reduced steady-state oscillation,” *IEEE Trans. Power Electron.*, vol. 27, no. 8, Aug. 2012, pp. 3627–3638.

[93] Á.-A. Bayod-Rújula and J.-A. Cebollero-Abián, “A novel MPPT method for PV sys-tems with irradiance measurement,” *Sol. Energ*., vol. 109, Nov. 2014, pp. 95–104.

[94] T. L. Nguyen and K.-S. Low, “A global maximum power point tracking scheme em-ploying DIRECT search algorithm for photovoltaic systems,” *IEEE Trans. Ind. Electron.*, vol. 57, no. 10, Oct. 2010,pp. 3456–3467.

[95] L.-R. Chen, C.-H. Tsai, Y.-L. Lin, and Y.-S. Lai, “A biological swarm chasing algorithm for tracking the PV maximum power point,” *IEEE Trans. Energy Convers.*, vol. 25, no. 2, Jun.2010, pp. 484–493.

[96] X. Chen and Y. Li, “A modified PSO structure resulting in high exploration ability with convergence guaranteed,” *IEEE Transactions on Systems*, Man, and Cybernetics, Part B, vol. 37, no. 5, 2007, pp. 1271–1289.

[97] A. Badram, A. Davoudi and R. S. Balog, "Control and circuit techniques to mitigate partial shading effects in photovoltaic arrays”, IEEE *J. Photovoltaics*, vol. 2, no. 4, 2012, pp.532 -546.

[98] B. N. Alajmi, K. H. Ahmed, S. J. Finney and B. W. Williams, "A maximum power point tracking technique for partially shaded photovoltaic systems in microgrids”, *IEEE Trans. Ind. Electron.*, vol. 60, no. 4, 2013,pp.1596 -1606.

[99] R. Gules, J. De Pellegrin Pacheco, H. L. Hey, and J. Imhoff, "A Maximum Power Point Tracking System with Parallel Connection for PV Stand-Alone Applications, *" IEEE Trans. Indust. Electronics*, vol. 55, 2008, pp. 2674-2683.

[100] A. Omole, Analysis, Modeling and Simulation of Optimal Power Tracking of Multiple-Modules of Paralleled Solar Cell Systems, Ph.D. dissertation, Dept. Electrical and Computer Engineering. The Florida State University, 2006.

[101] V. Phimmasone, T. Endo, Y. Kondo and M. Miyatake, "Improvement of the maximum power point tracker for photovoltaic generators with particle swarm optimization technique by adding repulsive force among agents," in *Electrical Machines and Systems, 2009. ICEMS 2009. International Conference on*, 2009, pp. 1-6.

[102] M. A. Elgendy, B. Zahawi, and D. J. Atkinson, "Assessment of the Incremental Conductance Maximum Power Point Tracking Algorithm, " IEEE Trans. Sustainable Energy, vol. 4, 2013, pp. 108-117.

[103] G. J. Shushnar et al., “Balance of System costs for a 5 MW photovoltaic generating station,” IEEE Trans. Power Apparatus System, vol. PAS-104, no.8, 1985,pp: 2006-2011.

[104] L. F. L. Villa, D. Picault, B. Raison, S. Bacha and A. Labonne, "Maximizing the power output of partially shaded photovoltaic plants through optimization of the interconnections among its modules", *IEEE Journal of Photovoltaics*, vol. 2, no. 2, 2012, pp.154 -163.

[105] J. A. Gow and C. D. Manning, "Development of a model for photovoltaic arrays suitable for use in simulation studies of solar energy conversion systems", *in Proc. 6th Int. Conf. Power Electron. Variable Speed Drives*, 1996, pp. 69-74.

[106] A. Dolara, R. Faranda and S. Leva, "Energy comparison of seven MPPT techniques for PV systems", J. Electromagn. Anal. Appl., vol. 3, 2009,pp.152 -162.

[107] J.G. Vera, "Operations for rural electrifications in Mexico," IEEE Trans. On Energy Conversion, vol.7, no.3, 1992,pp :426-433.

[108] E. J. Estebanez, V. M. Moreno, A. Pigazo, M. Liserre and A. Dell'Aquila, "Performance evaluation of active islanding-detection algorithms in distributed-generation photovoltaic systems: Two inverters case", *IEEE Trans. Ind. Electron.*, vol. 58, no. 4, 2011.pp.1185 -1193.

[109] D. Feldman, G. Barbose, R. Margolis, T. James, S. Weaver, N. Darghouth, R. Fu, C. Davidson, S. Booth and R. Wiser, "Behind the PV price declines", Renewable Energy Focus, vol. 15, no. 6, 2014, pp. 14-15.

[110] R. Kumar, J.E. Bigger, "Photovoltaic Systems," *proceedings of the IEEE*, vol. 81, np.3, pp: 365-377, 1993.

[111] H. A. Sher, A. F. Murtaza, K. E. Addoweesh and M. Chiaberge, "An intelligent off-line MPPT technique for PV applications", *Proc. IEEE Conf. Syst., Process Control*, pp.316 -320, 2013.

[112] S. Zhou, L. Kang, J. Sun, G. Guo, B. Cheng, B. Cao and Y. Tang, "A Novel Maximum Power Point Tracking Algorithms for Stand-alone Photovoltaic System", *International Journal of Control, Automation, and Systems*, vol. 8, 2011, pp.1364 -1371.

[113] J. M. Enrique, J. M. Andujar and M. A. Bohorquez, "A reliable, fast, and low cost maximum power point tracker for photovoltaic applications", Solar Energy, vol. 84, no. 1, 2010.pp.79 -89.

[114] S. M. Moosavian, N. A. Rahim, J. Selvaraj and K. H. Solangi, "Energy policy to promote photovoltaic generation", Renew. Sust. Energy Rev., vol. 25, 2013,pp.44 -58.

[115] T. Bhattacharya, Terrestrial solar photovoltaics, Narosa Publishing House, 1998.

[116] Antonio Luque and Steven Hegedus (2003), "Handbook of Photovoltaic Science and Engineering", John Wiley and Sons Ltd, Chichester, West Sussex P019 8SQ, England.

[117] F. Sick and T. Erge, Photovoltaic in buildings: a design handbook, International Energy Agency (1996).

[118] Z. Sen, Solar Energy Fundamentals and Modeling Techniques: Atmosphere, Environment, Climate Change and Renewable Energy, 2008: Springer-Verlag.

[119] J.A. Gow and C.D. Manning ''Photovoltaic converter system suitable for use in small scale stand-alone or grid connected applications'' *IEE Proc*, vol *147, No. 6, pp* 535-543, Nov 2000.

[120] W. Xiao, "Improved control of photovoltaic interfaces," 2008.

[121] L. Castañer and S. Silvestre, Modeling Photovoltaic Systems Using PSpice, 2002: Wiley.

[122] T. Yu and T. Chien, "Analysis and simulation of characteristics and maximum power point tracking for photovoltaic systems," in *Power Electronics and Drive Systems, 2009. PEDS 2009. International Conference on*, 2009, pp. 1339-1344.

[123] A. Woyte, J. Nijs, and R. Belmans, "Partial shadowing of photovoltaic arrays with different system configurations: literature review and field test results", Solar Energy, Vol. 74, Issue 3, March 2003, pp. 217-233.

[124] W. Xiao, N. Ozog, and W. G. Dunford, "Topology Study of Photovoltaic Interface for Maximum Power Point Tracking", IEEE Transactions on Industrial Electronics, Vol. 54, No. 3, June 2007, pp. 1696-1704.

[125] Tomas Markvart, Solar electricity, 2nd edition, Wiley, 1999, ISBN: 0471988537.

[126] G.-C. Hsieh, H.-I. Hsieh, C.-Y. Tsai and C.-H. Wang, "Photovoltaic power-increment-aided incremental-conductance MPPT with two-phased tracking", IEEE Trans. Power Electron., vol. 28, no. 6, pp.2895 -2911, 2013.

[127] F Lasnier and TG Ang. (1990), "Photovoltaic Engineering Handbook", IOP Publishing Ltd, Bristol, England.

[128] Florida solar energy center (1996), "Photovoltaic system Design", April 1996.

[129] A. Pandey, N. Dasgupta and A. K. Mukerjee, "High-performance algorithms for drift avoidance and fast tracking in solar MPPT system*", IEEE Trans. Energy Convers*., vol. 23, no. 2, pp.681 -689, 2008.

[130] Muhammdi H. Rashid (1993), "Power electronics- Converter application", Prentice Hall international edition, New Jercy, USA.

[131] I. Glasner and J. Applebaum, "Advantage of boost versus buck topology for maximum power point tracker in photovoltaic systems", Proc. *19th Annu. IEEE Conv. Electr. Electron. Eng. Israel*, 1996.pp.355 -358.

[132] C. Hua and C. Shen, "Control of DC/DC Converters for Solar Energy System with Maximum Power Tracking", *Proc. of IEEE, IECON*\'97, pp.827 -832, 1997.

[133] J. M. Enrique, E. Durán, M. Sidrach-de-Cardona and J. M. Andújar, "Theoretical assessment of the maximum power point tracking efficiency of photovoltaic facilities with different converter topologies", Sol. Energy, vol. 81, no. 1, pp.31 -38, 2007.

[134] D. D. C. Lu, R. H. Chu, S. Sathiakumar, and V. G. Agelidis, "A buck converter with simple maximum power point tracking for power electronics education on solar energy systems, " Power Engineering Conference, 2007. AUPEC 2007. Australasian Universities, vol. 1, no. 5, pp. 9-12 Dec. 2007.

[135] R. F. Coelho, F. Concer, and D. C. Martins, "A Study of the Basic DC-DC Converters Applied in the Maximum Power Point Tracking," in Proc. Brazilian Power Electronics Conference, 2009, pp. 673-678.

[136] Wilhelm Werner, Polynomial interpolation: Lagrange versus Newton, Math. Comp. 43 (1984), no. 167, 205–217.

[137] C. Candan, "An efficient filtering structure for Lagrange interpolation", *IEEE Signal Process. Lett.*, vol. 14, no. 1, pp. 17-19, 2007.

[138] S. Mirbagheri, M. Aldeen, and S. Saha. "A PSO-based MPPT re-initialised by incremental conductance method for a standalone PV system."Control and Automation (MED), 2015 23th Mediterranean Conference on. IEEE, 2015.

[139] Z. Fei, Z. X. Lin, Z. Junjun and H. Jingsheng, "Hardware-in-the-loop simulation, modeling and close-loop testing for three-level photovoltaic grid-connected inverter based on RT-LAB," in *Power System Technology (POWERCON), 2014 International Conference on*, 2014, pp. 2794-2799.

[140] A. Benigni and A. Monti, "A parallel approach to real-time simulation of power electronics systems," *IEEE Transactions on Power Electronics,* vol. 30, pp. 5192-5206, 2015.

[141] A. Friedman, S. J. Dyke, B. Phillips, R. Ahn, B. Dong, Y. Chae, N. Castaneda, Z. Jiang, J. Zhang and Y. Cha, "Large-scale real-time hybrid simulation for evaluation of advanced damping system performance," *J. Struct. Eng.*, vol.141, 2014.pp. 401-4150.

[142] J. Jung, "Power hardware-in-the-loop simulation (PHILS) of photovoltaic power generation using real-time simulation techniques and power interfaces," *J. Power Sources,* vol. 285, pp. 137-145, 2015.

[143] J. Jung and S. Ahmed, "Model construction of single crystalline photovoltaic panels for real-time simulation," in *2010 IEEE Energy Conversion Congress and Exposition,* 2010, pp. 342-349.

[144] R. B. A. Koad, A. F. Zobaa, "A Study of non-isolated DC–DC converters for photovoltaic systems," International Journal on Energy Conversion, vol.1, no.4, July 2013, pp.219-227.

[145] R. B. A. Koad, A. F. Zobaa, "Comparison study of five maximum power point tracking techniques for photovoltaic energy systems," International Journal on Energy Conversion, vol.2, no.1, January 2014, pp.17-25.

[146] R. B. A. Koad, and A. F. Zobaa, "Comparison between the conventional methods and PSO based MPPT algorithm for photovoltaic systems," International Journal of Electrical,

Computer, Energetic, Electronic and Communication Engineering, vol.8, no.4, April 2014, pp.690-695.

[147] R. B. A. Koad, A. F. Zobaa, and A. El-Shahat, “A novel MPPT algorithm based on particle swarm optimization for photovoltaic systems,” IEEE Transactions on Sustainable Energy.